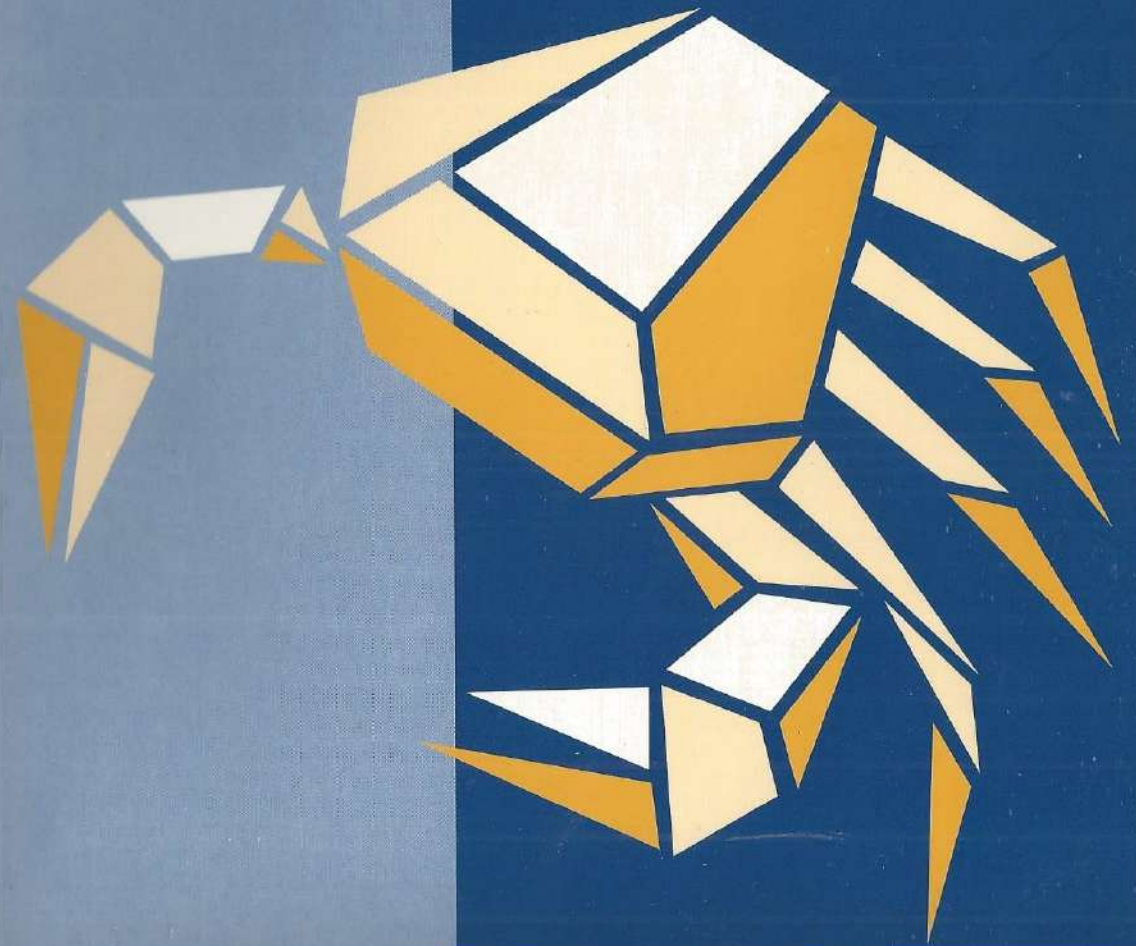


CD44v6 for diagnosis and targeting of head and neck squamous cell carcinoma



CD44v6 for diagnosis and targeting of head and neck squamous cell carcinoma



Nicole van Hal 1998

Nicole van Hal

CD44v6 for diagnosis and targeting of head and neck squamous cell carcinoma

Nicole van Hal

The research described in this thesis was performed at the Department of
Otolaryngology/Head and Neck Surgery, University Hospital *Vrije Universiteit*,
Amsterdam.

VRIJE UNIVERSITEIT

CD44v6 for diagnosis and targeting of head and neck squamous cell carcinoma

ACADEMISCH PROEFSCHRIFT

ter verkrijging van de graad van doctor aan
de Vrije Universiteit te Amsterdam,
op gezag van de rector magnificus
prof.dr. T. Sminia,
in het openbaar te verdedigen
ten overstaan van de promotiecommissie
van de faculteit der geneeskunde
op woensdag 23 december 1998 om 13.45 uur
in het hoofdgebouw van de universiteit,
De Boelelaan 1105

ISBN 90-646-4402-0

CD44v6 for diagnosis and targeting of head and neck squamous cell carcinoma
by Nicole Lucia Wilhelmina van Hal
Thesis University Hospital *Vrije Universiteit*, Amsterdam
with summary in Dutch

door

Nicole Lucia Wilhelmina van Hal

geboren te Boxmeer

Copyright © 1998 N.L.W. van Hal

Printing: Grafisch bedrijf Ponsen & Looijen BV, Wageningen, The Netherlands

Promotor: prof.dr. G.B. Snow

Copromotoren: dr. G.A.M.S. van Dongen
dr. R.H. Brakenhoff

*voor mijn ouders
voor Okke*

Contents

Chapter 1	General introduction	9
Chapter 2	Monoclonal antibody U36, a suitable candidate for clinical immunotherapy of squamous cell carcinoma, recognizes a CD44 isoform	51
Chapter 3	Sequence variation in the monoclonal antibody U36 defined CD44v6 epitope	69
Chapter 4	Characterization of CD44v6 isoforms in head and neck squamous cell carcinoma	81
Chapter 5	The role of CD44v6 splice variants in human cancer reconsidered	105
Chapter 6	Evaluation of soluble CD44v6 as potential serum marker for head and neck squamous cell carcinoma	123
Chapter 7	Summary, general discussion and perspectives	143
	Samenvatting, algemene discussie en perspectieven	151
	References	161
	Curriculum vitae	184
	List of publications	185
	Dankwoord	186
	List of abbreviations	188

Chapter 1

General introduction

Contents

1	Head and neck squamous cell carcinoma	11
1.1	Etiology and incidence	11
1.2	Metastasis	12
1.3	Staging of the disease	13
1.4	Treatment and survival rates	14
2	MAbs and squamous-associated antigens	16
2.1	MAbs directed against HNSCC	16
2.2	MAB U36 for targeting of HNSCC	18
2.3	Characterization of the MAB U36 defined antigen	22
3	CD44 proteins: structure, ligands, function and their role in tumor progression	23
3.1	General introduction	23
3.2	Generation of CD44 isoforms	24
3.2.1	Organization of the human CD44 gene	24
3.2.2	Post-translational modification of CD44 proteins	30
3.3	CD44 expression pattern in normal tissues	30
3.4	Molecular interactions of CD44	33
3.4.1	Interactions with the cytoskeleton	33
3.4.2	Interactions with the extracellular matrix	33
3.4.3	Other extracellular interactions	35
3.5	Functional characterization of CD44 isoforms	36
3.5.1	The role of CD44 in the immune system	36
3.5.2	The role of CD44 in the skin	38
3.5.3	Origin and function of soluble CD44	40
3.6	CD44 expression in tumors	42
3.6.1	Metastasis-inducing CD44 variants (rat model)	42
3.6.2	CD44v expression in various tumor types	43
3.6.3	Soluble CD44 as a tumor marker in serum	46
4	Aim and outline of this thesis	49

1 Head and neck squamous cell carcinoma

1.1 Etiology and incidence

Squamous cell carcinoma (SCC) is the most prominent malignancy of the head and neck region [1-3]. It arises from the mucosa of the upper aerodigestive tract. The most frequently affected sites are the oral cavity, the pharynx and the larynx (Fig. 1) [2,3]. The disease accounts for about 5% of all newly diagnosed malignant tumors in North Western Europe and the United States and each year about 500,000 new cases are registered world wide [2]. Head and neck squamous cell carcinoma (HNSCC) occurs more often in males than in females and shows a peak incidence in the sixth and seventh decade of life [2-4]. The most important risk factors for the development of HNSCC are smoking and alcohol abuse and there are indications that their combination has a synergistic effect [2,4-8]. It has been shown that carcinogens in cigarette smoke induce mutations in the p53 gene, the most common genetic alteration in human cancer [9-12]. When smoking was combined with alcohol consumption, the frequency of p53 mutations appeared to be increased [12]. Besides exposure to carcinogens, human papilloma viruses (HPV) may play a role in the carcinogenic process by inactivation of the

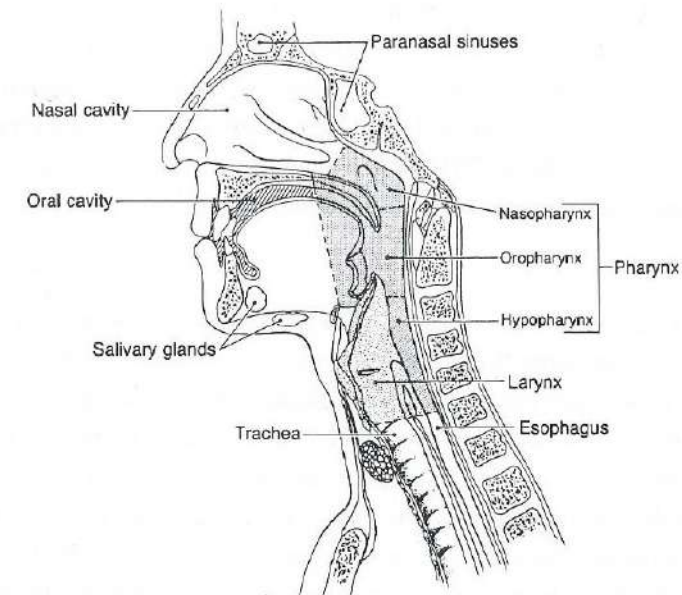


Figure 1 The upper aerodigestive tract [2].

cellular tumor suppressor gene products by means of interaction with the viral oncoproteins E6 and E7 [13]. Especially in tonsillar carcinoma, the presence of high risk HPV subtypes has been demonstrated, but a crucial role in the etiology of HNSCC is not proven. Besides mutations in the p53 gene, other genetic changes have been described for HNSCC, including amplification and overexpression of the epidermal growth factor receptor (EGFR) [14,15] and amplification of the oncogene PRAD-1 (located on 11q13) [16-18]. Also a frequent loss of heterozygosity (LOH) on chromosomal arms 9p (most often at position 9p21-22), 3p and 17p has been reported, suggesting the presence of tumor suppressor genes at these positions that are involved in the progression towards HNSCC [19-30].

Although smoking and alcohol are evident risk factors, only a small percentage of smokers and drinkers develop HNSCC. Therefore, it is assumed that there is an individual intrinsic sensitivity for these risk factors. It has been proposed that the risk for head and neck cancer (and in particular second primary tumors) is associated with the sensitivity of a person to carcinogenic agents [31]. This hypothesis was substantiated by an *in vitro* assay in which the genetic damage in lymphocytes, induced by the DNA-damaging compound bleomycin, was determined. Using this assay, it was found that HNSCC patients showed a significantly higher mutagen sensitivity than healthy control persons. In particular, HNSCC patients with multiple primary tumors appeared to be very sensitive. These differences were reproduced in a large multicenter trial and a hypersensitive phenotype in combination with smoking appeared to have a substantial effect on cancer risk estimates [32]. Recently, mutagen sensitivity was demonstrated to have a heritability estimate of 77% and the elucidation of the molecular mechanisms underlying this factor of cancer susceptibility is in progress.

1.2 Metastasis

HNSCC grows locally invasive, with a tendency to metastasize to the regional lymph nodes rather than to spread hematogeneously to distant sites. The incidence of lymph node metastasis mainly depends on the size and site of the primary tumor, varying from 1% for small glottic cancers to 80% for nasopharyngeal cancer [33]. Infiltration of the local lymph nodes can subsequently lead to further dissemination via the lymphatics and the bloodstream. The overall incidence of clinically detected distant metastases is 5-30% [34-38]. However, these figures should be interpreted with caution, as patients often die from loco-regional recurrences before distant metastases are clinically manifest. From

autopsy studies, it was concluded that about half of the patients suffered from distant metastases [39,40]. It should be noted, however, that in the latter studies cured patients were not taken into account, resulting in an overestimation of the overall incidence. The lungs are the most frequent initial site of distant metastases (about 70%) [35,38]. Other localizations of metastatic deposits are the skeletal system, liver, mediastinum, skin and brain [38,39].

The status of the lymph nodes in the neck is the most important prognostic factor for HNSCC. The presence of lymph node metastasis reduces the expected survival by approximately 50% [33,38]. Moreover, it has been shown that the incidence of distant metastases is directly related to the number of tumor positive neck nodes, extranodal spread and the involvement of lymph nodes in lower levels of the neck [34,35,37]. A study reported by Leemans *et al.* [38] indicated that the incidence of distant metastases is about twice as high for patients with histopathologically positive lymph nodes compared to patients with histopathologically negative nodes (13.6% versus 6.9%). Especially when more than three lymph nodes are involved, the risk to develop distant metastases appears to be highly increased (46.8%). In addition, the incidence of primary site recurrences is significantly increased, especially for patients with more than three positive nodes on histopathologic examination (26.2% versus 12.3%) [41].

1.3 Staging of the disease

Tumors can be classified according to the TNM system of the 'Union Internationale Contre le Cancer' (UICC) [42,43] (Table 1). The classification is based on the size of the primary tumor (T), the involvement of regional lymph nodes, including the size, number and laterality (N), and the presence of distant metastasis (M). Based on the TNM classification, tumors are grouped into clinical stages (Table 1). Stage I and II represent early stages of the disease, with relatively small tumors and no lymph node or distant metastasis. Stage III and IV are the more advanced clinical stages of HNSCC, with large tumors or tumors with lymph node or distant metastasis. About one third of the patients presents with a stage I or II disease, whereas the other two thirds of the HNSCC patients present with stage III or IV disease [2,44]. Accurate documentation of the stage of disease is important for optimal treatment planning and evaluation of experimental treatment strategies.

Table 1 TNM-classification and stage grouping according to the UICC [42,43].

TX	Primary tumor cannot be assessed
T0	No evidence of primary tumor
Tis	Carcinoma in situ
T1	Tumor ≤ 2 cm in greatest dimension
T2	Tumor > 2 cm, but ≤ 4 cm
T3	Tumor > 4 cm
T4	Tumor invades adjacent structures
<hr/>	
NX	Regional lymph nodes can not be assessed
N0	No regional lymph node metastasis
N1	Metastasis in a single ipsilateral lymph node (≤ 3 cm)
N2a	Metastasis in a single ipsilateral lymph node (> 3 cm, but ≤ 6 cm)
N2b	Metastasis in multiple ipsilateral lymph nodes (none > 6 cm)
N2c	Metastasis in bilateral or contralateral lymph nodes (none > 6 cm)
N3	Metastasis in a lymph node (> 6 cm)
<hr/>	
MX	Presence of distant metastasis cannot be assessed
M0	No evidence of distant metastasis
M1	Distant metastasis
<hr/>	
Stage 0	Tis, N0, M0
Stage I	T1, N0, M0
Stage II	T2, N0, M0
Stage III	T3, N0, M0
	T1-3, N1, M0
Stage IV	T4, N0-1, M0
	any T, N2-3, M0
	any T, any N, M1

1.4 Treatment and survival rates

Conventional treatment of HNSCC patients consists of surgery and/or radiotherapy. Patients with stage I or II disease are treated either by surgery or radiotherapy, which will cure about 60-80% of the patients [2]. The more advanced stages of HNSCC (stage III and IV) are treated with a combination of surgery and radiotherapy, but a curative result is reached in only 30% of the cases [2]. About 50-60% of the patients with advanced disease will develop locoregional recurrences after conventional therapy and 15-25% will develop distant metastases [38,41,45].

These data indicate that the currently applied treatment is not sufficient for many patients, despite the large improvements in the therapeutical modalities, *i.e.* surgery and radiotherapy. Apparently, small tumor deposits that are not detectable by routine histopathological examination remain in the body of the patient after conventional treatment, a phenomenon that is often referred to as 'minimal residual disease'. To improve the treatment of HNSCC patients, an effective systemic adjuvant therapy is needed to eliminate these remaining tumor cells at local, regional and distant sites. For this purpose, the efficacy of chemotherapy has been studied extensively and several drugs and drug combinations have been tested. However, the results were disappointing since the application of chemotherapy remained mainly palliative [2,46-48]. An important limitation of chemotherapy is its lack of selectivity, which can result in serious toxicity. Furthermore, it is important that new sensitive methods will be developed for the detection of tumor cells in surgical margins, in lymph nodes or at distant sites. The assessment of minimal residual disease will allow selection of patients for whom adjuvant therapy is to be recommended, and may be used to monitor the effect of the treatment.

At the Department of Otolaryngology/Head and Neck Surgery of the University Hospital *Vrije Universiteit*, monoclonal antibodies (MAbs) have been developed for selective targeting of HNSCC. Furthermore, efforts are made to identify HNSCC-associated markers that have potential for the detection and treatment of minimal residual head and neck cancer. The availability of squamous markers and specific antibodies will open new avenues for tumor (cell) detection. The most promising technologies for the detection of rare HNSCC cells in a background of normal cells are immunocytochemistry and polymerase chain reaction (PCR) based methods [49-54]. In addition, the 'magic bullet' concept can be explored, in which MAbs are used *in vivo* as missiles with a search-and-destroy function. This selective targeting approach can be used for the detection (*e.g.* by radioimmunoscinigraphy; RIS) and selective eradication (*e.g.* by radioimmunotherapy; RIT) of HNSCC tumors that are recognizable due to the presence of an HNSCC marker.

2. MAbs and squamous-associated antigens

2.1 MAbs directed against HNSCC

So far, at least 30 MAbs directed against HNSCC have been described in literature (a selection of MAbs is shown in Table 2), however, their suitability for detection of minimal residual disease and/or selective tumor targeting needs critical evaluation. One of the most important criteria is that the MAb shows an intense and homogeneous reactivity with all HNSCC tumors in the patient population and with all cancer cells within these tumors. Besides that, the MAb should not be reactive with surrounding normal tissue cells and ideally not be reactive with all other tissues. For *in vivo* tumor targeting, additional criteria have to be set, especially when the MAb is used in a therapeutic setting. In that case, the antigen should be localized at the outer surface of the HNSCC cell. Moreover, reactivity with normal tissues is generally not allowed, especially when these tissues are well accessible from the blood, such as blood vessels, bone marrow, and organs like liver and spleen. Besides that, the MAb should be preferably of the IgG subclass rather than of the IgM subclass, since the extravasation and penetration into the tumors will be better for the relatively small IgG molecules. Finally, the antibody should not react with an antigen that is shed in large amounts into the circulation.

The available HNSCC-reactive antibodies, as listed in Table 2, can be divided in two main categories. One group of MAbs also recognizes other tumor types besides HNSCC, the so-called pancarcinoma MAbs. A general shortcoming of these MAbs is their heterogeneous reaction pattern with HNSCC and their reactivity with several normal tissues. Another group of MAbs is reactive with squamous cell carcinoma and not with other tumor types. An advantage of these MAbs is their limited reactivity with normal tissues except for normal squamous epithelia.

Unfortunately, many of the MAbs mentioned in Table 2 are poorly characterized with respect to their reactivity profile on normal and malignant tissues. For these MAbs, it is difficult to speculate about their suitability for the previously mentioned diagnostic and therapeutic applications. The best characterized MAbs are 174H.64, E48, U36 and VFF18 of which the first three have been evaluated in radioimmunoscintigraphy (RIS) studies for their capacity to target HNSCC tumors in patients. Preoperative RIS with ^{99m}Tc -labeled MAb 174H.64 in 21 HNSCC patients revealed visualization of all 18 primary tumors,

Table 2 Monoclonal antibodies directed against squamous cell carcinoma.

MAb	Antigen	Reactivity with normal tissues	Reference
<i>Squamous cell specific:</i>			
174H.64	48 + 57 kDa	basal cells of normal squamous epithelia, cytoplasmic antigen	[55]
E48	16-20 kDa	basal and suprabasal cells of normal squamous epithelia	[56]
INS-2	40 kDa	normal squamous epithelia, cytoplasmic antigen, IgM	[57]
U36	CD44v6	basal and suprabasal cells of normal squamous epithelia	[58]
BM2	52 kDa	basal cells of normal squamous epithelia, IgM	[59]
VFF18	CD44v6	basal and suprabasal cells of normal squamous epithelia	[60]
<i>Pan-carcinoma:</i>			
SQM1	48 kDa	blood vessels, IgM	[61]
A9	$\alpha_5\beta_4$ integrin	blood vessels and basal cells of normal squamous epithelia	[62]
B10	various keratins	various normal tissues, cytoplasmic antigen, IgM	[63]
1H5	various keratins	various normal tissues, cytoplasmic antigen, IgM	[63]
425	EGF-receptor	various normal tissues	[64]
K931	Ep-CAM	various normal tissues	[65]
225	EGF-receptor	various normal tissues	[66]
K984	125 kDa	basal cells of normal squamous epithelia and various other normal tissues	[67]
K928	50 - 55 kDa	suprabasal cells of normal squamous epithelia and various other normal tissues	[67]
175F4	45-50 kDa	normal squamous epithelia	[68]
175F11	45-50 kDa	normal squamous epithelia	[68]
CAK1	40 kDa	mesothelium and basal epithelium of trachea	[69]
HMF61	>400 kDa, PEM	various normal tissues	[70]

while 15 out of 18 locoregional lymph node metastases and 2 out of 3 distant metastases were identified. Despite these promising results, eradication of intact HNSCC cells with MAb 174H.64 will be a problem due to the intracellular localization of this cytokeratin-like target antigen. MAb E48 recognizes a 16-22 kDa glycosylphosphatidyl-inositol-anchored surface antigen, which is apparently involved in cellular adhesion. The potential of this MAb-antigen combination for the targeting of primary HNSCC and lymph node metastases has been demonstrated in clinical RIS/biodistribution studies. In these studies, in which ^{99m}Tc -, ^{131}I - and ^{125}I -labeled E48 IgG or F(ab')₂ were administered, all primary tumors and about 60% of the lymph node metastases were detected. Only lymph nodes

containing just a small amount of viable tumor cells were not visualized, although the MAb had targeted also these cells as was demonstrated by immunohistochemistry. Unfortunately, a serious limitation met by MAb E48 is the heterogeneity of the E48 expression in 30% of HNSCC [71]. With respect to this, MAb U36 seems to be better qualified for *in vivo* tumor targeting as a high and homogenous expression of the U36 antigen was found in 96% of the primary HNSCC tumors and HNSCC lymph node metastases as determined by immunohistochemistry [71]. MAb VFF18 was shown to recognize the same antigen as MAb U36 and showed similar characteristics [60].

2.2 MAb U36 for targeting of HNSCC

MAb U36 was generated by immunizing BALB/c mice intraperitoneally with viable cells of the HNSCC cell line UM-SCC-22B [58]. It is an antibody of the IgG1 subclass that binds with an affinity of $3.5 \times 10^{10} \text{ M}^{-1}$ (as determined by Scatchard plot) to a surface antigen of squamous tumor cells [58]. Its high and homogeneous expression on most HNSCC tumors makes the MAb U36 defined antigen a suitable HNSCC marker antigen. Immunohistochemical staining of a large panel of HNSCC cryosections showed that in 188/196 (96%) of the HNSCC tumors, at least 50% of the tumor cells are intensely stained [71]. The reactivity of MAb U36 to normal tissues appears to be mainly restricted to squamous epithelia. Immunohistochemical evaluation of a wide range of normal tissues showed an intense staining of the squamous cells of the oral cavity, pharynx, larynx, esophagus, tonsil, cervix, vagina and epidermis as well as the epithelial cells of hair follicles [58]. An example of normal oral mucosa immunohistochemically stained with MAb U36 is shown in Fig. 2. From a few other tissues only specialized cells were reactive (*e.g.* sebaceous glands, the basal layers of transitional epithelium of the urinary bladder, terminal bronchioli of the lung and myoepithelial cells from various organs), but the fraction of positive cells in these tissues was low. For antibody-based therapy, antigen expression in normal tissues is expected to cause a problem when the tissue is well accessible to the antibody. Squamous epithelia, however, are poorly accessible to intravenously injected immunoglobulins, due to the presence of an effective blood/tissue barrier. Therefore, the high expression of the MAb U36 defined antigen on normal squamous epithelia is not expected to be a limitation for *in vivo* tumor targeting, as was confirmed by various scintigraphy studies (see below). The physio-

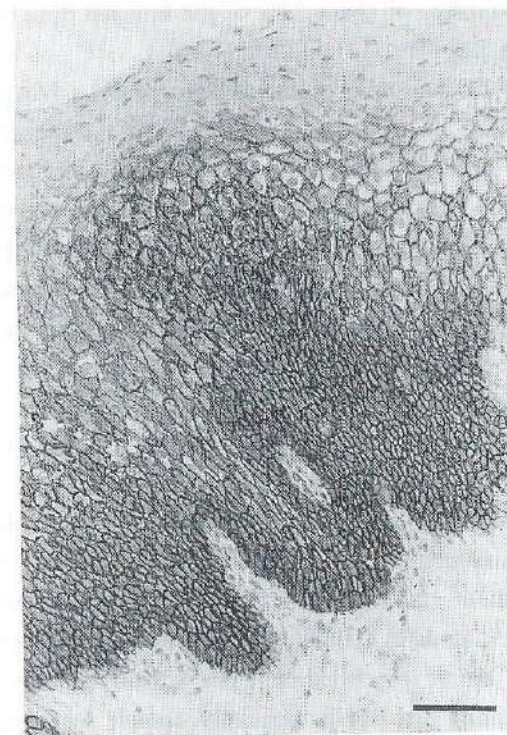


Figure 2 Immunohistochemical staining of normal oral mucosa, using MAb U36. The antibody strongly reacts with the outer cell surface of both the basal cell layer and the stratum spinosum and less intensely with cells in the stratum granulosum. The keratinized squames are negative. The plasma membrane at the basal side of cells in the basal cell layer appears to be predominantly negative. Scale bar represents 50 μm .

logical barrier in malignant tissues often appears to be less effective, and the fenestrated structure of the endothelium leads to a high uptake of MAbs [72].

The capacity of MAb U36 for selective tumor targeting *in vivo* was studied using ^{131}I trace-labeled MAb U36 in athymic nude mice bearing human HNSCC xenografts. These mice are immunodeficient since they lack T-cells, permitting the growth of human tumor tissue when transplanted subcutaneously. The localization of radioactively labeled MAb U36 in this mouse model was determined qualitatively by imaging with a gamma camera (RIS) and quantitatively by γ -counting of the radioactivity in dissected tissues. MAb U36 immuno-

conjugates appeared to be capable of selective tumor targeting in this mouse model, and tumor uptakes of about 25% of the injected dose per gram (%ID/g) have been observed [58].

Its capacity for selective tumor targeting makes MAb U36 a suitable candidate for the use as targeting vehicle in antibody-based therapy. Since HNSCC has an intrinsic sensitivity for radiation, RIT using monoclonal antibodies conjugated with radionuclides seems to be a promising option [73]. An advantage of RIT is that it is unnecessary for radiolabeled MABs to bind to each single tumor cell to achieve maximal therapeutic effects, because radionuclides (especially β -emitters) are cytotoxic at a distance of several cell diameters. Although the use of radioimmunoconjugates seems to have the most favorable perspectives, also MAB conjugates containing toxins, cytostatics, photosensitizers or enzymes capable of converting non-toxic prodrugs to active cytotoxic drugs might find a way in therapy of head and neck cancer [74,75].

For the use of MAB U36 in RIT, procedures for the stable coupling of the therapeutic β -emitting radionuclide ^{186}Re were developed [76]. When mice bearing xenografts of about 100 mm^3 were injected with a therapeutic dose of $500\text{ }\mu\text{Ci}$ ^{186}Re -labeled MAB U36, 100% complete remissions were observed [77]. Furthermore, small tumors responded more dramatically upon RIT treatment than larger tumors, indicating that RIT is especially suitable for treatment of minimal residual disease [78].

Based on the promising data obtained from preclinical experiments, a clinical RIS study was initiated to evaluate the biodistribution of MAB U36 in HNSCC patients [79]. In this clinical RIS study, 10 HNSCC patients received $1.8\text{--}53\text{ mg}$ U36 IgG labeled with $^{99\text{m}}\text{Tc}$ ($756 \pm 95\text{ MBq}$; $20.4 \pm 2.6\text{ mCi}$) intravenously. Two days after injection, the uptake of MAB U36 was measured in biopsies of the tumor, in positive and negative lymph nodes and in various additional tissues including blood and bone marrow. Activity uptake was the highest in the tumor ($20.4 \pm 12.4\text{ }\% \text{ID/kg}$). In addition, a relatively high uptake was observed in the normal mucosa ($10.1 \pm 6.4\text{ }\% \text{ID/kg}$), the thyroid gland ($7.1 \pm 4.0\text{ }\% \text{ID/kg}$) and bone marrow aspirate ($7.2 \pm 1.4\text{ }\% \text{ID/kg}$). It should be noted, however, that the activity in bone marrow aspirate was almost the same as in blood ($7.8 \pm 1.7\text{ }\% \text{ID/kg}$), suggesting that it was mainly based on plasma activity.

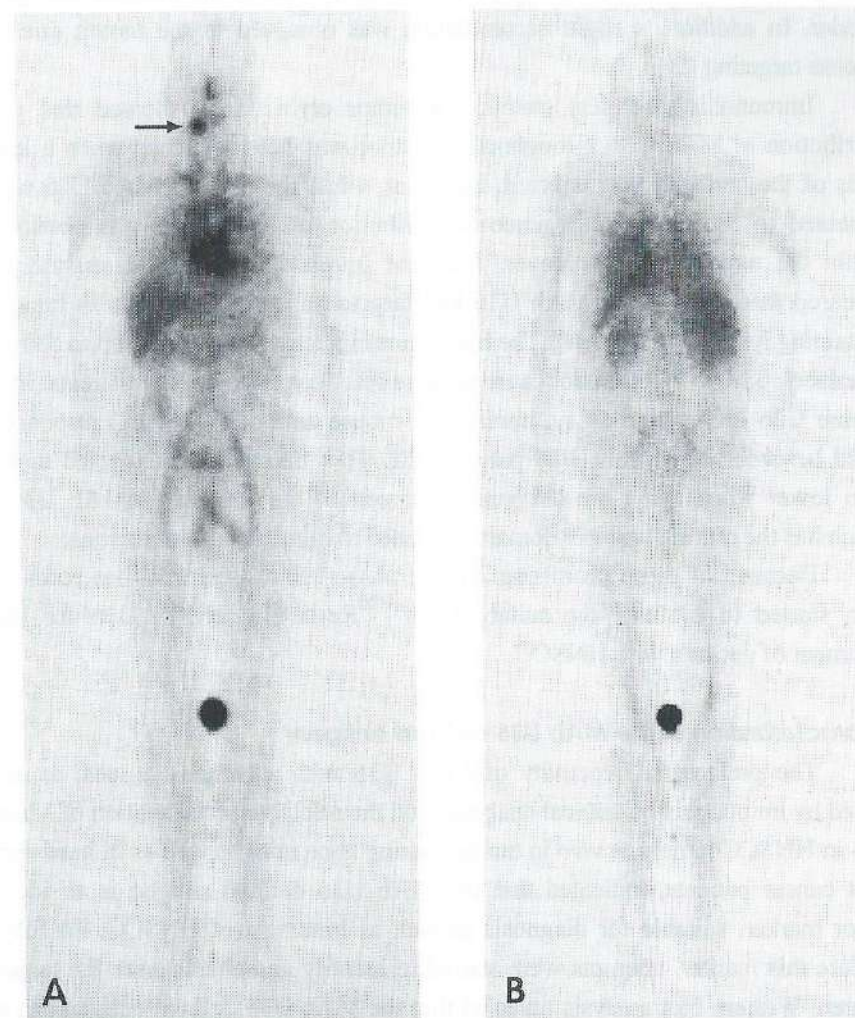


Figure 3 (A) Anterior and (B) posterior whole body images (16 hr p.i.) of an HNSCC patient injected with 13 mg MAB U36 radiolabeled with 756 MBq $^{99\text{m}}\text{Tc}$.

Thus, accumulation of MAB U36 in the bone marrow, which is generally the dose limiting organ in RIT, appears to be limited. In Fig. 3a an anterior and in Fig. 3b a posterior whole body image 16 hr p.i. is shown. Besides activity uptake in tumor tissue (indicated by an arrow), the heart, bloodvessels, lungs, liver, spleen and

kidneys were visualized, most likely also due to activity in the blood. Uptake of activity was also seen in the scrotal area and sometimes in the intestine and gall bladder. In addition, a slight accumulation was observed in the mouth due to mucosa targeting [79].

Immunohistochemical staining of tumor cryosections showed that the distribution of MAb U36 throughout the tumor was heterogeneous when a low dosis of the antibody was injected. However, when the dose of MAb U36 was increased to 53 mg, a homogeneous distribution of MAb U36 was obtained within the tumors [80]. Moreover, from the immunohistochemical analyses it appeared that at this dose MAb U36 had targeted all tumor deposits in tumor-containing lymph nodes [53,80]. The intravenous injection of amounts up to 53 mg of unlabeled MAb U36 did not cause adverse reactions in any of the patients. In a murine U36 IgG-related assay, human anti-mouse antibody (HAMA) responses could be observed in only 3/18 patients [80]. This frequency is expected to be even lower when using the chimerized version of the antibody (cMAb U36), which has the murine variable domains attached to human constant regions.

Because of these promising data, a phase-I/II clinical trial has recently been started to evaluate the suitability of ^{186}Re -labeled cMAb U36 for the treatment of patients with HNSCC.

2.3 Characterization of the MAb U36 defined antigen

The preferential reactivity of MAb U36 with squamous tissues, as assessed by immunohistochemical analyses, and the selective accumulation of MAb U36 in HNSCC tumors *in vivo* in tumor-bearing nude mice as well as in head and neck cancer patients, indicated that the MAb U36 defined antigen is an ideal tumor marker, suitable for diagnosis as well as treatment of HNSCC. To fully explore this marker, attempts were started to identify and characterize the target antigen. Western blot analysis revealed that the MAb U36 defined antigen has a molecular weight of about 200 kDa and that its epitope is primate-specific. In this thesis, the target antigen of MAb U36 is identified by cDNA cloning, to enable molecular diagnosis of minimal residual head and neck cancer and to enable functional characterization. As will be discussed in Chapter 2 of this thesis, the epitope recognized by MAb U36 appeared to be located in the **v6 domain of the CD44 proteins**.

3 CD44 proteins: structure, ligands, function and their role in tumor progression

3.1 General introduction

In the mid-eighties, several research groups identified independently the first CD44 proteins, which were at that time designated by a variety of names as indicated in Table 3. Eventually, all these proteins were shown to be immunologically identical or related to each other [93,96-100]. Since the F10-44-2 antigen [81] had been designated 'CD44' at the Third International Workshop on Leukocyte Antigens, according to the 'Cluster of Differentiation' (CD) designation [101], this became the official nomenclature for this protein.

Table 3 The first CD44 proteins that have been identified.

Protein name	Source	References
F10-44-2 antigen	human brain, granulocytes, T-lymphocytes and cortical thymocytes	[81]
phagocytic glycoprotein-1 (Pgp-1) or Ly-24	mouse 3T3 cells, murine macrophages and granulocytes	[82,83]
ln(Lu)-related p80 protein	human erythrocytes	[84]
p80-A1G3	human medullary thymocytes and mature T cells	[85]
gp85	baby hamster kidney cells	[86]
p85	human B cells	[87]
hyaluronate receptor	SV-3T3 cells	[88,89]
human homologue of Pgp-1	human fibroblasts, leukocytes, bone marrow cells and thymocytes	[90]
Hermes antigen or lymphocyte homing receptor	human lymphocytes	[91,92]
class III extracellular matrix receptor (ECMRIII)	human fibroblasts	[93-95]
Hutch-1 antigen	human fibroblasts and peripheral blood mononuclear cells	[93]

Soon, the first CD44-encoding cDNA clones were isolated and it became apparent that a large set of CD44 isoforms existed [102-114]. The isolated cDNA clones provided some insight into the complexity and structural relationship of the CD44 proteins, and an underlying mechanism of alternative splicing was hypothesized. This hypothesis was confirmed when in 1992 the CD44 gene was cloned and physically mapped [115]. To study the tissue-distribution of the various CD44 isoforms, a large set of monoclonal antibodies directed against variant CD44 domains were generated. CD44 isoforms appeared to have a tissue-restricted expression profile, which suggests a difference in function.

In the early nineties, it was noted that two CD44 isoforms expressed by a metastatic rat tumor cell line were able to confer metastatic behavior upon a non-metastasizing rat carcinoma cell line [109,116]. Since then, the role of the surface antigen CD44 in tumor progression and metastasis formation became an important direction in oncological research (see below).

3.2 Generation of CD44 isoforms

3.2.1 Organization of the human CD44 gene

The human CD44 gene is located on the short arm of human chromosome 11 (11p13) and spans about 50-60 kb [115,117]. Fig. 4 shows a schematical representation of the CD44 gene and its encoded proteins. The amino acid sequence encoded by the CD44 exons is depicted in Fig. 5. The first exon of the CD44 gene is thought to encode a signal peptide that is necessary for translocation of the protein to the membrane [105,109,118]. The predicted signal peptide cleavage site is indicated in Fig. 5 [105]. Exons 2-16 encode the extracellular domain, exon 17 encodes the transmembrane domain and the first 3 amino acids of the cytoplasmic tail. The further composition of the intracellular domain is encoded by exons 18 and 19.

All CD44 isoforms, varying in the composition and size of their extracellular and intracellular domain, are encoded by alternatively spliced transcripts of this single gene. Two particular regions of the CD44 mRNA precursors are alternatively spliced. The first region subjected to alternative splicing encompasses exons 6-14, also often indicated as the variant exons v2-v10 [119], and accounts for the variations observed in the extracellular domain (Fig. 4). The data demonstrate that increasing numbers of adjacent variant exons are removed from the 5' end of the variant region [120], although several transcripts have been

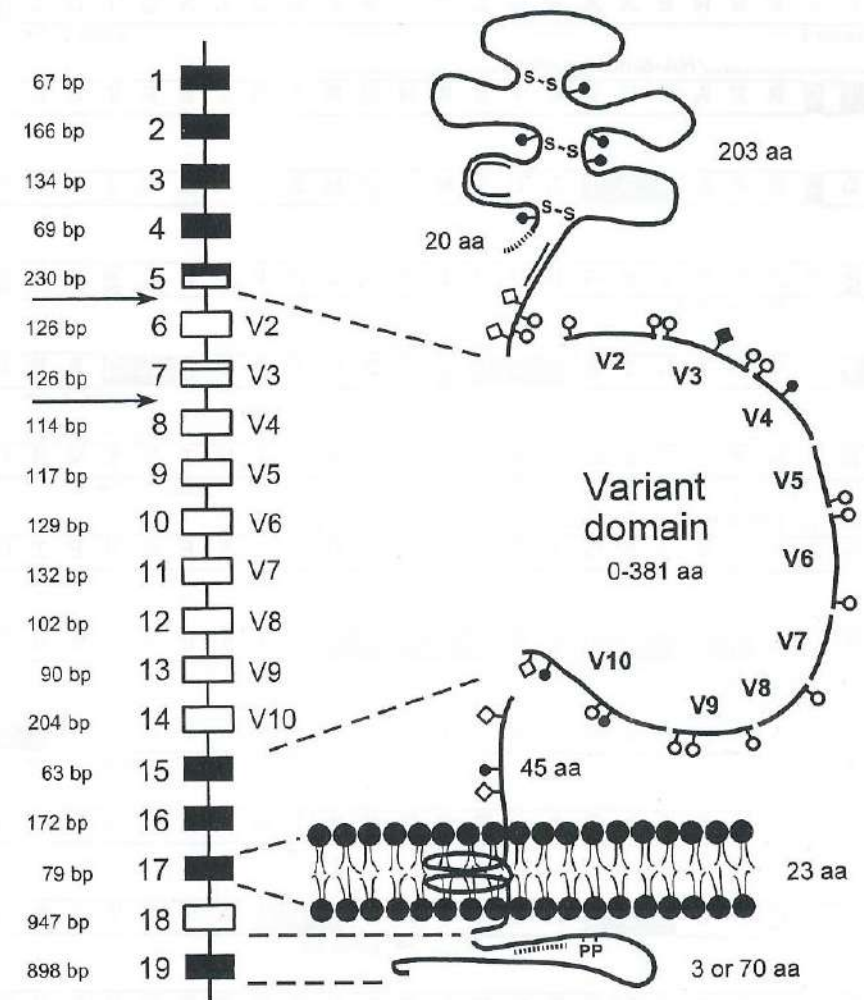


Figure 4 Schematic representation of the CD44 gene and its encoded proteins. As a result of alternative splicing, CD44 isoforms vary in the size of their extracellular domain and cytoplasmic tail. The alternatively spliced exons are indicated by open boxes on the left. The location of two additional exons, recently identified, is indicated by arrows. In the protein structure, all putative glycosylation attachment sites are indicated: O-glycosylation (open circles), N-glycosylation (closed circles), chondroitine sulfate (open squares) and heparan sulfate (closed squares) attachment sites. In addition, the HA-binding sites (double line), the putative signal peptide (dotted line), the disulfide bonds (S-S), the ankyrin binding site (dotted/undotted line) and the phosphorylation sites (-P) are indicated.

26

27

Figure 5 (on previous two pages) The human CD44 amino acid sequence. Indicated are the putative signal peptide, the HA-binding sites, the cysteines involved in the formation of disulfide bonds, the transmembrane domain, the ankyrin binding site and the two cytoplasmic serines that can be phosphorylated. The putative glycosylation sites are indicated by boxes: O-glycosylation (three amino acid motifs containing S and/or T), N-glycosylation (NXT or NXS), chondroitine sulfate (SG) and heparan sulfate (SGSG) attachment sites. The following footnotes is referred to: ¹Putative signal peptide with cleavage site. ²The HA-binding B(X₂)B motifs described by Yang *et al.* [151] are: **KNGRYSISR**, **RDGTRYVQKGEYR** and **RRRCGQKKK** (located in the cytoplasmic domain). ³Y [104,125] or S [102,114]. ⁴Additional 5' splice site. ⁵R [125] or A [102,104,107,114]. ⁶Depends on splicing. ⁷T [115] or A [120]. ⁸D [115] or L [120]. ⁹E [120] or S [110,113-115,119]. ¹⁰Additional 3' splice site. ¹¹S [113,120] or N [110,114,115,119]. ¹²P [120] or A [110,114,115,119]. ¹³V [114] or E [110,115,119,120]. ¹⁴K [114] or R [110,115,119,120]. ¹⁵Theoretical cleavage site for trypsin-like proteases. ¹⁶H [125] or T [107,108,110,111,113-115,119,120]. ¹⁷E [104] or G [102,114,115,125].

found that do not obey this general rule [109,110,121-123]. From this observation, however, it cannot be concluded whether the mechanism of alternative splicing is step-wise or block-wise. In exons 5 and 7, additional splice donor and acceptor consensus sequences are present, which account for an even higher diversity in the extracellular CD44 domain (Fig. 4 and 5). A second region subjected to alternative splicing is located at the 3' end of the CD44 mRNA precursors. This region accounts for a variation in the size of the cytoplasmic domain. Exon 17 may be spliced to exon 19, resulting in a long cytoplasmic tail of 70 amino acids, of which the first 3 amino acids are encoded by exon 17. However, the presence of exon 18, which starts with a stop codon, will result in a short cytoplasmic tail of only 3 amino acids [102,104,115,124]. CD44 proteins with a long cytoplasmic tail appear to be most abundant. A few examples of CD44 splice variants frequently found are depicted in Fig. 6. The splice variant that does not contain any variant exons was previously called the hemopoietic isoform (CD44H), since this variant is found in large amounts on hemopoietic cells [81,82,84,85,87,91,92]. In 1993, Tölg *et al.* [119] proposed a new nomenclature, and since then this variant is usually called the CD44 standard form (CD44s). A short tailed variant of CD44s has also been described. On epithelial cells, a variant with exon 5 spliced to exon 12 (v8) appeared to be highly expressed. This variant was previously called CD44R1 or the epithelial isoform (CD44E) [107,111,125], but according to the nomenclature of Tölg *et al.* [119], this variant is now called CD44v8-v10. One of

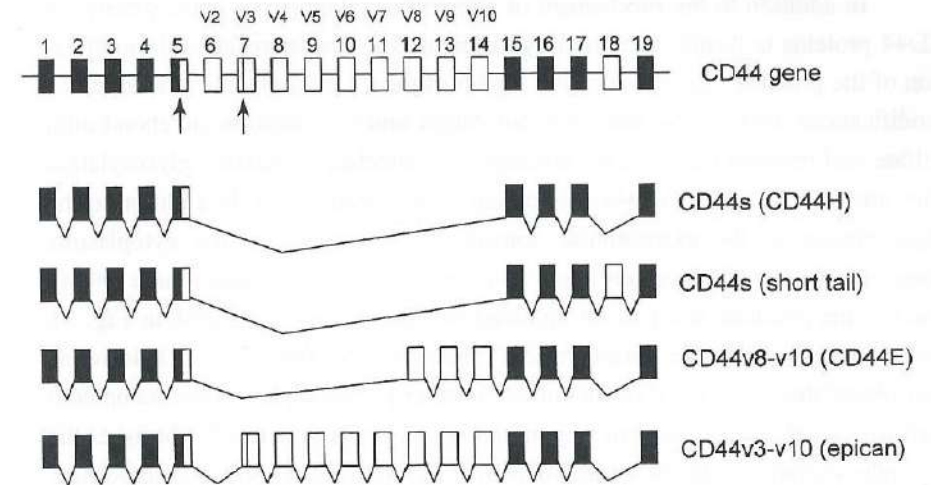


Figure 6 Nomenclature of CD44 splice variants. In the upper part the CD44 gene is shown. The solid boxes represent the standard exons, the open boxes represent the exons that undergo alternative splicing. In the lower part a few examples of CD44 splice variants are shown.

the largest CD44 variants found in humans is CD44v3-v10. This variant is highly expressed on keratinocytes, and was earlier called epican [114].

CD44 protein isoforms are encoded by at least three different mRNA transcripts. These transcripts only differ in the size of their non-coding 3' end, due to the existence of multiple polyadenylation signals [109,126,127]. For CD44s three major CD44 mRNA transcripts of approximately 1.6, 2.2 and 4.8 kb have been observed [102,104,107,127].

The numbering of the exons suggests that the CD44 gene consists of 19 exons. However, at a later stage two additional exons have been found. Firstly, an additional exon was found in the region between exons 5 and 6. In humans, this exon was shown to be interrupted by a stop codon. Transcripts containing this variant exon have not been detected in man, suggesting that it is not functional [120]. A second additional exon is located between exons 7 and 8 [128]. Transcripts containing this new exon have been described, but as yet only in malignant cells [128,129]. Despite the identification of these new exons, this thesis will keep to the exon-numbering as depicted in Fig. 6.

3.2.2 Post-translational modification of CD44 proteins

In addition to the mechanism of alternative splicing, the heterogeneity of CD44 proteins is further increased by differences in post-translational modification of the proteins. The extracellular region of the CD44 molecule is a target for modifications such as *N*- and *O*-glycosylation and the addition of chondroitin sulfate and heparan sulfate (HS) proteoglycan sidechains. Putative glycosylation sites are indicated in the CD44 amino acid sequence of Fig. 5. In addition to the glycosylation of the extracellular domain, it is known that the cytoplasmic domain is subject to phosphorylation by a serine/threonine protein kinase [90,94]. Two serine residues seem to be involved in this process (indicated in Fig. 5), since mutation of either serine residue abolishes the ability of CD44s to be phosphorylated [130,131]. It is not known whether phosphorylation occurs on both serine residues, nor is it known why mutation of either serine totally abolishes the phosphorylation of CD44s. Alternative splicing and post-translational modification together result in a considerable variation in the composition and size of the CD44 molecules expressed on different cell types. For example, the predicted size of the CD44s core protein is 37-38 kDa [102-104,132]. The addition of *O*- and *N*-linked carbohydrate chains doubles the apparent molecular weight on gel, bringing it to 85-95 kDa [133]. Finally, addition of chondroitin sulfate further increases the size to 180-200 kDa [134].

3.3 CD44 expression pattern in normal tissues

CD44 proteins are widely expressed in various tissues of man. Immunohistochemical staining with antibodies against the standard domain of CD44 showed a strong reactivity with most hemopoietic and epithelial cell populations [135-138]. Only in a few tissues the expression of CD44 could not be detected, including the kidney (very weak), the islets of Langerhans, the acini of the pancreas, hepatocytes, adrenal glands and the ovaries.

The expression of CD44 proteins containing variant domains (CD44v) was studied by using monoclonal antibodies generated against specific variant domains. Staining results with these antibodies indicated that most of the variant domains show a tissue-specific expression pattern. The expression of the variant CD44 domains appeared to be mainly restricted to epithelial cells [136-138]. Tissues, like the stromal elements, connective tissue, blood vessels, muscles and the brain only showed expression of the standard isoform CD44s [98,135-137]. In

addition, cells of the hemopoietic system (B and T lymphocytes, granulocytes, monocytes and erythrocytes) mainly express the standard isoform CD44s [137,139].

The CD44 expression on hemopoietic cells appears to be dependent on the activation state. After activation with PHA, PMA or anti-CD3, an upregulation of CD44v9 and CD44v6 was seen on T cells [137,139]. The upregulation occurred within 24 hr and was transient, decreasing to pre-stimulation levels within a week. In contrast to mature T cells, thymocytes do not express CD44v9 or v6 at all [137]. Immunohistochemical staining of the thymus showed that CD44v molecules were only expressed by the epithelial cells within Hassall's Corpuscles (v4, v6 and v9). In the bone marrow, where the blood cell precursors are formed, only the plasma cells showed CD44v expression (v9 and v3) [137,138]. Similar to T cells, an upregulation of CD44v has also been observed in activated B cells and macrophages [121].

In epithelia, CD44v expression is often restricted to the generative epithelial cells in the basal cell layer [137,140]. Table 4 shows a compilation of the data that have been published about the differential expression of CD44s, -v9, -v6 and -v4 in epithelial cells of various human tissues. Most epithelial cells appear to express CD44v9, whereas fewer epithelial cells express the CD44v6 domain. The expression of CD44v4 appears to be even more restricted. In general, detection of CD44v9 paralleled the reaction with anti-CD44s [137,140], with the stomach, the small and the large intestine showing a less intense staining than most other epithelia [136,137,140]. The CD44v6 domain is predominantly expressed in squamous epithelia, like the skin (epidermis, hair follicles, sweat and sebaceous glands) and the oesophagus [137,140]. At a lower level, the CD44v6 domain was detected in the ducts of the mammary gland, ducts of the salivary gland, in the lung, tonsil, the Hassall's Corpuscles of the thymus and only very weakly in the urinary bladder, the prostate gland [137,140], the crypt epithelium of the gastrointestinal tract [141,142] and the thyroid gland [136]. Finally, the v4-containing isoforms were only detected in the epidermal layer and hair follicles of the skin, the oesophageal epithelium and the tonsil [137,140].

Table 4 Compilation of the data that have been published about the expression of CD44s, -v9, -v6 and v4 in human epithelial tissues.¹

Tissue type	CD44s	CD44v9	CD44v6	CD44v4
adrenal gland	-	-	-	-
brain	+ ²	-	-	-
endometrium	+++	++	-	-
epididymis	+++	+++	-	-
intestine (small-)	++(+)	+	-	-
intestine (large -)	++(+)	+(+)	-	-
kidney				
tubular region	(+)	(+)	-	-
liver				
bile ducts	++(+)	+++	-	-
hepatocytes	-	-	-	-
lung				
pneumocytes	+++	+++	+(+)	-
respiratory epith.	+++	+++	+	-
mammary gland	+++	+++	+	-
oesophagus	+++	+++	+++	+++
ovary	- ³	-	-	-
pancreas				
acini	-	-	-	-
ducts	++(+)	++(+)	-	-
prostate gland	+++	+++	+	-
salivary gland	+++	+++	(+)	-
skin				
epidermis	+++	+++	+++	+++
hair follicles	+++	+++	+++	+++
sebaceous glands	+++	+++	+++	-
sweat glands	+++	+++	+++	-
stomach	++(+)	+(+)	-	-
thymus	+++	+	-	-
Hassall's Corpuscles	+	++	+	+
thyroid gland	+++	++	-	-
tonsil	+++	+++	++	++
urinary tract, bladder	+++	+++	(+)	-
	+++	++	-	-

¹Immunohistochemical data based on results published by Mackay *et al.* [137] and Terpe *et al.* [140]. ²Located exclusively in the white matter Flanagan *et al.* [135]. ³Ovary follicular epithelium was scored +++ by Terpe *et al.* [140].

3.4 Molecular interactions of CD44

3.4.1 Interactions with the cytoskeleton

Several interactions of CD44 with the cytoskeleton have been described. Firstly, CD44 was shown to bind to the cytoskeleton component ankyrin, a molecule known to link transmembrane proteins with the underlying cytoskeleton [143,144]. The ankyrin binding site has been mapped to a particular 15 amino acid sequence in the long cytoplasmic domain of CD44 encoded by exon 19 (indicated in Fig. 5). The mapping was performed by screening of deletion mutants, by competition binding assays with a synthetic peptide of the ankyrin binding sequence and by fusion of the sequence to a trans-membrane protein incapable of binding ankyrin [145]. In addition to ankyrin, CD44 is also thought to interact indirectly with the actin-filaments. Immunoprecipitation studies and immunofluorescence co-localisation studies indicated that CD44 interacts with proteins located just beneath the plasma membrane, which are thought to be involved in the actin filament/plasma membrane association [146,147].

3.4.2 Interactions with the extracellular matrix

The extracellular matrix is a network of various macromolecules surrounding the cells and influencing their development, migration, proliferation, shape and metabolic functions. The macromolecules, which are mainly secreted locally by the cells in the matrix, can be subdivided into glycosaminoglycans and fibrous proteins. Glycosaminoglycans (*e.g.* hyaluronic acid (HA), chondroitin 4-sulfate, heparin and HS) are long unbranched negatively charged polysaccharide chains that attract cations, causing large amounts of water to be sucked into the matrix. In this way, a hydrated gel is formed that provides mechanical support to tissues while still allowing the diffusion of water-soluble molecules and the migration of cells. Large complexes of glycosaminoglycans and core proteins are present in the extracellular matrix. Fibrous proteins are embedded in the hydrated gel formed by the glycosaminoglycans. Two functional types can be distinguished, structural proteins (*e.g.* collagen, elastin) or adhesive proteins (*e.g.* fibronectin, laminin). Although in practice their functions show overlap, the structural protein fibers generally confer mechanical strength upon a tissue, whereas the adhesive fibers help cells to attach to the extracellular matrix by binding both to cells and to other macromolecules in the matrix.

CD44 proteins can interact with several macromolecules of the extracellular matrix. Firstly, CD44 proteins are able to bind to HA, a glycosaminoglycan that is found in variable amounts in all tissues and in the synovial fluid. In fact, HA seems to be the principal ligand of CD44 [88,89,99,100,102,104,148,149]. By truncation and site-directed mutagenesis, two clusters of basic residues could be identified in the extracellular domain of CD44 that appeared to be associated with HA-binding [150]. Both clusters are indicated in Fig. 5. Comparison of the HA-binding sites of various HA-binding proteins showed that this motif could be defined as B(X₇)B, where B is a basic amino acid (either arginine (R) or lysine (K)) and X is any non-acidic residue [151]. As indicated in Fig. 5, a third B(X₇)B motif is present in the membrane proximal part of the CD44 cytoplasmic tail. The N-terminal non-variant region of CD44, encoded by exon 1-5, contains 6 conserved cysteine residues, which can be used to form disulfide bonds. The three-dimensional structure of the N-terminal domain resulting from the formation of these disulfide bonds seems to be critical for the binding of HA [152].

The ability of CD44 to bind HA appears to be isoform dependent [125]. However, as transfection of the same CD44 cDNA into different cell lines confers HA binding properties upon some cell lines but not on others, there must also be some cellular factors that influence the ability of the CD44 molecule to bind HA [153,154]. Several lines of evidence indicate that clustering of CD44 in the plasma membrane plays a central role in the process of HA binding [154-157]. The concept is that a multivalent interaction of HA with several molecules of CD44 will have a higher affinity than that of a monovalent interaction [158,159].

Various experiments have shown that truncation of the cytoplasmic domain of CD44s reduces the ability to bind HA efficiently [145,155,160]. The absence of a cytoplasmic domain could be bypassed by artificial cross-linking of the CD44 receptor, which indicates that the cytoplasmic domain might be involved in clustering of the CD44 molecules [155-157]. There are several indications that clustering is induced by interactions of the cytoplasmic domain with the cytoskeleton [144,145,161], although not all data confirm this [154]. Possibly, the effect of the cytoplasmic domain and its interactions with the cytoskeleton are dependent on the cell type.

The carbohydrate side-chains of CD44 proteins can also influence the interaction with HA. The attachment of *O*-linked or *N*-linked carbohydrates can result in an increase or inhibition of the capacity to bind HA [133,154,162-165]. Most likely, the effect of carbohydrate chains depends on the site of addition.

With respect to CD44 clustering, glycosylation might prevent the formation of aggregates by charge repulsion or induce aggregation by charge attraction. However, carbohydrate side-chains could also alter the shape of the CD44 molecules or interfere with HA-binding by steric hindrance.

Finally, the composition of the variant domain has also been described to influence HA-binding [125]. The effect of alternative splicing can probably be ascribed to the resulting changes in protein glycosylation (Fig. 5) [162]. Interestingly, it has been shown that when different CD44v proteins are present on the same cell, they exclusively form homoaggregates [154].

Besides HA, CD44 also interacts with the extracellular fibrous proteins fibronectin, collagen (type I and VI) and laminin [94,95,166]. The adhesion to fibrous proteins seems to be mediated through the chondroitin sulfate sidechains, which are linked to some types of CD44 (Fig. 5). Removal of this chondroitin sulfate by enzymatic digestion abolished the capacity of purified CD44 to bind to collagen type I, laminin and fibronectin [166,167].

3.4.3 Other extracellular interactions

Another putative ligand for CD44 is Mucosal Vascular Addressin (MAd), a 58-66 kDa molecule isolated from murine mucosal vascular endothelial cells [168,169]. The process of lymphocyte homing is thought to be based on the binding of CD44s expressed on the surface of lymphocytes to MAd on specialized endothelial cells of high endothelial venules (HEV). Binding studies have shown that MAd directly interacts with affinity-purified human CD44s molecules [170]. The binding was shown to be saturable and could be blocked by anti-MAd and anti-CD44s. The isoform CD44E lacked this capacity [98,170]. The insert in the middle domain presumably prevents its interaction with MAd.

V3-containing CD44 isoforms have been implicated in the presentation of heparin-binding growth factors. The v3 domain contains a highly conserved SGSG motif (Fig. 5), that can be modified with HS [171]. *In vitro*, HS-modified CD44 isoforms appeared to be able to bind several HS-binding growth factors, like basic-fibroblast growth factor (b-FGF) and heparin binding-epidermal growth factor (HB-EGF). By pretreating the protein with heparitinase or by blocking with free heparin, this interaction could be eliminated [171]. In contrast to HS modifications, chondroitin sulfate modifications did not bind these growth factors. Finally, several other putative ligands of CD44 have been described, although their specific functions *in vivo* have not been determined yet [172-174].

3.5 Functional characterization of CD44 isoforms

Most functional studies of CD44 have focused on CD44s as it is the most widely expressed CD44 variant. A multitude of functions has been described for this CD44 variant and especially its role on lymphocytes has been studied intensively. The functions of other CD44 variants are largely unknown but their tissue-specific and cell state-dependent expression seems to indicate that they have their own specific functions. In this section, putative functions of CD44 are discussed.

3.5.1 The role of CD44 in the immune system

All types of hemopoietic cells (including erythrocytes, T and B lymphocytes, monocytes, macrophages, granulocytes and natural killer cells) preferentially express CD44s [139]. As noted above, the function of CD44s has been studied most intensively on lymphocytes. CD44s is thought to play an important role during lymphocyte hemopoiesis and on mature lymphocytes in homing and lymphocyte activation.

Already during the early stages of B and T cell differentiation, CD44s is strongly expressed. The expression of CD44s is lost during maturation, but again present on the more mature thymocytes and B-cells [175,176]. The expression of CD44s during the first steps of hemopoiesis in the bone marrow was shown to be critical for the differentiation of lymphoid cells [148,177]. Furthermore, the relatively high expression of the CD44s antigen in the earliest phases of T and B cell development is thought to be involved in the migration of bone marrow derived lymphoid precursors to their site of maturation [176].

One of the major functions of the isoform CD44s on mature lymphocytes is to mediate lymphocyte homing [91,92]. Lymphocyte homing is the process in which circulating lymphocytes migrate from the bloodvessel to the lymphoid tissue. One of the most important control points in this process are the HEVs (reviewed by Berg *et al.* [170]). Circulating lymphocytes recognize specialized endothelial cells of the HEV in lymph nodes, the mucosal associated lymphoid organs (Peyer's patches, appendix) and sites of inflammation (synovium) and selectively interact with these cells during their transit through the vessel wall into the surrounding lymphoid tissue. It seems that distinct organ-specific receptor systems exist for the homing of lymphocytes to each of these sites [178-180]. Whether CD44s regulates the homing of lymphocytes to one specific site is not totally clear at the moment [92,181]. From murine mucosal vascular endo-

thelial cells, a putative ligand of CD44s, termed MAd, has been isolated as already described in section 3.4.3 [168-170]. For the homing of lymphocytes to the lymphoid organs it has been suggested that this occurs via the interaction of CD44s with HA [99,125,155]. However, other groups could not confirm this [100]. Besides HA-dependent adhesion of lymphocytes to high endothelial cells, HA-dependent cell adhesion has also been observed to mediate the aggregation of macrophages [182] and the adhesion between stromal cells and lymphoid precursor cells in the bone marrow [148].

Besides being an adhesion molecule, CD44 also seems to function as a signal-transducing molecule on T cells and monocytes. The addition of anti-CD44s MAbs markedly enhances both CD2 and CD3 mediated activation of mature T cells [183-186]. *In vitro* assays showed that CD44 antibodies enhance CD2-mediated T cell triggering by 3 mechanisms. Firstly, anti-CD44 binding to monocytes induced monocyte IL-1 release, which is an important signal for T cell activation. Secondly, anti-CD44 enhanced the adhesion of T cells and monocytes in CD2 stimulated cultures. Thirdly, anti-CD44 binding to T cells elevated IL-2 production and the expression of the high affinity IL-2 receptor on the T cell surface [185]. Since the antibody probably mimics the specific interaction of a natural CD44 ligand, these results imply that CD44-mediated binding of T cells to endothelial cells or components of the extracellular matrix may induce or upregulate T cell activation *in vivo*. [183,185]. There is indeed some evidence that interaction between CD44 and HA in conjunction with CD3-mediated stimuli has a costimulatory effect on T cell proliferation and IL-2 release [187].

The activation of T cells by antigenic or mitogenic stimuli leads to a strong transient upregulation of CD44v9 and CD44v6 on normal human T lymphocytes [137,139]. These CD44 variants seem to have a specific function during T cell activation, since antibodies to these variant domains were shown to hinder T cell activation *in vivo* [121]. Although CD44v expression seems to be an early event in lymphocyte activation, the precise function of CD44v molecules expressed on human T cells is still unknown. Transgenic mice, which constitutively express rat CD44v4-v7 on their thymocytes and peripheral T cells, responded faster to activating stimuli. This indicates that CD44 variant isoforms might be involved in the process of signal transduction during T cell activation [188]. Similar to T cells, an upregulation of CD44v has also been observed in activated B cells and macrophages [121].

3.5.2 The role of CD44 in the skin

Besides their role in the immune system, the wide distribution of CD44 proteins indicates that they have specific functions in various other tissues. CD44 has indeed been implicated in a variety of physiologic events, including cell-cell adhesion, cell-matrix adhesion, HA metabolism, cell migration and cell proliferation. Most of these functions can be attributed to the interaction between CD44 and HA. Despite the abundant evidence of its involvement in multiple processes, the biological role of CD44 *in vivo* in various tissues remains to be determined. In this paragraph, the putative physiological role of CD44 in human tissues will be discussed, focusing especially on the function of CD44 in the skin in which large CD44 isoforms are expressed, including the variants CD44v2-v10 [189,190], CD44v3-v10 [110,114,190], CD44v4-v10 and CD44v6-v10 [190] (see also Chapter 4). Consequently, a high expression of the 5' located variant exons (e.g. v3, v4 or v6) is observed in this part of the body (Table 4, section 3.3).

As has been mentioned in section 3.4.3, the v3 domain of CD44 contains a HS attachment site and has probably a function in growth factor binding [171]. This suggests a role for CD44 in signal transduction and cell proliferation. Since the v3 domain is abundantly expressed in the human skin, it seems likely that CD44 plays an important role in the proliferation of keratinocytes [136,171]. Experiments with transgenic mice that had manipulated low levels of CD44 expression on their keratinocytes, support this putative function of CD44 [191]. The CD44 expression in these mice was downregulated by the expression of an antisense CD44 cDNA driven by the keratin-5 promoter. These transgenic mice showed a delayed wound healing, and injection of bromodeoxyuridine (BrdU) indicated that this was due to a reduced keratinocyte proliferation in the wound. A reduction of cell proliferation was also observed for the hair follicle keratinocytes, resulting in slower regrowth after hair removal. *In vitro* experiments showed that, in contrast to keratinocytes of control mice, the keratinocytes of transgenic mice were defective in their response to the mitogen TPA and the growth factors bFGF and HB-EGF, which are known ligands of CD44v3 (section 3.4.3). For TPA this was also shown by *in vivo* experiments. Besides mitogenic stimuli and growth factors, also incubation with low concentrations of HA caused a slightly increased proliferation of normal murine keratinocytes. In contrast, keratinocytes from transgenic mice showed an impaired proliferative response to exogenous HA. This indicates that the interaction between CD44 and HA plays a role in keratinocyte proliferation as well.

In addition to cell proliferation, CD44 may play a role in cell migration. Cell migration is especially important during processes like embryogenesis [192] and wound healing [193]. Cells are thought to migrate by synthesizing new extracellular matrix, binding to this matrix, and then degrading the matrix. During the process of cell migration, CD44 seems to be involved in the degradation of HA [192]. This multistep process involves HA-binding, internalization and the subsequent degradation by lysosomal enzymes. Antibodies to CD44s were shown to prevent both the binding of HA to the cell surface and its subsequent uptake and degradation. In addition, agents such as chloroquine and NH₄Cl, which block the activity of lysosomal enzymes, prevented the breakdown of HA [192]. Besides HA [194-196], several types of collagen seem to promote the adhesion and migration of cells via CD44 [167,197-199].

CD44-mediated HA degradation indeed seems to take place in the skin. The selective suppression of CD44 in keratinocytes of mice, described by Kaya *et al.* [191], resulted in a loss of HA in the interkeratinocyte spaces. In addition, an abnormal accumulation of HA in the superficial dermis and corneal stroma was observed. Culturing of keratinocytes from dorsal skin of control and transgenic mice in the presence of fluorescein-tagged HA revealed cell surface binding and internalization of HA by normal but not by CD44 negative transgenic keratinocytes. Despite the inability of CD44 negative keratinocytes to bind and internalize HA, the cells were still able to synthesize HA [191]. As described above, the delayed wound healing observed in the transgenic mice was shown to be caused by a defective keratinocyte proliferation. In addition, a reduced skin elasticity, resulting from the defective HA homeostasis, seemed to be an inhibiting factor by increasing the size of the wound. Whether an impaired migration of keratinocytes also contributed to the delayed wound healing has not been determined yet.

Finally, several lines of evidence suggest that the interaction between CD44 and the extracellular matrix component HA plays a role in divalent cation-independent cell aggregation (reviewed by Underhill [200]). As already described in section 3.5.1, CD44s mediated HA-dependent cell-cell interactions are thought to take place between hemopoietic cells or between hemopoietic and non-hemopoietic cells [99,125,148,155,182]. Similarly, this kind of interactions have also been described to occur between non-hemopoietic cells using CD44v. Milstone *et al.* showed that transfection of the keratinocyte CD44 variant epican (CD44v3-v10) in CD44 negative L cells resulted in a self-aggregating phenotype that was

only observed in the presence of HA [201]. The aggregation occurred in the absence of divalent cations and was inhibited by hyaluronidase or by an anti-CD44v6 MAbs. Results of Hudson *et al.* [190] also indicated that CD44v participates in cell-cell interactions among keratinocytes. Whether these *in vitro* observations, which imply an adhesive function of epican in intact epidermis, indeed match the biological role of this variant is not known.

3.5.3 Origin and function of soluble CD44

Besides their expression on cell membrane surfaces, CD44 proteins are also present in body fluids. Already in 1980, Dalchau *et al.* [81], found evidence for the presence of soluble CD44s in serum. This observation was later confirmed by others [84,98,202]. Besides in serum, the presence of soluble CD44 has also been described in synovial fluid [203]. Soluble CD44 proteins were shown to lack the cytoplasmic domain [204], resulting in a molecular weight difference of about 15 kDa with the membrane bound forms [202,205]. The main protein detected in human serum has a molecular weight of about 70-80 kDa [202,205]. Since the CD44 protein that is released by *in vitro* cultured lymphocytes appeared to be of identical size, soluble CD44 is thought to have its main origin in lymphocytes [205,206]. Besides the small main protein, probably representing tailless CD44s, several larger forms of 100-150 kDa have been detected in normal human serum [205,207,208]. At least several of these larger forms seem to originate from the variant isoforms, since variant domains have been detected in normal human serum [207-212,214] (Table 6, section 3.6.3). However, variations in protein glycosylation and the addition of chondroitin sulfate sidechains are also likely to attribute to the observed size differences. The origin of the 100-150 kDa soluble CD44 proteins has not been determined yet, although granulocytes [205] and activated lymphocytes [208] have been mentioned as a possible source.

Circulating CD44 might simply represent the products of normal catabolism. However, it is rather uniform in size and molecular weights of less than 80 kDa have never been detected. This, in addition to the relatively high CD44 serum levels of about 500 ng/ml [207-212,214] (Table 6, section 3.6.3), suggests that it might have functional significance. In addition, serum levels of soluble forms have been described for several other adhesion molecules, for example the intercellular adhesion molecule-1, vascular cell adhesion molecule-1 and E-selectin (reviewed by Gearing and Newman [215]). The physiological role of these circulating soluble adhesion molecules is also still unknown. It has been

shown that circulating CD44 is functionally active with respect to its binding to HA and fibronectin [204,216]. However, *in vivo* experiments with mice indicated that under normal conditions soluble CD44 is not associated with HA [216]. The circulating CD44 seems to be monomeric and not (firmly) associated with other proteins.

Whether soluble CD44 is shed or excreted by cells is not known at the moment. Some evidence for a mechanism of CD44 excretion is provided by the observation of a new alternatively spliced exon in mice [217]. This 93 bp exon, located between exons 13 (v9) and 14 (v10), contains a stop codon after the 12th amino acid in the predicted peptide sequence. However, the mRNA transcripts containing the new exon seem restricted in their expression and have only been observed in cultured murine G8 myoblasts and *in vivo* in embryonic muscle and cartilage tissues. In humans, this additional exon has not been detected until now. In contrast to the murine situation, exon v1 of the human CD44 gene contains a stop codon and could therefore give rise to the formation of a short soluble CD44 protein. However, no v1-containing CD44 transcripts have been detected in man until now.

There are also several indications that soluble CD44 proteins are generated by proteolytic cleavage. A trypsin-type proteolytic cleavage site, represented by an arginine dipeptide motif, has been identified in exon 14 (v10) [108] (indicated in Fig. 5). In addition, studies involving the release of CD44 from cultured cells indicate that several protease inhibitors, especially inhibitors of metalloproteases and serine proteases, are able to decrease the amount of CD44 released from the cell surface [218,219].

The mechanism regulating enzymatic cleavage is unknown. *In vitro* and *in vivo* experiments suggest that the natural ligands trigger the release from the membrane. Binding to its natural ligand may change the conformation of CD44, exposing the cleavage site for one or more enzymes [220]. For example, *in vitro* experiments have shown that the surface expression of CD44 can be modulated by anti-CD44 antibodies. The treatment of cultured neutrophils and lymphocytes with antibodies against CD44 resulted in a diminished surface expression of CD44s on both of these cell types and elevated levels of soluble CD44s in their culture medium [205]. In addition, intravenous injection of anti-CD44 MAbs in mice caused CD44 release from certain lymphocyte populations [221].

CD44 protein release has been postulated to have a function in lymphocyte homing [205]. It seems that lymphocytes trafficking into lymphoid organs have in

general a high CD44 surface expression, while the CD44 surface expression of lymphocytes leaving the lymphoid organs is mainly low [222]. This might indicate that CD44 release is induced upon interaction with the high endothelium, regulating the trafficking of lymphocytes through the high endothelial venules. One possible explanation might be that soluble CD44 is released to allow the detachment of cells bound to a ligand such as HA. Another hypothesis is that soluble CD44 functions as competitive inhibitor of the transmembrane receptor, as has been suggested for some other cell adhesion molecules [215,223,224].

3.6 CD44 expression in tumors

3.6.1 Metastasis-inducing CD44 variants (rat model)

In an attempt to clone metastasis-associated surface antigens, Günthert *et al.* [109] made the first observation of a potential correlation between CD44 expression and tumor metastasis in an experimental rat tumor system. The approach was based on the generation of monoclonal antibodies against membrane proteins that were expressed by the metastatic rat pancreatic carcinoma cell line BSp73ASML [225]. Antibodies that were incapable of recognizing the non-metastatic rat pancreatic carcinoma cell line Bsp73AS, a cell line derived from the same tumor as the cell line BSp73ASML, were selected and used to screen a bacterial cDNA expression library. A cDNA clone called pMeta-1 was isolated, which appeared to encode a new CD44 isoform containing the variant exons v4-v7 and lacking exon 15. Overexpression of pMeta-1 in the nonmetastatic BSp73AS cells appeared to be sufficient to establish full metastatic behavior [109]. In 1993, Rudy *et al.* [116] described the presence of a second CD44 variant on the metastatic rat pancreatic carcinoma cell line BSp73ASML, that was able to confer metastatic properties upon the nonmetastatic tumor cell line BSp73AS. This cDNA clone, designated pMeta-2, encoded the variant CD44v6-v7 without exon 15. Intravenous injections of a MAb recognizing the v6 domain of both CD44 variants, appeared to inhibit or prevent metastasis formation in the rat system [226,227]. These injections were only efficient when applied before the establishment of metastatic colonies. However, the CD44 variants did not seem to play a role in tumor cell invasion, since experiments with radioactively labeled tumor cells showed that comparable numbers of tumor cells reached the draining lymph nodes in rats, irrespective whether injected with anti-v6 MAb or not.

Therefore, the CD44 variants pMeta-1 and pMeta-2 rather seem to play a role in the outgrowth of tumor cells [227].

The observations made with the experimental rat system initiated a whole new direction for research. Since then, many research groups have focused on the role of CD44 in human tumor progression and the process of metastasis formation. Especially CD44 variants containing the v6 domain were extensively studied, due to the observation that an anti-v6 MAb (1.1ASML) was able to block metastasis formation in the rat model. Numerous tumor types were investigated by immunohistochemistry and reverse transcriptase-polymerase chain reaction (RT-PCR) to find CD44 splice variants related to metastatic behavior of cells and several follow-up studies were performed to find a correlation between the level of CD44v6 expression and patient-survival. This research line was further substantiated by the observation of various groups that most normal tissues hardly express CD44v6 and that a gain in CD44v6 expression causes tumor cells to disseminate. Based on these results, predictions were made about the applicability of CD44 for the development of new therapeutic strategies and the use of CD44 as a prognostic marker.

3.6.2 CD44v expression in various tumor types

The expression of CD44 variants has been studied in a wide range of tumor types. For this purpose, a large panel of monoclonal antibodies directed against epitopes encoded by the variant exons has become commercially available, facilitating the study of CD44v expression. However, immunohistochemical staining only provides partial information, as it does not allow the discrimination between different splice variants. Therefore, RT-PCR analysis is often performed in addition to immunohistochemistry, providing an accurate analysis of the CD44 alternative splicing pattern.

Using immunohistochemical analysis, an upregulation of the v6 domain has indeed been observed in several types of primary human tumors, including colon carcinoma, breast carcinoma, high grade lymphoma, gastric carcinoma, cervix carcinoma, vulva carcinoma and kidney carcinoma (Table 5). For colon carcinoma, also correlations have been observed between the level of CD44v6 expression and the Dukes stage [233,235,236,262]. In addition, a few groups described that metastases show even a higher CD44v expression than primary tumors [228,229]. The indications for involvement of CD44v6 in tumor progression and metastasis formation became even stronger, as for several of these

Table 5 Immunohistochemical detection of CD44 in various human carcinomas compared to the expression in normal tissues.

Tumor type	CD44 expression	References
breast carcinoma	v3 ↑	[228]
	v5 ↑	[228,229]
	v6 ↑	[228,229]
	v7,8 ↑	[229]
cervix carcinoma	v6 ↑	[230]
	v7,8 ↑	[231,232]
colon carcinoma	v5 ↑	[233,234]
	v6 ↑	[233-238]
	no change	[141]
endometrium carcinoma	CD44v ↓	[239]
gastric carcinoma	v5 ↑	[240-242]
	v6 ↑	[240,242,243]
	v9 ↑	[244,245]
kidney carcinoma	v6 ↑	[246]
	v9 ↑	[246]
	v10 ↑	[247]
lymphoma (high grade)	v3 ↑	[248]
	v6 ↑	[138,139,248,249]
melanoma	v5 ↑	[250]
	v10 ↑	[250]
multiple myeloma	v9 ↑	[251]
neuroblastoma	CD44s ↓ no CD44v	[127,252]
pancreatic carcinoma	v5 ↑	[253]
prostate adenocarcinoma	CD44v ↓	[254]
small cell lung carcinoma	no CD44	[123,255-257]
urothelial and bladder carcinoma	CD44v ↓	[258-260]
vulva carcinoma	v6 ↑	[261]

tumor types Kaplan-Meier curves indicated that the CD44v6 expression level was correlated with overall patient survival. This was found for colon carcinoma [234,236], breast carcinoma [228,229], cervix carcinoma [231], vulva carcinoma [261] and non-Hodgkin's lymphoma [138,249]. Based on these findings, it was suggested that CD44v6 expression could be a valuable prognostic marker for the progression of these tumor types.

Unfortunately, results were not always consistent. For example, doubts about the involvement of CD44v6 in the process of metastasis formation were raised by the observation that not only the metastatic colon carcinomas but also non-invasive adenomas expressed the v6 domain, indicating that the v6 domain is not directly associated with metastasis [235,237,263,264]. The role of CD44v6 in tumor invasion became even more doubtful when Finke *et al.* [235] reported that the domain is preferentially downregulated in distant metastases of colon carcinomas when compared with primary tumors. In addition, Gotley *et al.* [141] even stated that the CD44v6 expression in colon carcinoma and normal colon mucosa is identical [141]. Also the correlation between the CD44v6 expression level and patient survival is still uncertain, since these results could not be reproduced by several other groups, *e.g.* for colon [265] and breast carcinoma [122,266].

In addition to CD44v6, the overexpression of several other variant exons has been described to be important for metastasis formation of human tumors (Table 5). However, an elevated CD44v expression does not necessarily correlate with the tumor's progression or metastatic capacity. In some tumors CD44v expression is reported to be downregulated, for example in endometrium carcinomas [239], prostate adenocarcinomas [254] and urothelial and bladder carcinomas [258-260]. In addition, no expression of CD44v could be detected in neuroblastoma, and the aggressiveness of these tumors appeared to be correlated with repression of CD44s expression [127,252]. In highly metastatic small cell lung cancer practically no CD44 expression could be detected [123,255-257] (Table 5).

From RT-PCR experiments it has been concluded that elevated CD44v levels in tumor cells are caused by an disorganized splicing mechanism. When using primers flanking the variant region, tumors appeared to yield a much more complex pattern of amplification products than the corresponding normal tissues. This has been described for various human tumors, such as breast cancer [142,267-269], colon cancer [142,264,267,269-272], gastric carcinoma [240,241,273], cervical cancer [232], aggressive and metastatic non-Hodgkin lymphoma [138,139] and

bladder carcinoma [142,274,275]. It is assumed that the whole spectrum of splice variants can be generated by tumor cells, due to a disorganized splicing mechanism. In this way, also metastatic CD44 isoforms can be generated, giving the tumor cells the opportunity to metastasize. The data also suggest that RT-PCR might be a sensitive method for the detection of tumor cells in small clinical specimens by amplification of abnormal alternative CD44 splice variants [267]. Besides aberrantly spliced transcripts, also incomplete processing of CD44 transcripts has been observed in tumors, resulting in the retention of introns. Intron 9 was shown to be often retained in bladder carcinoma [128] and adenocarcinomas of the digestive tract [129,276,277] and may therefore be a helpful marker for the diagnosis of these tumors. For patients with bladder cancer the retention of intron 9 might be applicable for the detection of exfoliated cancer cells in urine [128].

3.6.3 Soluble CD44 as a tumor marker in serum

Knowledge about the release of soluble CD44 proteins and the fact that several tumor types show an increased CD44v expression, raised the question whether CD44 released by tumor cells could be used as a simple new diagnostic tool to assess tumor load and metastases in patients [213]. Various reports have been published about soluble CD44 molecules and their clinical significance. Using exon-specific enzyme-linked immunosorbent assays (ELISAs) that have recently been developed and which are commercially available, serum levels have been studied in patients with different types of tumor. Table 6 shows an overview of most of the data that have been published until now. For some tumor types, elevated CD44 serum levels were indeed observed (e.g. B cell chronic lymphocytic leukemia, node positive breast cancer, gastric cancer and lymphoma; see Table 6). Elevated levels were shown to correlate with tumor burden, metastasis formation, or the response to treatment. However, for other tumor types soluble CD44 levels were found to be identical to or even lower than those observed in control persons (e.g. ovarian, pancreatic, prostatic, bladder and renal cancer; see Table 6).

The observation that patients with ovarian cancer did not show an elevation of soluble CD44s, CD44v5 or CD44v6, could be explained by the low expression of these CD44 isoforms in malignant ovarian tumors. In this case, the serum CD44 production by hemopoietic cells probably overrules the production by ovarian tumor cells [214]. Besides the expression level of CD44 variants, also

Table 6 Overview of the serum levels of soluble CD44s, CD44v5 and CD44v6 in patients (P) with various types of cancer compared to those of healthy control persons (C).

Type of cancer		CD44s ¹ (ng/ml)			CD44v5 ¹ (ng/ml)			CD44v6 ¹ (ng/ml)		
		P	C		P	C		P	C	
B cell chronic lymphocytic leukemia	n=122 (P); n=48 (C) [207]	+	750±350	478±133	0	nr ²	39±20	0	nr	154±55
bladder cancer	n=19 (P); n=30 (C) [211]	0	443±124	501±87	-	43±24	54±23	0	151±62	179±64
breast cancer (node positive)	n=14 (P); n=30 (C) [212]	0	430±30	420±30	+	46±10	24±3	+	250±50	154±13
cervical cancer	n=44 (P); n=? (C) [209]	0	644±284	568±207 ³	0	53±27	51±23 ³	+	227±90	199±135 ³
colon cancer	n=25 (P); n=43 (C) [213]	+	nr	nr	nr	nr	nr	nr	nr	nr
	n=30 (P); n=30 (C) [208]	0	723±45	700±50	nr	nr	nr	0	190±21	221±21
(advanced) gastric cancer	n=25 (P); n=30 (C) [213]	+	nr	nr	nr	nr	nr	nr	nr	nr
	n=32 _{st} , 41 _{v5} , 35 _{v6} (P);									
	n=10 (C) [210]	0	270±22	289±18	+	69±6	25±2	+	217±33	148±3
	n=20 (P); n=30 (C) [208]	- ⁴	574±47	700±50	nr	nr	nr	-	141±22	221±21
lymphoma	n=25 (P); n=12 (C) [206]	+	510	15	nr	nr	nr	+ ⁵	nr	nr
ovarian cancer	n=22 (P); n=? (C) [214]	0	468±138	443±124	0	15±12	35±13	0	111±47	170±54
pancreatic cancer	n=93 (P); n=30 (C) [208]	-	515±18	700±50	nr	nr	nr	-	117±11	221±21
prostate cancer	n=49 (P); n=30 (C) [211]	0	475±119	501±87	-	36±20	54±23	0	173±62	179±64
renal cancer	n=18 (P); n=30 (C) [211]	-	399±145	501±87	-	34±19	54±23	0	160±59	179±64

¹Serum levels of patients (P) and healthy controls (C) in ng/ml as determined by ELISA. Indicated is whether patient levels are higher (+), equally high (0) or lower (-) than those of healthy control persons. ²Not reported (nr). ³Patients with a complete remission. ⁴According to the authors this was not significantly different. ⁵Slight elevation.

the draining of the tumor is expected to determine the contribution of the tumor to the total level of soluble CD44 in the circulation.

The significantly lower serum levels that were observed in patients with bladder, pancreatic, prostatic and renal cancer, are more difficult to explain [208,211,278]. Actually, these results indicate that other factors should be involved. It has been shown that serum concentrations of CD44s, CD44v5 and CD44v6 are not age or sex dependent [278,279]. However, there are some indications that the activity of the immune system influences the levels of soluble CD44. Soluble CD44s levels were shown to be significantly reduced in immunodeficient mice and significantly increased in murine models of autoimmune disease [216]. In addition, Guo *et al.* [280] observed HIV-induced loss of CD44s in a monocytic cell line. Gansauge *et al.* [208] found decreased levels of soluble CD44v6 in septic patients who are known to be immunosuppressed. And finally, in pancreatic carcinoma patients who developed autoantibodies against mutant p53 showing immunoreactivity against the tumor, soluble CD44v6 levels were significantly higher than in patients without anti-p53 autoantibodies [208]. Consequently, infections and inflammatory conditions are also expected to be of influence. On the other hand, patients with lymphoproliferative diseases like common viral infections of the upper respiratory tract, mononucleosis, or chronic rheumatic diseases do not seem to have elevated levels of circulating CD44 [206,213]. Also smoking has been recognized to be an important influencing factor [279]. About 35% of the biological variability of soluble CD44v5 and CD44v6 serum levels could be explained by smoking habits. The influence of smoking on the serum level of soluble CD44s has not been determined. It was hypothesized that the smoking-effect is due to chronic bronchial inflammation. Of course, influences like infections and smoking habits would considerably diminish the diagnostic specificity of soluble CD44. Whether soluble CD44 can indeed be used as a prognostic marker in certain tumor types remains to be seen.

4 Aim and outline of this thesis

Identification and molecular characterization of tumor-associated antigens can be helpful to improve the current treatment of patients with head and neck squamous cell carcinoma, to develop novel methods for tumor detection and detection of minimal residual disease as well as to obtain more insight into the process of carcinogenesis. MAb U36 recognizes a surface antigen highly expressed on HNSCC cells. Clinical RIS and biodistribution studies have shown that the MAb U36 defined antigen is a suitable target molecule for antibody-based therapy of HNSCC. The aim of this thesis is the identification and molecular characterization of the MAb U36 defined antigen. The subsequent possibilities for diagnosis and therapy, and its association with malignant progression are addressed. **Chapter 2** deals with the identification of the MAb U36 defined antigen and the mapping of the epitope recognized by MAb U36. As the antibody is shown to recognize a CD44 splice variant, a literature survey about the CD44 protein family is provided in the introduction section. **Chapter 3** focuses on amino acid variations that have been observed in the epitope recognized by MAb U36. The basis of this sequence variation and the influence on the binding affinity of MAb U36 are presented. **Chapter 4** describes the identification of CD44 variants expressed in HNSCC and normal oral mucosa that might be recognized by MAb U36. The role of these CD44 isoforms in progression and metastasis of HNSCC is discussed. In addition, in **Chapter 5** the role of these variants in the progression of colon, breast and lung carcinomas is investigated and discussed. **Chapter 6** addresses the question whether soluble CD44 proteins in plasma of patients can be used for HNSCC detection. CD44v6 plasma levels of HNSCC patients and control persons are compared by ELISA and a further characterization of the soluble CD44v6 variants is performed by immunoprecipitation. In **Chapter 7** results described in this thesis are summarized and discussed, while future perspectives are outlined.

Chapter 2

Monoclonal antibody U36, a suitable candidate for clinical immunotherapy of squamous cell carcinoma, recognizes a CD44 isoform

Nicole L.W. van Hal

Guus A.M.S. van Dongen

Ellen M.C. Rood-Knippels

Paul van der Valk

Gordon B. Snow

Ruud H. Brakenhoff

Published in: *Int. J. Cancer* 68:520-527 (1996)

Abstract

At present, tumor targeting with monoclonal antibodies (MAbs) is among the most promising novel adjuvant therapy modalities for the treatment of patients with minimal residual disease of head and neck squamous cell carcinoma (HNSCC). For this purpose, we developed MAb U36, recognizing a 200 kDa antigen expressed on the outer cell surface of squamous cell carcinomas and their normal counterparts. Clinical radioimmunoscinigraphy (RIS) and biodistribution studies have shown that the MAb U36 defined antigen is a suitable target molecule for antibody-based therapy of head and neck cancer. In this Chapter, we describe further characterization of the antigen by cDNA cloning. The cDNA was isolated by expression cloning in COS-7 cells. Sequence analysis and database searching revealed that the MAb U36 defined antigen is identical to the squamous cell specific CD44 splice variant epican. The epitope recognized by MAb U36 was mapped by screening overlapping synthetic peptides of the epican-specific region encoded by exon 7-11 (v3-v7), and appeared to be located in the v6 domain. The applicability of MAb U36 for targeting human tumors of various origin expressing the CD44v6 domain is discussed.

Introduction

Squamous cell carcinoma is the major histological type among tumors of the head and neck. The early stages are treated with either surgery or radiotherapy, and advanced stages with combined surgery and radiotherapy. In patients with advanced disease (stage III and IV), locoregional recurrences develop in 50 to 60% of the cases after primary therapy and 15 to 25% of the patients develop distant metastases [75]. The actual incidence of distant metastases in HNSCC patients is probably even higher since autopsy studies report an incidence of 40 to 57% [75]. These data indicate that there is an urgent need for an effective adjuvant therapy for the eradication of (minimal) residual disease after initial treatment, to prevent the eventual development of locoregional recurrences and/or distant metastases. The high expectations raised by chemotherapy have not been fulfilled, and its application is in general limited to palliation. We therefore have decided to exploit the tumor targeting capacity of monoclonal antibodies for delivery of radionuclides to the remaining tumor deposits. A panel of MAbs directed against squamous cell carcinoma associated antigens was selected by *in vitro* techniques and evaluated in *in vivo* models of tumor bearing nude mice [75]. The antibodies selected by this procedure were tested in RIS and biodistribution studies in patients with HNSCC [75,79]. MAb U36 appeared to be the most promising antibody for specific targeting of HNSCC in patients. Immunohistochemical evaluation showed that in 188/196 (96%) of the HNSCC tumors at least 50% of the tumor cells were intensely stained by MAb U36, indicating that the antigen is very homogeneously expressed [71]. Moreover, extensive biodistribution and RIS studies in HNSCC patients have shown that ^{99m}Tc -labeled U36 IgG accumulates selectively and to a high level in these tumors [79], and during a follow-up of 3 years no adverse reactions have been observed. These data showed that the MAb U36 defined antigen is a suitable target molecule for antibody-based adjuvant therapy of squamous cell carcinoma of the head and neck. The antibody recognizes a 200 kDa cell surface antigen highly expressed by human normal squamous epithelia and squamous cell carcinomas of distinct sites of origin: head and neck, lung, esophagus, cervix and epidermis [58]. The abundant expression of the target antigen in normal human squamous epithelia, *i.e.* mucosa and skin, is not an absolute restriction for radioimmunotherapy (RIT), since only a slight uptake of MAb U36 in the oral mucosa has been observed in biodistribu-

tion studies [79]. The suitability of this specific antigen as a target molecule for immunotherapy, confirmed by extensive clinical RIS studies, justified further identification of the antigen.

Materials and methods

Cell culture

UM-SCC-11B (kindly provided by dr. T.E. Carey, Ann Arbor, MI) and COS-7 cells were cultured under 5% CO₂ at 37°C in Dulbecco's modified Eagle's medium (DMEM; Gibco Life Technologies, Breda, The Netherlands) supplemented with 2 mM L-glutamine, 16 mM NaHCO₃, 5% fetal calf serum (FCS; Hyclone Laboratories, Logan, UT), 1% penicillin, 1% streptomycin and 15 mM HEPES, pH 7.4.

Western blot analysis

Antigen was isolated from UM-SCC-11B cells essentially as described for the MAb E48 defined antigen [281], with a few minor modifications. First, 1% Nonidet P-40 was used as detergent instead of 1% *n*-octyl- β -D-glucoside. Second, after ultracentrifugation the supernatant was directly incubated with the immuno-absorbative. Finally, the acetone-methanol precipitation was omitted. The proteins were separated by sodium dodecyl sulfate polyacrylamide gel electrophoresis (SDS-PAGE) on a 5% gel and transferred to nitrocellulose membrane (Schleicher & Schuell, Dassel, Germany). The free binding sites were blocked by incubation of the blot in 1% bovine serum albumin in phosphate buffered saline (1% BSA/PBS) for 1 hr [282]. Subsequently, the filter was incubated for 1 hr with 1×10^5 cpm/ml ¹²⁵I-labeled MAb U36 in 1% BSA/PBS [58]. Unbound MAb was removed by washing three times with 0.05% Tween-20 in PBS for 5 min, and bands were visualized by autoradiography for 24 to 64 hr using intensifying screens. Alternatively, the antigen was stained by alkaline-phosphatase anti-alkaline-phosphatase (APAAP), as described by Brakenhoff *et al.* [281].

Construction of the cDNA library

Construction of the cDNA library in shuttle vector pCDM8 by use of non-selfcomplementary *Eco*RI/*Bst*XI adaptors (Invitrogen, Leek, The Netherlands) and the subsequent transformation into *E. coli* K12 MC1061/P3 by electroporation have been described previously [281].

DNA isolation, COS cell transfection, immunocytochemistry and Hirt extraction

Plasmid DNA was isolated according to the miniprep method based upon alkaline lysis [282] or using the QIAprep-spin Plasmid Kit (Westburg, Leusden, The Netherlands), according to the supplier's instructions. From DNA isolated by the miniprep method the RNA was removed by RNase A digestion, phenol extraction and ethanol precipitation [282].

COS-7 cells were transfected using the Profection Mammalian Transfection System-DEAE-Dextran (Promega, Leiden, The Netherlands) and stained immunocytochemically 2 days after transfection as described previously [281].

Scraping of positively stained COS cells from the culture dish, Hirt extraction of plasmid DNA and electroporation into *E. coli* K12 MC1061/P3 was performed as described previously [281].

Library screening by progressively smaller pools of bacterial colonies

The U36-encoding clone was isolated by screening progressively smaller pools of bacterial colonies from the cDNA library. The pools were prepared as follows: the frozen glycerol cultures of the library were titrated and a distinct number of colonies was inoculated in Luria-Bertani medium [282] supplemented with 40 μ g/ml kanamycin, 7.5 μ g/ml tetracyclin (both from Boehringer Mannheim, Almere, The Netherlands), and 12.5 μ g/ml ampicillin (Sigma, Bornem, Belgium) and grown overnight. Frozen glycerol cultures were prepared and plasmid DNA was isolated and transfected into COS-7 cells. After immunocytochemical staining using MAb U36 as first antibody, the library fraction with the most positive COS cells was selected and used for the next fractionation round. In the first step, 7×10^5 clones were screened. The screening was repeated for 8 cycles until the clone containing the U36-encoding cDNA could be isolated. Detailed protocols are available upon request.

DNA sequencing

The U36 cDNA clone in pCDM8 was cut with *Pst*I and subcloned in the *Pst*I site of pUC19. The obtained subclones were partially sequenced, using the Sequenase version 2.0 DNA Sequencing Kit (USB, Cleveland, OH) or using the DyeDeoxy Terminator Cycle Sequencing Kit on an Applied Biosystems 373A DNA Sequencer (Applied Biosystems, Maarssen, The Netherlands).

Construction of the *epican*^{U36} clone

To obtain other *epican*-encoding clones, the cDNA library was rescreened by colony hybridization [282], using the U36 cDNA clone as a probe.

A full-length *epican* clone was constructed from the incomplete *epican* clone designated 'clone 54', missing exons 1-4, and the U36 cDNA clone. The *Eco*RV site within the U36 cDNA and the *Hind*III site within the polylinker of pCDM8 were used to replace the 530 bp *Eco*RV/*Hind*III fragment of *epican* clone 54 by the 1320 bp *Eco*RV/*Hind*III fragment of the U36 cDNA clone. The resulting clone was designated *epican*^{U36} (Fig. 1).

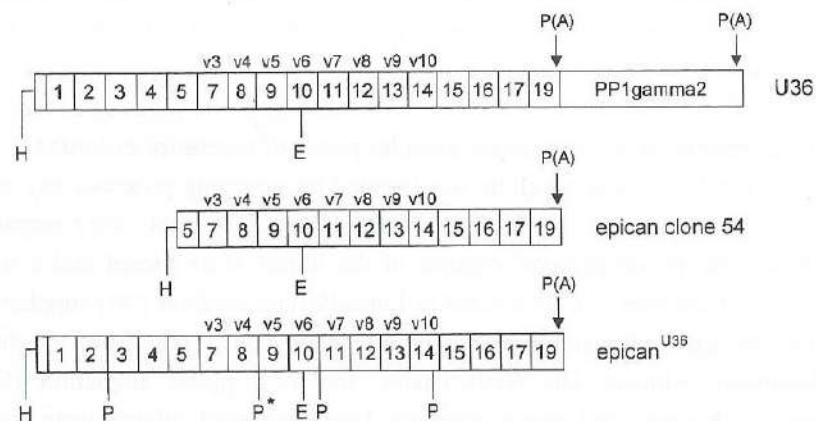


Figure 1 Physical map of the U36 cDNA clone and the *epican*^{U36} construct. The *epican*^{U36} construct was built from the originally isolated U36 clone and *epican* clone 54 by swapping the 5' *Hind*III (H)/*Eco*RV (E) fragments, as described in 'Materials and methods'. Note that the *Pst*I (P) restriction pattern of the *epican*^{U36} clone is slightly different from the one described by Kugelman *et al.* [114]. An alternative splice acceptor site in intron 8 (shifted 3 bases upstream) results in an additional *Pst*I site, indicated with an asterisk, in the cDNA sequence [115]. P(A) indicates the presence of a poly(A) tail in the sequence. Exons are represented by a box and numbered according to Screaton *et al.* [115].

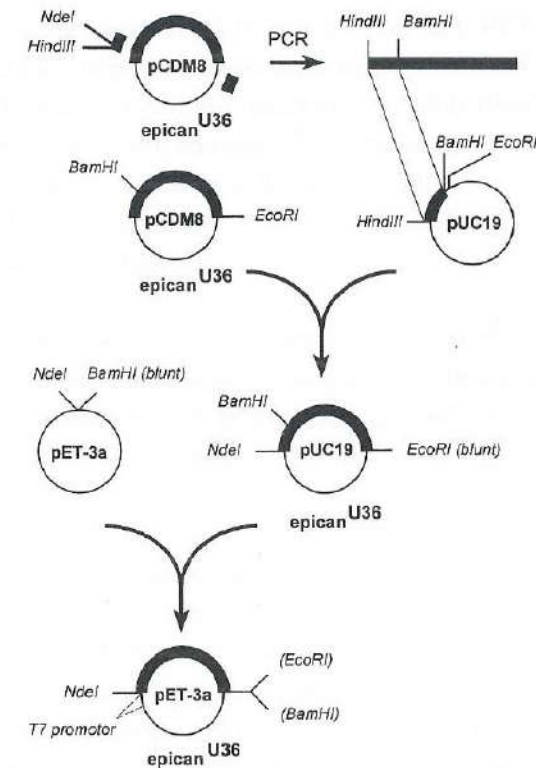


Figure 2 Construction scheme of the *epican*^{U36} clone in pET-3a. The *epican*^{U36} sequence from exon 2-19 was inserted behind the T7 promoter in pET-3a. Details are described in 'Materials and methods'.

Expression of *epican*^{U36} in *E. coli*

A gene expression system based on bacteriophage T7 RNA polymerase was used to express *epican*^{U36} in *E. coli* [283]. The *epican*^{U36} sequence from exon 2-19 was inserted behind the T7 promoter in pET-3a. The construction of this clone is illustrated in Fig. 2. The *epican* sequence from exon 2-19 was amplified by polymerase chain reaction (PCR) using the sense primer 5'-TGTGAAGCTTC-ATATGTTGAATATAACCTGCCGC-3' located in exon 2 [115], and the pCDM8 reverse primer (Invitrogen). *Nde*I and *Hind*III restriction sites were added at the 5' end of the sense primer to facilitate the cloning steps and to introduce the ATG start codon. The PCR product was cut with *Hind*III (primer) and *Bam*HI (internal) and the 210 bp fragment, containing exon 2 and part of exon 3, was purified by agarose gel electrophoresis and inserted in the *Hind*III/

*Bam*HI sites of pUC19. The 1986 bp *Bam*HI/*Eco*RI fragment of epican^{U36}, containing exon 3-19, was then inserted in the *Bam*HI (internal) and *Eco*RI (pUC19) sites. Finally, the *Eco*RI (filled in with Klenow polymerase)/*Nde*I fragment of the resulting clone, containing the epican^{U36} sequence from exon 2-19, was inserted behind the T7 promoter in the *Bam*HI (filled in with Klenow polymerase)/*Nde*I sites of the expression plasmid pET-3a [283]. The resulting clone was transformed to the *E. coli* strain BL21(DE3)/pLysE [283]. All relevant steps were checked by sequencing.

Expression of the epican^{U36} protein was induced with 1 mM isopropylthio- β -D-galactoside, essentially as described by Sambrook *et al.* [282]. Samples before and 2 hr after induction were analyzed by Western blotting under reducing conditions, and the expressed protein was visualized by APAAP-staining.

Epitope mapping

Based on the sequence of the epican-specific exons 7-11 (v3-v7) published by Kugelman *et al.* [114], 218 overlapping dodecapeptides were synthesized essentially as described by Geysen *et al.* [284]. To include the splice junctions to exon 5 and 12 (v8), the series of peptides started with amino acids 212-223 and ended with amino acids 429-440 (numbering according to Kugelman *et al.* [114]). In addition, 7 overlapping dodecapeptides starting with amino acids 362-373 and ending with amino acids 368-379 were synthesized, based on the sequence published by Hofmann *et al.* [110] and Screatton *et al.* [115]. The enzyme-linked immunosorbent assay (ELISA) as described by Geysen *et al.* [284] was used to assess the binding of MAb U36 to the panel of synthetic peptides.

Competitive antibody inhibition assay

The competitive immunoreactivity assay was performed in duplicate, essentially as described by Lindmo *et al.* [285]. In short, UM-SCC-11B cells were detached with cell dissociation medium (Sigma), fixed in 0.1% glutaraldehyde and serially diluted in 1% BSA/PBS, ranging from 2.3×10^6 to 1.4×10^5 cells per tube. MAb U36 (200 μ g) was labeled with 1 mCi ¹²⁵I in iodogen coated vials, and free iodine was removed by PD10 chromatography [58]. To the diluted cell suspensions, 3 μ g of the dodecapeptides WHVGYRQTPKED, WHEGYRQTPRED or HRPQGRWYDEE was added. After adding 10,000 cpm (1.5 ng) ¹²⁵I-labeled MAb U36, the cells were incubated overnight at 4°C. To the most diluted sample, an excess of unlabeled MAb U36 was added to determine the level of

non-specific binding. After the cells were spun, the radioactivity in the pellet and supernatant was determined in a gamma counter. The percentage of ¹²⁵I-labeled MAb U36 bound to the cells in the presence or absence of a particular dodecapeptide was calculated.

Immunohistochemical staining of frozen tumor sections

Cryosections of 4 μ m were mounted on microscopical glass slides coated with 1 mg/ml poly-L-lysine, air dried for 1 hr and fixed with acetone for 10 min. The sections were rinsed with PBS, and incubated for 10 min with normal rabbit serum (DAKO, Glostrup, Denmark) diluted 1:50 in 1% BSA/PBS. Subsequently, the sections were incubated for 1 hr with specific antibody diluted to 10 μ g/ml in 1% BSA/PBS (or 1:5 for hybridoma supernatant), biotin-labeled rabbit anti-mouse F(ab)₂ fragments diluted 1:500 in 1% BSA/PBS and streptavidin-labeled horseradish peroxidase diluted 1:500 in 1% BSA/PBS. After each incubation step, the sections were rinsed three times with PBS. The sections were stained with 0.5 mg/ml 3,3-diaminobenzidine tetrahydrochloride/0.01% H₂O₂ in PBS for 3 to 5 min. The sections were rinsed once with PBS, and the nuclei were counterstained with haematoxylin for 45 sec. Finally, the sections were dehydrated and covered with Depex. All incubation and washing steps were carried out at 20 to 25°C.

Results

The protein recognized by MAb U36 is a cell surface antigen that is highly expressed by squamous epithelia and squamous cell carcinomas. Western blotting showed that the protein recognized by MAb U36 is approximately 200 kDa (Fig. 3), and the heterogeneity in molecular weight suggested that it is a glycoprotein. Staining of affinity purified antigen, using periodic acid in combination with Schiff's reagent, indeed confirmed that the protein is glycosylated (data not shown).

The antigen was characterized further by the molecular cloning of its encoding cDNA. A human HNSCC cDNA library inserted in shuttle vector pCDM8, containing 7×10^5 independent clones, was transfected into COS-7 cells and screened *in situ* by immunocytochemical staining with MAb U36. Plasmid DNA was extracted from the positive COS cells by Hirt extraction and trans-

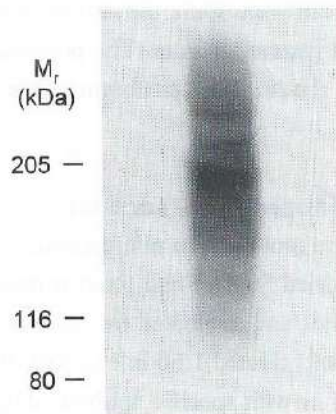


Figure 3 U36 antigen isolated from UM-SCC-11B cells, run on an SDS-PAGE gel, blotted and incubated with ^{125}I -labeled MAb U36 as described in 'Materials and methods'. The relative molecular weights of protein standards run on the same gel are indicated on the left.

formed into *E. coli*, as described earlier [281]. About 200 colonies were obtained, pooled and rescreened. Unfortunately, all clones appeared to be negative upon rescreening in COS-7 cells, most likely due to plasmid DNA modification by the eukaryotic cells. We therefore analyzed the cDNA library by screening progressively smaller pools of bacterial colonies [281], starting with 9 pools of 75,000 bacterial colonies. Plasmid DNA was isolated from overnight cultures inoculated with the 9 pools of bacterial colonies and transfected into COS-7 cells. Pools containing U36-encoding cDNA clones were identified by immunocytochemical staining of the transfected cells. The pool with the highest number of positive cells and consisting of the smallest number of colonies was selected for further fractionation. After 8 subsequent fractionation rounds, the cDNA clone encoding the U36 antigen was isolated.

Sequence analysis and database searching revealed that the U36-encoding cDNA consisted of two open reading frames, both containing a poly(A) tail (Fig. 1). The first frame appeared to encode epican, the squamous cell specific variant of CD44 [110,114], and the second frame encoded the serine/threonine phosphatase PP1 γ_2 [286]. To show that this fusion clone was the result of a cloning artefact, the UM-SCC-22A cDNA library was rescreened by hybridization with the isolated U36 clone as a probe. Restriction mapping and Southern hybridization revealed that only separate clones encoding either phosphatase

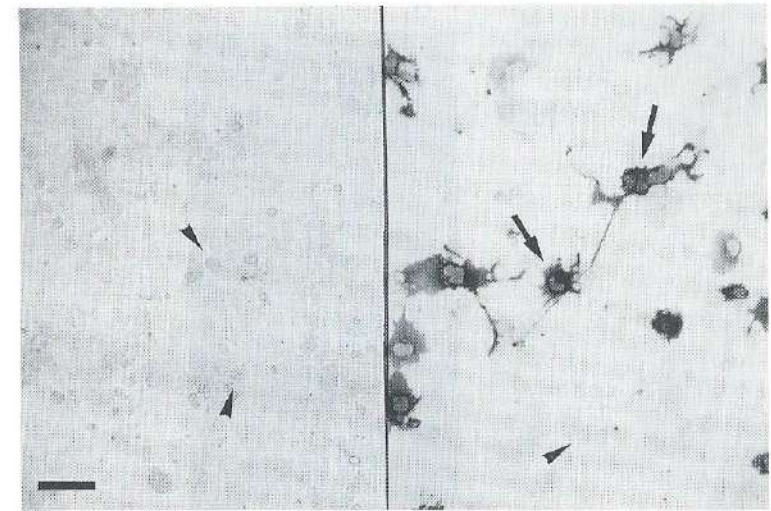


Figure 4 COS-7 cells were transiently transfected (efficiency about 50%) without (left panel) or with the epican^{U36} clone (right panel), and stained immunocytochemically *in situ* by MAb U36 and APAAP, as described in 'Materials and methods'. Cells positively stained with MAb U36 are indicated with an arrow; negative cells of which only the nuclei are visible are indicated with an arrowhead. Scale bar represents 10 μm .

PP1 γ_2 or (incomplete) epican could be isolated. Other epican-PP1 γ_2 fusion clones were not present (data not shown). A correct epican-encoding clone was then constructed from a clone containing part of the epican-encoding sequence, lacking exon 1-4, and the U36 clone originally isolated by expression cloning (Fig. 1). The resulting clone, designated epican^{U36}, was transfected into COS-7 cells and stained immunocytochemically. The transfected cells stained positive, confirming that epican indeed contains the epitope recognized by MAb U36 (Fig. 4).

Epican is an isoform of the large CD44 protein family. These isoforms are encoded by alternatively spliced transcripts of a single gene [115]. The presence of these protein isoforms makes it conceivable that different regions of the CD44 protein are responsible for the reported variety of biological activities in different tissues. We therefore decided to identify the epican domain containing the MAb U36 defined epitope.

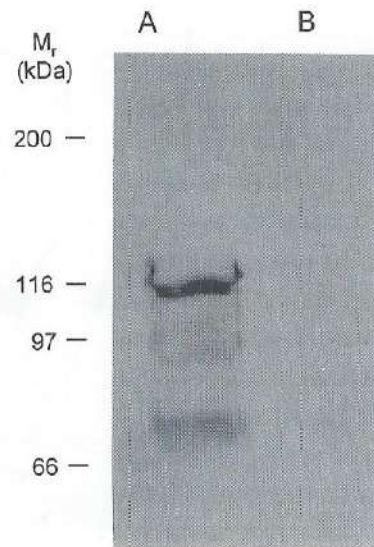


Figure 5 A culture of *E. coli* BL21(DE3)/plysE transformed with pET-3a/epican^{U36} lysed 2 hr after induction (A) and before induction (B). The proteins were analyzed by Western blotting and APAAP-staining, as described in 'Materials and methods'. Although the expected protein has a theoretical molecular weight of 74 kDa, the relative molecular weight on SDS-PAGE is apparently 116 kDa. The smaller fragments are probably due to protein degradation. The relative molecular weights of protein standards run on the same gel are indicated on the left.

As a first step, we determined whether MAb U36 recognized a linear polypeptide epitope. A gene expression system based on bacteriophage T7 RNA polymerase was used to express epican^{U36} in the *E. coli* strain BL21(DE3)/plysE [283]. Binding of MAb U36 to the antigen produced by *E. coli* was analyzed by Western blotting under reducing conditions and by APAAP-staining. Upon induction a protein was produced that was recognized by MAb U36 (Fig. 5).

The epitope recognized by MAb U36 was mapped by an ELISA screening of 218 overlapping synthetic peptides spanning the translated sequence of the epican-specific exons 7-11 (v3-v7) (Fig. 6). The sequences of the peptides consisted of 12 amino acids and overlapped each other by 11 amino acids. The analysis was hindered by the fact that a variation in the amino acid sequence of these domains has been described [110,114,115]. The published protein sequences differ in amino acids 367 and 374 (amino acid numbering according to Kugelman *et al.* [114]), being V and K (Kugelman *et al.* [114]) or E and R (Hofmann *et al.*

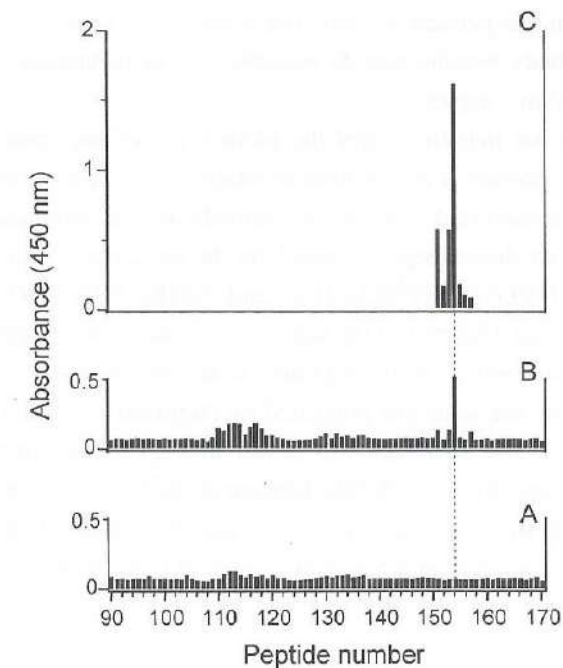


Figure 6 Mapping of the MAb U36 defined epitope. A set of overlapping dodecapeptides covering the epican-specific exons 7-11 (v3-v7) was screened by ELISA. On the Y-axis the ELISA absorbance of OPD at 450 nm is indicated. On the X-axis the peptides 90-170 are shown. The peptide regions 1-89 and 171-218 have not been depicted. The ELISA absorbance of these peptides was below the level of detection (0.15). The peptide panel based on the amino acid sequence published by Kugelman *et al.* [114] was screened without (A) and with (B) MAb U36, showing a signal on peptide 154. When the variant amino acids as found in the sequences published by Hofmann *et al.* and Screaton *et al.* [110,115] are included, a much higher signal was found on peptide 154 (C). Each pepscan was performed in duplicate.

and Screaton *et al.* [110,115]), respectively. Because of this sequence variation, we decided to include in the panel 7 additional peptides covering the region with the variable amino acids. Signal was observed in the region of peptide 154 (amino acids 365-376) located in exon 10 (v6), and a very weak signal was present in the region of peptide 113 (amino acids 324-335) located in exon 9 (v5). The signal in this exon is probably not significant since the negative control showed a similar trend. Surprisingly, the epitope in exon 10 (v6) appeared to include the observed variation in amino acid sequence, and these variations have an impact on the

antibody binding in this pepscan system. The basis of this sequence variation, its relevance for antibody binding and its possible role in metastasis and carcinogenesis is described in Chapter 3.

To confirm our hypothesis that the MAb U36 defined epitope is indeed localized on the v6 domain, a competitive antibody-binding assay was performed. In this assay, we investigated whether the antibody-antigen interaction could be blocked by 2 variant dodecapeptides based on the sequence of the MAb U36-binding region WHVGYRQTPKED [114] and WHEGYRQTPRED [110,115]. The HNSCC cell line UM-SCC-11B was used in the antibody-binding assay, with and without competitive dodecapeptides. A scrambled sequence (HRPQGRWYDEE) based on the sequence published by Hofmann *et al.* and Screaton *et al.* [110,115] was used as a control. As shown in Fig. 7, both peptides of the epitope sequence were able to inhibit the binding of the U36 antibody to the cells. In agreement with the pepscan results, the peptide based on the sequence published by Hofmann *et al.* and Screaton *et al.* [110,115] was the most effective competitor.

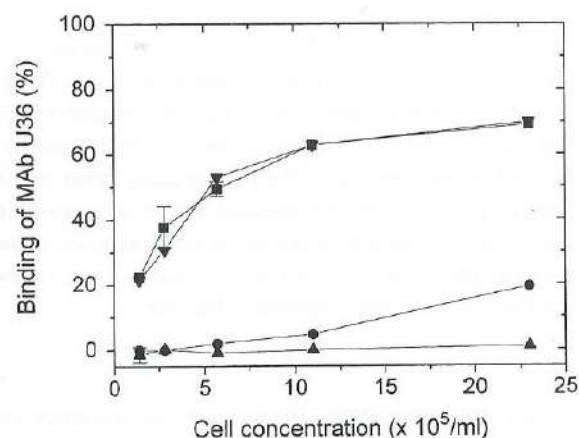


Figure 7 The binding of a constant concentration (1.5 ng/ml) of ¹²⁵I-labeled MAb U36 as a function of the concentration of UM-SCC-11B squamous carcinoma cells in the absence (■) or in the presence of 3 µg/ml of the synthetic peptides WHVGYRQTPKED (●; Kugelman *et al.* [114]) and WHEGYRQTPRED (▲; Hofmann *et al.* and Screaton *et al.* [110,115]). A scrambled sequence (▽; HRPQGRWYDEE) based on the sequence published by Hofmann *et al.* and Screaton *et al.* [110,115] was used as a control. Error bars have been omitted when the standard deviation was smaller than 2% binding.

Discussion

MAb U36, directed against a 200 kDa squamous cell associated surface antigen was selected as the most promising MAb for RIT of HNSCC since (a) it recognized 188 of the 196 tumors analyzed (at least 50% of the cells intensely stained [71]), (b) it has a favorable biodistribution in HNSCC patients, (c) it hardly induces undesired human anti-mouse antibody (HAMA) responses after a single dose administration, and (d) did not show any adverse effects when administered to patients at dosages up to 50 mg [79]. Because of these promising data, we have started a phase I/II clinical RIT trial to evaluate the suitability of ¹⁸⁶Re-labeled MAb U36 for the treatment of minimal residual disease in patients with head and neck cancer.

Obviously, these data justified the characterization of the target antigen by cDNA cloning. In this Chapter, we show that the MAb U36 defined antigen is identical to the keratinocyte-specific splice variant of CD44, epican. CD44 is an assortment of protein isoforms encoded by various splice variants of a single copy gene located on chromosome 11 [115]. Epican, the squamous cell specific variant, is one of the largest isoforms encoded by the standard exons 1-5, the variant exons 7-14 (v3-v10) and the standard exons 15-17 and 19 [110,114]. Besides the isoforms expressed in normal tissues, a number of tumor-associated isoforms encoded by specific alternatively spliced transcripts have been described. Interestingly, it has been shown that the expression of tumor-associated splice variants is related to tumor metastasis in animal models [109]. Moreover, there appears to be a correlation between these changes in CD44 expression and the progression of several human tumors, such as breast and colon cancers [267], cervical cancer [232], aggressive and metastatic non-Hodgkin lymphoma [139] and bladder carcinoma [274]. For colon carcinoma [234] and breast carcinoma [228] Kaplan-Meier curves indeed showed a correlation between CD44v6 expression and poor overall survival, indicating that especially the expression of splice variants containing the v6 domain seems to be valuable as a prognostic marker for the progression of these tumors. However, the data are still controversial [265,287].

The observation that the MAb U36 defined epitope is localized on the v6 domain and the knowledge that various tumors express v6 splice variants raised the question whether this MAb might also be suitable for targeting tumors other than squamous cell carcinoma. For a target antigen to be suitable for RIT, some

important criteria must be met. First, the expression of the antigen in normal tissues that are in direct contact with the blood circulation should be low. Second, the target antigen should be a surface antigen that is not shed to a high level into the circulation. Finally, the antigen should be expressed abundantly and homogeneously in the tumor tissue, and in a high percentage of the tumors. To test the expression level of CD44v6 in various tumor types, we analyzed the reactivity of MAb U36 on frozen sections of primary tumors and metastases from colon, breast, lung, cervix, and bladder carcinoma as well as from non-Hodgkin lymphoma by immunohistochemistry. Reactivity of MAb U36 with these tumors was scored semi-quantitatively as described previously [58,71] and was compared with its reactivity on HNSCC sections. Since all tumors were stained in a single run, intensity and homogeneity of the staining pattern provided an indication for the relative CD44v6 expression level. In comparison with the high, homogeneous and membrane restricted staining of HNSCC, staining of the other tumors was variable (Table 1). A large proportion of the tumors did not show staining at all, while for some tumors the staining was homogeneous but weak and others were stained heterogeneously. Taking these staining patterns into account, RIS or RIT studies would most likely result in relatively low tumor uptake and ineffective targeting of these tumors. Only a proportion of the breast and bladder carcinomas as well as of the squamous cell carcinomas of the cervix and lung showed intense and homogeneous staining similar to that of HNSCC. Other anti-v6 antibodies such as MAb17 (kindly provided by dr. L.M. Milstone), MAb U39 (Van Dongen *et al.*, unpublished results) and MAb CD44v6 (kindly provided by dr. S. Jalkanen), which recognize epitopes on the v6 domain consisting of amino acids 354-365 (MAb17) or 356-367 (U39), showed a similar reactivity pattern (amino acid numbering according to Kugelman *et al.* [114]). The epitope of MAb CD44v6 could not be determined.

From these data it can be concluded that expression of the v6 domain in squamous cell carcinoma as part of epican is of a different order of magnitude than v6 expression accomplished by tumor-associated splice variants in other tumor types. Analysis of epican-encoding transcripts and other v6-encoding splice variants in HNSCC cell lines revealed that in these tumor types the v6 domain is mainly expressed as part of epican (Chapter 4). As a consequence of this difference in expression level, the applicability of anti-v6 MAbs for tumor targeting of radioisotopes seems to be restricted to squamous cell carcinomas and

Table 1 Immunohistochemical staining of frozen tumorsections with MAb U36¹

Tumor	Positive cells (%)	Primary tumors	Metastases
HNSCC	0-10	2/196	1/31
	10-50	6/196	2/31
	50-95	124/196	20/31
	>95	64/196	8/31
cervix carcinoma	0-10	1/5	0/2
	10-50	2/5	0/2
	50-95	0/5	0/2
	>95	2/5	2/2
colon carcinoma	0-10	12/19	5/9
	10-50	2/19 ²	3/9 ⁶
	50-95	3/19 ³	0/9
	>95	2/19 ⁴	1/9 ⁴
breast carcinoma	0-10	7/21	1/9
	10-50	5/21 ²	2/9 ²
	50-95	7/21 ⁵	2/9 ²
	>95	2/21	4/9 ⁷
bladder carcinoma	0-10	2/4	3/3
	10-50	0/4	0/3
	50-95	1/4	0/3
	>95	1/4	0/3
lung adenocarcinoma	0-10	4/8	3/3
	10-50	1/8 ²	0/3
	50-95	1/8 ²	0/3
	>95	2/8 ²	0/3
lung squamous cell carcinoma	0-10	1/7	0/1
	10-50	0/7	0/1
	50-95	2/7 ²	1/1 ²
	>95	4/7 ²	0/1
non-Hodgkin lymphoma	0-10	6/6	6/6
	10-50	0/6	0/6
	50-95	0/6	0/6
	>95	0/6	0/6

¹Frozen sections of primary tumors and metastases of HNSCC, cervix, colon, breast, bladder and lung carcinomas as well as non-Hodgkin lymphomas were stained immunohistochemically by MAb U36 as described in 'Materials and methods'. The staining pattern was scored semi-quantitatively. Per score range (percentage of positive cells) the number of positive tumors/number of tumors was determined. The data from HNSCC were taken from De Bree *et al.* [71].

²1 tumor weakly stained. ³1 tumor weakly and 1 tumor very weakly stained. ⁴1 tumor very weakly stained. ⁵4 tumors weakly and 1 tumor very weakly stained. ⁶All tumors weakly stained.

⁷2 tumors weakly stained.

previously selected breast and bladder carcinomas, although this statement can be proven only by biodistribution studies in cancer patients.

Although other anti-v6 antibodies may be equally well suited for targeting HNSCC, it is important to realize that differences in suitability cannot be excluded. For example, Salmi *et al.* [288] found downregulation of v6 expression in all squamous cell carcinomas (n=30) with MAb Var3.1, an antibody raised against a synthetic peptide of 16 amino acids derived from the v6 domain. It appeared that more differentiated carcinomas displayed a more intense reactivity than undifferentiated ones. Remarkably, for normal stratified squamous epithelia a particularly strong reactivity of MAb Var3.1 was seen with the mid and upper layers, while for the other four MAbs tested in our study the reactivity was particularly strong with the basal layers and almost lacking in the upper layers. This example indicates that evaluation in patients, as has been performed with MAb U36, is necessary before MAbs directed against v6 epitopes can be ranked for their tumor targeting capacity.

Acknowledgements

The authors are indebted to dr. W. Puijk, dr. J. Slootstra and dr. R.H. Melen (ID-DLO, Lelystad, The Netherlands) for the epitope mapping, P. den Otter (Department of Pathology, University Hospital *Vrije Universiteit*, Amsterdam, The Netherlands) for immunohistochemical analysis of the various tumors with the anti-v6 antibodies, and dr. S.T. Pals (Department of Pathology, Academic Medical Center, University of Amsterdam, The Netherlands) for valuable discussions. We are grateful to dr. S. Jalkanen (National Public Health Institute, University of Turku, Finland) and dr. L.M. Milstone (Department of Dermatology, Yale University School of Medicine, New Haven, USA), for providing their antibodies MAb CD44v6 and MAb17, respectively.

Chapter 3

Sequence variation in the monoclonal antibody U36 defined CD44v6 epitope

Nicole L.W. van Hal

Guus A.M.S. van Dongen

Corlinda B.M. ten Brink

Jim N. Herron

Gordon B. Snow

Ruud H. Brakenhoff

Published in: *Cancer Immunol. Immunother.* 45:88-92 (1997)

Abstract

Monoclonal antibody (MAb) U36 was developed for the treatment of minimal residual disease of head and neck squamous cell carcinoma (HNSCC). The MAb U36 defined antigen was characterized by cDNA cloning and was shown to be identical to the keratinocyte-specific CD44 splice variant epican. The epitope recognized by MAb U36 was shown to be located in the v6 domain. Two amino acids within the epitope appeared to differ from the sequences that have been described in literature. The sequence of the epitope appeared to contain glutamic acid at position 367 and lysine at position 374, while valine and arginine, respectively, have been described before. Interestingly, another anti-CD44v6 antibody with possible clinical application, VFF18, recognizes an epitope in the same area. With respect to the applicability of these antibodies for tumor targeting, this variation might have an influence on antibody-antigen interaction and MAb accumulation in the tumor. Furthermore, this observation raised the question whether the different epitopes are related to the malignant behavior of tumor cells.

In this Chapter, we determine the relative affinity of MAb U36 for the variant epitope sequences by tumor cell binding assays, using synthetic peptides for competition. The presence of glutamic acid instead of valine at position 367 caused a strong competition. Further evaluation showed that the published valine variant does not exist *in vivo* and is the result of a sequencing artefact. The effect of substitution of lysine for arginine at position 374 had no effect on the binding of MAb U36 to the cells. This amino acid variation was shown to be due to allelic polymorphism. There was no trend towards allelic imbalance in tumor cells as compared to normal cells.

Introduction

MAb U36, an antibody developed for the treatment of minimal residual disease of HNSCC [79], recognizes an epitope in the CD44v6 domain (Chapter 2). By the use of overlapping synthetic peptides it was shown that the region of amino acids 365-376 (numbering according to Kugelman *et al.* [114]) forms the MAb U36 epitope. It is exactly in this antibody-binding region, that slight differences were observed in comparison to the various CD44v6 sequences that have been published and stored in the databases. These published protein sequences differ in amino acids 367 and 374, being valine and lysine according to Kugelman *et al.* [114] or glutamic acid and arginine according to Hofmann *et al.* and Sreaton *et al.* [110,115]. (The sequences are accessible in the EMBL/GenBank databases by the numbers X66733, X62739 and L05415). The sequence of our epican^{U36} cDNA clone appeared to be a combination of the other two published sequences, encoding glutamic acid at position 367 and lysine at position 374 (Fig. 1). These sequence variations could possibly be explained by the source used for cDNA/gene analysis: an *in vitro* tumor cell line ([110], Chapter 2) or normal primary keratinocytes [114], suggesting that CD44v6 mutations are favored in the malignant progression of normal cells to tumor cells.

Kugelman *et al.* [114]:

```

365 W H V G Y R Q T P K E D 376
    ttg cat gtg gga tat cgc caa aca ccc aaa gaa gac
  
```

Hofmann *et al.* [110]; Sreaton *et al.* [115]:

```

365 W H E G Y R Q T P R E D 376
    ttg cat gag gga tat cgc caa aca ccc aga gaa gac
  
```

Van Hal *et al.* (Chapter 2):

```

365 W H E G Y R Q T P K E D 376
    ttg cat gag gga tat cgc caa aca ccc aaa gaa gac
  
```

Figure 1 The amino acid region in the CD44v6 domain that forms the epitope recognized by MAb U36 (amino acids 365-376; numbering according to Kugelman *et al.* [114]). Two amino acids within this region show a variation: valine (V) or glutamic acid (E) at position 367 and lysine (K) or arginine (R) at position 374.

The observation that several sequence variants have been described raised questions about the applicability of MAb U36 for tumor targeting as well. When different epitopes with different affinity for MAb U36 exist *in vivo*, this might influence the accumulation of MAb U36 in tumors and normal tissues. This is also true for VFF18, an anti-CD44v6 MAb that was recently described as a promising targeting vehicle for immunotherapy of squamous cell carcinoma [60]. The epitope of VFF18 is formed by amino acids 360-370 and contains the variable amino acid at position 367. That differences in antibody affinity indeed have implications for immunotherapy is shown by the results of Kievit *et al.* [289]. Comparison of the anti-EGP40 antibodies 17-1A and 323/A3 showed that antibodies with different affinities for the same antigen show a different efficacy in immunotherapy, at least in tumor-bearing nude mouse models.

To investigate whether the observed amino acid variation has an impact on the binding affinity of the antibody, we determined the relative affinity of MAb U36 for the variant epitopes by a competition binding assay using synthetic peptides. In addition, the presence and frequency of the various epitope sequences *in vivo* was investigated by analysis of the genomic exon v6 sequence of normal cells and various HNSCC cell lines.

Materials and methods

Competitive antibody inhibition assay and data analysis

The competitive antibody inhibition assay was performed in triplicate and was based on the assay described by Lindmo *et al.* [285]. Briefly, 200 µg MAb U36 was labeled with 1 mCi ^{125}I in a glass vial coated with 25 µg iodogen [58]. Free iodine was removed by PD10 chromatography. UM-SCC-11B cells were detached with cell dissociation medium (Sigma, Bornem, Belgium), as the MAb U36 defined epitope is destroyed by trypsinization, and fixed in 0.1% glutaraldehyde. Subsequently, 1.0×10^6 cells/ml were incubated with 10,000 cpm (8.0×10^{-12} M) ^{125}I -labeled MAb U36 in the presence of synthetic peptide (concentration ranging from 6.5×10^{-11} M to 2.0×10^{-5} M) in a final volume of 1 ml 1% bovine serum albumine in phosphate buffered saline (1% BSA/PBS). Incubations were performed overnight at 4°C. Cells were spun down and the radioactivity in the pellet and supernatant was determined in a gamma counter. The percentage of ^{125}I -labeled MAb U36 bound to the cells was calculated.

The calculation of the dissociation constants for the antibody/peptide complexes was based on the following equilibria:

$$K_d^{\text{Ag}} = \frac{[\text{F}_{\text{ab}}^{\text{unb}}] \times [\text{Ag}^{\text{unb}}]}{[\text{F}_{\text{ab}}\text{Ag}]} \quad 1$$

$$K_d^{\text{Pep}} = \frac{[\text{F}_{\text{ab}}^{\text{unb}}] \times [\text{Pep}^{\text{unb}}]}{[\text{F}_{\text{ab}}\text{Pep}]} \quad 2$$

where K_d^{Ag} is the dissociation constant for the surface antigen/antigen-combining site complex, which is equal to 2.9×10^{-11} M [58], and K_d^{Pep} the dissociation constant for the peptide/antigen-combining site complex. Note that each IgG antibody contains two antigen-combining sites which are assumed in this model to bind independently. Therefore, K_d^{Pep} values obtained by the model are 'apparent' affinity constants. $[\text{F}_{\text{ab}}^{\text{unb}}]$ is the concentration of unbound antigen-combining sites. The parameters $[\text{Ag}^{\text{unb}}]$ and $[\text{Pep}^{\text{unb}}]$ are the concentrations of unbound surface antigen and unbound peptide. $[\text{F}_{\text{ab}}\text{Ag}]$ and $[\text{F}_{\text{ab}}\text{Pep}]$ are the concentrations of the complex of antigen-combining sites with, respectively, the surface antigen and peptide. Assuming that $[\text{Pep}^{\text{unb}}]$, the unbound peptide concentration, is equal to the total peptide concentration, the following quadratic expression for $[\text{F}_{\text{ab}}\text{Ag}]$ can be derived:

$$[\text{F}_{\text{ab}}\text{Ag}] = \frac{([\text{F}_{\text{ab}}^{\text{tot}}] + [\text{Ag}^{\text{tot}}] + A \times K_d^{\text{Ag}}) \pm \sqrt{([\text{F}_{\text{ab}}^{\text{tot}}] + [\text{Ag}^{\text{tot}}] + A \times K_d^{\text{Ag}})^2 - 4 \times [\text{F}_{\text{ab}}^{\text{tot}}] \times [\text{Ag}^{\text{tot}}]}}{2} \quad 3$$

where:

$$A = 1 + \frac{[\text{Pep}^{\text{unb}}]}{K_d^{\text{Pep}}} \quad 4$$

In this equation $[\text{F}_{\text{ab}}^{\text{tot}}]$ is the total concentration of antigen-combining sites and $[\text{Ag}^{\text{tot}}]$ the total concentration of surface antigen. Equation 3 was used for curve-fitting of the data and thereby providing an estimation of K_d^{Pep} and $[\text{Ag}^{\text{tot}}]$. (Derivation of equation 3 is available upon request).

PCR amplification

Polymerase chain reaction (PCR) analysis was performed on 0.25 µg chromosomal DNA isolated from the HNSCC cell lines UM-SCC-22A, UM-SCC-22B, UM-SCC-11B, UM-SCC-14C and UM-SCC-35 (kindly provided by dr. T.E. Carey, Ann Arbor, MI) and exfoliated cells collected from the oral cavity of four control persons by scraping with a Cytobrush plus (Medscand, Malmö, Sweden). The exfoliated cells were resuspended in 200 µl 10 mM TRIS (pH 8.3) and frozen. Before use, the samples were heated at 100°C for 10 min and subsequently 10 µl was used in a PCR reaction. The sense primer was identical to the sequence of the intron 9/exon 10 boundary and contained an *EcoRI* site at the 5' end to facilitate subcloning (5'-GGAATTCCTGATATTCTTCTCACAGTCC-AGGC-3'). The antisense primer was complementary to the sequence of the exon 10/intron 10 boundary with an *XbaI* site at the 5' end (5'-GCTCTAGACTTGTT-AAACCATCCATTACCAGC-3'). The PCR reactions were performed in a total volume of 50 µl, using 200 µM deoxyribonucleoside triphosphates, 10 mM TRIS-HCl (pH 8.3), 50 mM KCl, 1.5 mM MgCl₂, 0.5 µM sense, 0.5 µM antisense primer and 1 U AmpliTaq DNA polymerase (Perkin Elmer, Gouda, The Netherlands). The PCR conditions were as follows: 4 min at 95°C, 40 cycles of 1 min at 95°C, 1 min at 55°C, 2 min at 72°C, followed by a final incubation of 4 min at 72°C. PCR amplification was performed on a Hybaid Omnigene thermal cycler (Biozym, Landgraaf, The Netherlands).

DNA sequencing

The PCR fragments obtained were cut with *EcoRI* and *XbaI* and subcloned into pUC19. DNA of the obtained subclones was sequenced, using a DyeDeoxy Terminator Cycle Sequencing Kit (Perkin Elmer, Gouda, The Netherlands) and an Applied Biosystems 373A DNA Sequencer (Applied Biosystems, Maarssen, The Netherlands).

Results and discussion

The epitope recognized by MAb U36, an antibody that binds to the CD44v6 domain, was shown to be located in the v6 domain of CD44 (amino acids 365-376; numbering according to Kugelman *et al.* [114]). In the literature two variant sequences have been described encoding a valine and a lysine [114] or a glutamic acid and an arginine [110,115] at positions 367 and 374, respectively. Sequence analysis of the epican^{U36} clone revealed a combination of these sequences, encoding a glutamic acid at position 367 according to Hofmann *et al.* and Sreaton *et al.* [110,115] and a lysine at position 374 according to Kugelman *et al.* [114].

As differences in affinity may have implications for therapeutic applications [289], we investigated whether the amino acid variations influence the binding affinity of the antibody. A competition experiment was performed to determine the relative binding affinity of MAb U36 for the three epitope variants. In this experiment, a constant amount of cells that expressed CD44v6 was incubated with a constant amount of radioactive MAb U36. To these mixtures several concentrations of synthetic peptide, representing one of the epitope variants, was added to inhibit the binding of MAb U36 to the cells. A concentration of 1.0×10^6 cells/ml was chosen for this competitive inhibition assay. At this concentration, the binding of MAb U36 to the cells was about 80% and had nearly reached its maximum value (Fig. 2). Apparent K_d^{Pep} values were obtained by optimal curve-fitting of the experimental data with equation 3 mentioned in 'Materials and methods' (Table 1). Fig. 3 shows the optimal curve-fit for all peptides. Differences in binding affinity of MAb U36 for the various synthetic peptides could be observed. The peptides W H E G Y R Q T P R E D (based on the sequence of Hofmann *et al.* and Sreaton *et al.* [110,115]) and W H E G Y R Q T P K E D (based on the sequence of the epican^{U36} clone) blocked antibody binding with an equal efficiency ($K_d^{\text{Pep}} = 7.5 \times 10^{-9}$ M). This implies that substitution of lysine at position 374 to arginine does not affect the binding of MAb U36. This could be explained by the fact that lysine and arginine are both hydrophilic amino acids with strong polar side chains, which are positively charged at a physiological pH. The synthetic peptide W H V G Y R Q T P K E D (sequence described by Kugelman *et al.* [114]) appeared to be less effective in blocking the binding of MAb U36 to the cells ($K_d^{\text{Pep}} = 1.1 \times 10^{-7}$ M). So, the substitution of glutamic acid at position 367 (which is nearly always negatively

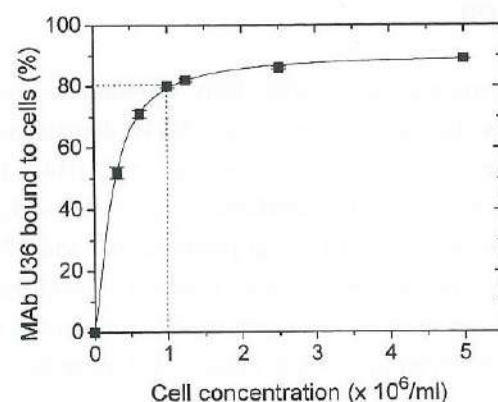


Figure 2 The binding of a constant concentration (8.0×10^{-12} M) of 125 I-labeled MAb U36 as a function of the concentration of UM-SCC-11B squamous carcinoma cells. No synthetic peptides were added. The dashed line indicates the concentration of 1.0×10^6 cells/ml, which was chosen for the competitive inhibition assay (Fig. 3). At this concentration, the binding of MAb U36 to the cells was about 80% and had nearly reached its maximum value.

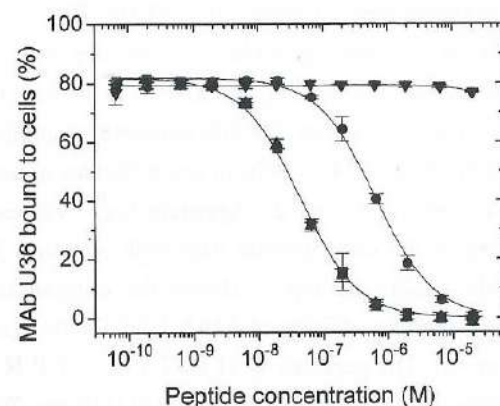


Figure 3 The binding of a constant concentration (8.0×10^{-12} M) of 125 I-labeled MAb U36 to a constant concentration of HNSCC cells UM-SCC-11B (1×10^6 cells/ml) as a function of the concentration of the synthetic peptides (Δ) WHEGYRQTPRED (Hofmann *et al.* and Sreaton *et al.* [110,115]), (\blacksquare) WHEGYRQTPKED (Chapter 2), (\bullet) WHVGYRQTPKED (Kugelman *et al.* [114]) and (∇) HRPQGRWTYDEE, a scrambled version of the sequence of Hofmann *et al.* and Sreaton *et al.* [110,115]. Optimal curve-fit ($r^2 \geq 0.999$) with equation 3, mentioned in 'Materials and methods', is shown for all peptides. This resulted in an estimation of the total concentration of surface antigen (1.4×10^{-10} M), and the K_d^{Pep} of the synthetic peptides based on the sequences of Sreaton *et al.* (7.5×10^{-9} M), Chapter 2 (7.5×10^{-9} M) and Kugelman *et al.* (1.1×10^{-7} M). Error bars of a triplicate experiments are indicated.

Table 1. Apparent K_d^{Pep} values obtained by optimal curve-fitting of the experimental data with equation 3 mentioned in 'Materials and methods'.

Synthetic peptide	K_d^{Pep} (M)	r^2
WHEGYRQTPRED ¹	7.5×10^{-9}	0.9986
WHEGYRQTPKED ²	7.5×10^{-9}	0.9996
WHVGYRQTPKED ³	1.1×10^{-7}	0.9994

¹Hofmann *et al.* [110]; Sreaton *et al.* [115]. ²Chapter 2. ³Kugelman *et al.* [114].

charged at a neutral pH) for valine (an apolar amino acid) significantly reduced the competitive effect of the synthetic peptide, indicating that this amino acid is important for the binding of MAb U36 to the epitope. Finally, the control peptide HRPQGRWTYDEE, a scrambled version of the sequence of Hofmann *et al.* and Sreaton *et al.* [110,115], did not block antibody binding at these concentrations. The calculated K_d^{Pep} values are comparable to values that have been described in literature for antibody-peptide interactions [290]. The K_d^{Pep} values indicate that the epitope conformation apparently has an influence on the binding affinity of the antibody, since the dissociation constant for the surface antigen/antigen-combining site complex ($K_d^{\text{Ag}} = 2.9 \times 10^{-11}$ M [58]) is lower than for the synthetic peptides. Other studies have shown that the affinity of antigen-mimicking peptides is often more than 100-fold lower than the affinity of the native antigen [290]. This observation is due to the fact that a short peptide has a greater conformational freedom than the same sequence in the native antigen, thus binding of the peptide results in a significant loss of configurational entropy. To summarize, the amino acid variation at position 374 has no effect on the affinity of the antibody for the synthetic peptides. Therefore, differences in affinity for the antigen epitopes *in vivo* are only to be expected when the amino acid variation causes masking of the epitope (*e.g.* by changing the conformation or the glycosylation of the protein). However, these changes are unlikely to occur since the amino acid variation concerns two amino acids with very similar physico-chemical properties. In contrast, the amino acid variation at position 367 has a large impact on antibody binding.

The observation that an epitope variant that showed a lower affinity for MAb U36 had been described in literature needed further analysis. It can be anticipated that the presence of the low affinity epitope *in vivo* will influence the antibody accumulation in the tumor during immunotherapy with MAb U36, as was shown by Kievit *et al.* [289] in nude mouse models with anti-EGP40 antibodies 17-1A and 323/A3. Moreover, the same holds true for MAb VFF18, an anti-CD44v6 antibody with potential applicability for immunotherapy of squamous cell carcinoma that was recently described by Heider *et al.* [60]. When a library of 218 overlapping synthetic peptides, based on the v3-v10 sequence of Kugelman *et al.* [114], was screened with MAb VFF18 (obtained from Boehringer Ingelheim), no signal on the peptide that was shown to contain the VFF18 epitope could be observed (data not shown). This observation strongly indicates that the VFF18 epitope with valine at position 167 instead of glutamine is not recognized by the antibody.

To establish the presence of these three epitope sequences *in vivo*, the genomic exon v6 sequence of several HNSCC tumor cell lines and of normal keratinocytes from control persons was determined. As shown in Table 2, the sequence described by Kugelman *et al.* [114], which showed a lower affinity for MAb U36, was not found. All sequences had –gag– in the first variable position, encoding glutamic acid at position 367. Resequencing of the epican-encoding clone pKG1, described by Kugelman *et al.* [114] (which was a generous gift from dr. L.M. Milstone), revealed that this variant was the result of a sequencing artefact. In contrast, the other two variants with –gag– in the first variable position, encoding glutamic acid and –aaa– or –aga– in the second variable position encoding lysine or arginine, respectively, were both observed *in vivo*. Both sequence variants were often present in the same cell line sample or in the same normal cell sample of a control person, indicating that this variation is probably due to allelic polymorphism. Remarkably, only –aga– and not –aaa– homozygotes were found, although this could be due to the relatively low number of cell lines and control persons that were screened. Although only a few cell lines were analyzed, we have no indications that one of the variable sequences is more frequently present in malignant cells.

Table 2 Genomic CD44 sequence of several HNSCC cell lines and normal keratinocytes of control persons. The number of clones that were sequenced and the sequence they contained are indicated.

Cell type		Amino acid 367		Amino acid 374	
		gtg (V)	gag (E)	aaa (K)	aga (R)
HNSCC cell lines	UM-SCC-22A ¹	0	5	2	3
	UM-SCC-22B ²	0	6	3	3
	UM-SCC-11B ¹	0	7	0	7
	UM-SCC-14C ³	0	4	2	2
	UM-SCC-35 ¹	0	7	0	7
Normal Keratinocytes	Control 1	0	8	0	8
	Control 2	0	4	2	2
	Control 3	0	5	2	3
	Control 4	0	5	3	2

¹Cell line derived from a primary tumor (hypopharynx). ²Cell line derived from a lymph node metastasis (primary site: hypopharynx). ³Cell line derived from a skin metastasis (primary site: floor of the mouth).

Acknowledgements

We are grateful to dr. L.M. Milstone (Department of Dermatology, Yale University School of Medicine, New Haven, USA), who kindly provided us with their full-length epican clone pKG1 and sequence data.

Chapter 4

Characterization of CD44v6 isoforms in head and neck squamous cell carcinoma

Nicole L.W. van Hal

Guus A.M.S. van Dongen

Marijke Stigter-van Walsum

Gordon B. Snow

Ruud H. Brakenhoff

Submitted

Summary

CD44 splice variants, especially those containing the v6 domain, are assumed to play a critical role in the malignant progression of many human tumors. This concept was based on (a) the aberrant expression of CD44v6 in malignant cells, often encoded by alternatively spliced transcripts, and (b) the absence of CD44v6 expression in the corresponding normal tissues. Remarkably, data on CD44v6 expression in squamous cells do not support this hypothesis: the v6 domain is already highly expressed in normal squamous tissues and even a downregulation in the majority of squamous cell carcinomas of the head and neck (HNSCC) has been described. In this Chapter, we compared the v6 expression of normal oral mucosa and HNSCC in a qualitative and quantitative way, firstly to elucidate the observed downregulation of CD44v6 expression in HNSCC, and secondly to characterize the v6-encoding splice variants.

Immunohistochemistry was performed on a large panel of HNSCC cell lines and tumors using three different anti-v6 antibodies (U36, U39 and VFF18). The v6-encoding splice variants were characterized by screening a cDNA library of a human HNSCC cell line and reverse transcriptase-polymerase chain reaction (RT-PCR) on HNSCC cell lines, microdissected normal mucosa as well as HNSCC primary tumors and metastases.

These analyzes revealed that there is no, or only marginal downregulation of CD44v6 in HNSCC. About 97% of the primary HNSCC tumors showed a high and homogeneous staining pattern (U36: 270/277; U39: 268/277 tumors with more than 50% positive cells). Furthermore, it appeared that the v6-containing CD44 splice variants present in HNSCC primary tumors and metastases are identical to those expressed in normal mucosa. These data indicate that v6-containing as well as other CD44 splice variants do not play a role in the malignant progression of HNSCC.

Introduction

A variety of tumor-associated proteins has been described during the last decades, which are of interest for tumor detection and therapy [291-294]. In tumor therapy, these proteins might be used as a target antigen for immunotherapy, for example by using antibodies conjugated with radionuclides, toxins, cytotoxic drugs or enzymes [74]. For diagnostic purposes immunocyto(histo)chemical or polymerase chain reaction (PCR)-based techniques can be developed to detect these tumor-associated proteins or the transcripts encoding them as a marker for the presence of tumor cells. Moreover, some tumor-associated proteins have been shown to be useful as a serum marker [295,296]. A protein family, which seems to be specifically associated with several human tumor types and which might be applicable as indicated above, is CD44.

The CD44 protein family consists of an assortment of protein isoforms encoded by alternatively spliced transcripts of a single gene [115]. In most cells, such as cells of the hemopoietic lineage, the standard form (CD44s) of the molecule is expressed, which is the isoform without variant domains. In addition to CD44s, several tissues also express larger CD44 isoforms, encoded by alternatively spliced transcripts. CD44 isoform expression appears to be tissue dependent, which relies on a tissue-specific splicing mechanism rather than on differential gene activation.

Interestingly, it has been established in numerous reports that tumor-specific CD44 splice variants are expressed in malignant cells, especially variants containing the v6 domain, indicating that the differential splicing machinery is disorganized [233,267-269,297]. This notion directed the exploitation of this domain for tumor detection and therapy [60,277]. The biological significance of these isoforms was stressed in model experiments showing that v6-containing splice variants were able to confer metastatic potential upon tumor cells [109]. In addition, the prognostic significance of CD44v6 expression in for example non-Hodgkin lymphoma, breast carcinoma and colon carcinoma further substantiated the hypothesis that CD44 plays a critical role in the malignant progression of many human tumors [138,228,234].

Remarkably, the situation in squamous cells does not support this hypothesis. In contrast to other normal tissues, the expression of the v6 domain in normal squamous cells is homogeneous and high. The role of CD44 in HNSCC seems even more confusing as several groups reported that the expression of

CD44v6 is down regulated during the development of tumors of squamocellular origin [288,298,299]. This downregulation, observed by immunohistochemistry, could result from (a) differential glycosylation of the molecule by malignant cells and thus masking the epitope recognized by the used antibody, (b) diminished gene transcription, (c) a switch in the expression of splice variants, or (d) a combination of these biological mechanisms.

In this Chapter, we present a detailed qualitative and quantitative analysis of the CD44v6 expression in normal as well as malignant squamous cells, firstly to explain the observed downregulation of CD44v6 expression in HNSCC, and secondly to identify the v6-encoding splice variants. To evaluate CD44v6 expression on normal oral mucosa and HNSCC, a large panel of tissues was immunohistochemically stained with 3 monoclonal antibodies (MAbs) directed against different epitopes of the v6 domain. The v6-encoding splice variants were characterized by RT-PCR and sequencing of PCR fragments from microdissected normal and malignant tissues. To exclude putative stroma or lymphocyte contamination, the analysis was extended to HNSCC cell lines using similar and more profound techniques to confirm and validate the data.

Materials and methods

Anti-CD44v6 monoclonal antibodies

Immunocytochemical and immunohistochemical stainings were performed with the anti-CD44v6 monoclonal antibodies U36, U39 and VFF18. MAb U36 was obtained from Centocor (Leiden, The Netherlands), MAb U39 was produced and purified by in house procedures and MAb VFF18 (also called BIWA-1) was obtained from Bender MedSystems (Vienna, Austria). According to the numbering of Kugelman *et al.* [114], the epitope recognized by MAb U36 consists of amino acids 365-376 (Chapter 2), the epitope recognized by MAb U39 consists of amino acids 356-367 (Chapter 2) and the epitope recognized by MAb VFF18 consists of amino acids 360-370 [60].

Immunohistochemical staining of frozen tissue sections

Cryosections (6 μ m) of tumors and normal tissues were mounted on glass slides coated with a solution containing 0.5% gelatin and 1 mM chromium (III) potassium sulfate, air dried for 1 hr and fixed with freshly prepared 2% para-

formaldehyde in phosphate buffered saline (PBS) for 10 min. The sections were rinsed for 5 min with PBS, and pre-incubated for 30 min with normal rabbit serum (NRS; DAKO, Glostrup, Denmark) diluted 1:50 in PBS with 1% bovine serum albumin (1% BSA/PBS). Subsequently, the sections were incubated for 1 hr with anti-CD44v6 specific antibody (MAb U36, U39 or VFF18) diluted to 10 μ g/ml in 1% BSA/PBS, followed by 1 hr incubation with rabbit anti-mouse immunoglobulin peroxidase conjugate (RAMPO; DAKO) diluted 1:100 in 1% BSA/PBS. Between all incubation steps the sections were rinsed three times for 5 min with PBS. Finally, the sections were stained for 5 min with a solution containing 1 mg/ml 3,3'-diaminobenzidine (DAB; Sigma, Bornem, Belgium) and 0.1% H₂O₂ in PBS. After rinsing the sections once with PBS, the nuclei were counter stained with haematoxylin for 45 sec. Stained sections were washed with running tap water and covered with Kaiser's glycerol gelatin. The staining pattern of the sections was scored semi-quantitatively by two independent observers. In 80-90% of the cases the scoring was similar. For differences a consensus was reached. Since all cells, when positive, showed an intense staining, tumors were classified only depending on the percentage of positive cells (0-10%, 10-50%, 50-90% or 90-100%). Keratinized parts were excluded from scoring.

Cell culture

HNSCC cell lines (UM-SCC-14A, UM-SCC-14B, UM-SCC-14C, UM-SCC-22A, UM-SCC-22B, UM-SCC-11B and UM-SCC-35) were cultured in Dulbecco's modified Eagle's medium (DMEM; Gibco Life Technologies, Breda, The Netherlands) supplemented with 5% fetal calf serum (FCS; Hyclone Laboratories, Logan, UT), 16 mM NaHCO₃, 15 mM HEPES (pH 7.4), 2 mM L-glutamine, 1% penicillin and 1% streptomycin. The UM-SCC cell lines were kindly provided by dr. T.E. Carey (Ann Harbor, MI). The origin of the HNSCC cell lines is summarized in Table 3.

Immunocytochemical staining of HNSCC cell lines

As the MAb U36 epitope is trypsin sensitive, cells were stained *in situ*. Cells were seeded in 6-well tissue culture plates (Costar, Badhoevedorp, The Netherlands) at a density of 0.5×10^5 cells/well a few days before staining. After fixing the cells with freshly prepared 2% paraformaldehyde (pH 7.2-7.4) in PBS for 10 min, the cells were stained by alkaline-phosphatase anti-alkaline-phosphatase (APAAP) as described previously [281], using the anti-CD44v6 MAbs U36 and VFF18 as first

antibody. Endogenous enzyme activity was inhibited by adding 1 mM levamisole (Sigma) to the substrate. Staining was scored semi-quantitatively by two independent observers. Since all HNSCC cell lines showed a homogeneous staining, the staining intensity was classified into the following 5 categories: 0) no staining, 1) weak staining, 2) moderate staining, 3) intense staining and 4) very intense staining.

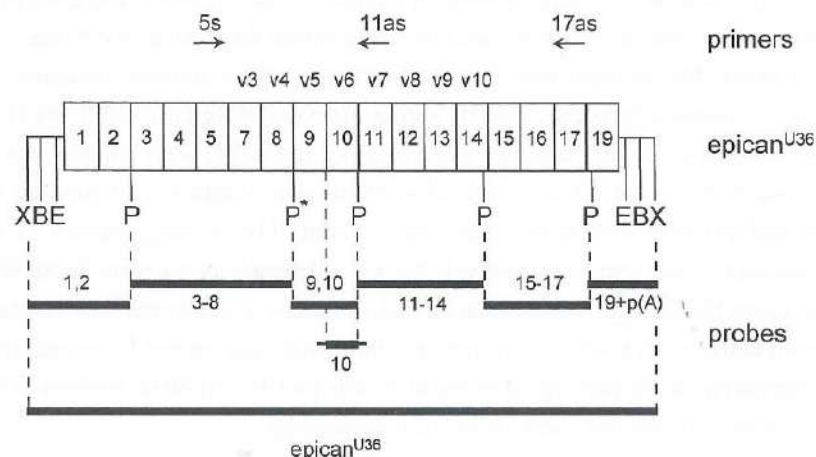


Figure 1 Physical map of the *epican*^{U36} (CD44v3-v10) cDNA construct. The location of the primers, the restriction sites *EcoRI* (E), *BstXI* (B), *PstI* (P) and *XhoI* (X) as well as the probes used in the experiments are indicated. The exon 10 (v6) probe was made by subcloning the PCR-product obtained by amplification on chromosomal DNA using primers corresponding to the intron 9/exon 10 and exon 10/intron 10 boundary, respectively. The other probes were made by subcloning the *PstI* and *XhoI* restriction fragments. Note that the *PstI* restriction pattern of the *epican*^{U36} (CD44v3-v10) clone is slightly different from the one described by Kugelman *et al.* [114]. An alternative 3' splice site in intron 8 (shifted 3 bases upstream) results in an additional *PstI* site, indicated with an asterisk).

Probes

In Fig. 1, the probes are depicted that were used for the library screening, RT-PCR analysis and Northern blot hybridization. The exon 10 (v6) probe was constructed by subcloning the PCR-product amplified with a sense primer identical to the sequence of the intron 9/exon 10 boundary (5'-GGAATTCCTGATATTCT-TCTCAGTCCAGGC-3') and an antisense primer complementary to the sequence of the exon 10/intron 10 boundary (5'-GCTCTAGACTTGTTAAACCA-

TCCATTACCAGC-3') using UM-SCC-22A chromosomal DNA as template. The primers contained additional restriction sites (*EcoRI* and *XbaI*, respectively) to facilitate subcloning. All other region-specific probes were made by subcloning the *PstI* (P) and *XhoI* (X) restriction fragments of the *epican*^{U36} (CD44v3-v10) clone (Chapter 2). DNA digests of the various subclones were run on an NA agarose gel (Pharmacia LKB, Uppsala, Sweden), bands were cut out of the gel and frozen. The frozen blocks were squeezed between parafilm, followed by a phenol/chloroform/ isoamyl alcohol (25:24:1) extraction and ethanol precipitation [282]. The isolated inserts were labeled with [α -³²P]dCTP by random primer elongation [301] using the Klenow fragment of DNA polymerase I (Boehringer Mannheim, Almere, The Netherlands).

Northern blot analysis

Total RNA was extracted from HNSCC cell lines using RNAzol (Campro Scientific, Veenendaal, The Netherlands) according to the supplier. Of each sample, 20 μ g of RNA was separated on a 1.0% (w/v) agarose/formaldehyde gel and transferred to a positively charged nylon membrane (Qiabrane; Westburg, Leusden, The Netherlands) using 10 \times saline sodium citrate (10 \times SSC) as transfer buffer according to Sambrook *et al.* [282]. The filters were baked for 2 hr at 80°C, prehybridized for 1 hr at 65°C in hybridization solution (containing 0.5 M Na₂HPO₄, pH 7.2, 7% sodium dodecyl sulfate (SDS), 1 mM EDTA) and subsequently hybridized overnight at 65°C after addition of the ³²P-labeled probe. A cDNA clone encoding murine GAPDH was used as a probe to check the RNA content and quality of the samples. After 2 washes with 2 \times SSC/0.01% SDS, and 2 washes with 0.2 \times SSC/0.01% SDS at 65°C, the blot was exposed to Kodak X-AR 5 film and autoradiographed for 2 weeks at -80°C using intensifying screens. Signals were quantified by phosphor-imaging.

Screening of the UM-SCC-22A cDNA library

Construction of the cDNA library in shuttle vector pCDM8 by use of non-self complementary *EcoRI*/*BstXI* adaptors (Invitrogen, Leek, The Netherlands) as well as the subsequent transformation into *E. coli* K12 MC1061/P3 by electroporation have been described previously [281].

The library was plated onto LB-agar plates containing 40 μ g/ml kanamycin, 7.5 μ g/ml tetracyclin (both from Boehringer Mannheim), and 12.5 μ g/ml ampicillin (Sigma, Bornem, Belgium). In total about 1.8 \times 10⁶ clones were screened

by hybridization of colony-lifts on nitrocellulose [282] with the ^{32}P -labeled isolated insert of the epican^{U36} (CD44v3-v10) clone as a probe (Fig. 1; see also Chapter 2). The hybridizing clones were purified and the cDNA inserts characterized by physical mapping of their *Pst*I/*Xho*I restriction pattern in combination with Southern blot analysis using the ^{32}P -labeled probes indicated in Fig. 1, and partial sequence analysis. The hybridization pattern was combined with the sequence information to establish the presence and order of the alternatively spliced exons in the cDNA inserts. Sequencing was performed, using a DyeDeoxy Terminator Cycle Sequencing Kit (Perkin Elmer, Gouda, The Netherlands) and an Applied Biosystems 373A DNA Sequencer (Applied Biosystems, Maarssen, The Netherlands).

Microdissection

Frozen sections (10 μm) of normal and malignant tissues were stained for 15 sec with a solution containing 1% toluidine blue and 0.2% methylene blue. After rinsing with millipore filtered water, microdissection was carried out immediately, using a Zeiss Stemi SV 11 stereo-microscope. Microdissection was performed in duplicate, for each sample 2–5 areas of tumor or normal tissue were dissected, depending on the size of these regions. Microdissected tissue was stored on ice until RNA was isolated.

RNA isolation, reverse transcription and PCR amplification

RNA was extracted from microdissected cryosections or from cultured HNSCC cells using RNeasy (Qiagen) according to the supplier. For the microdissected cryosections, this procedure was scaled down to a volume of 100 μl RNeasy, and 5 μg glycogen was added as a carrier. The RNA pellets of the microdissected tissues were dissolved in 25 μl water. First strand cDNA was synthesized from 5 μl of the RNA sample obtained from microdissected tissue. For the HNSCC cell lines first strand cDNA synthesis was carried out with 10 ng of RNA. The RNA samples were heated for 3 min at 70°C and immediately put on ice. The RNA was reverse transcribed to cDNA by AMV reverse transcriptase (Promega, Leiden, The Netherlands), using oligonucleotides complementary to a sequence in exon 11 (11as: 5'-CTTCCTGCTTGATGACCTCGTCC-3') or exon 17 (17as: 5'-CAAAGCCAAGGCCAAGAGGGATGC-3') as primers. The reverse transcription reaction was performed in a volume of 20 μl and contained 1 mM deoxyribonucleoside triphosphates, 1 mM DTT, 50 mM TRIS-HCl pH 8.3, 60 mM

KCl, 3 mM MgCl_2 , 1.25 μM antisense primer, 2 U RNasin (Promega) and 0.75 U AMV reverse transcriptase (Promega). The reactions were incubated for 2 hr at 42°C.

The obtained cDNA products were used as a template for PCR amplification using the same antisense primer and a sense primer located in exon 5 (5s: 5'-TGTCCAGAAAGGAGAATACAGAACG-3'). The RT-PCR reactions were performed in a total volume of 50 μl using 5 μl of the cDNA product as template. The final concentrations in the RT-PCR reactions were: 200 μM deoxyribonucleoside triphosphates, 0.625 μM antisense primer, 0.5 μM sense primer, 10 mM TRIS-HCl pH 8.3, 50 mM KCl and 1.5 mM MgCl_2 . To the negative control, water was added instead of RNA template. As a positive control PCR-amplification was performed on the epican^{U36} (CD44v3-v10) clone (100 pg) using the same primer pairs. To check the quality of the RNA, an RT-PCR reaction was performed in parallel using Abelson primers [302]. Strict precautions were taken to prevent carry-over contamination. PCR-mix pipetting, RNA isolation/cDNA synthesis and PCR amplification were carried out in three separate laboratories. The PCR conditions used were as described by Hudson *et al.* [190] with a 'hot start' of 5 min at 95°C and cooling to 72°C. Subsequently, 1 U AmpliTaq DNA polymerase (Perkin Elmer) was added. This was followed by 3 min 57°C, 3 min 72°C, 30 cycles of 1 min 94°C, 1 min 57°C, 2 min 72°C and subsequently a final incubation of 4 min 72°C. PCR amplification was performed on a Hybaid Omnigene thermal cycler (Biozym, Landgraaf, The Netherlands) with paraffin oil to prevent evaporation. Ten μl of the reaction mixtures was loaded on an 1.5% (5s/11as amplification products) or an 1% (5s/17as amplification products) agarose gel and transferred to a charged nylon membrane (Qiabran; Westburg) using a transfer buffer containing 0.4 M sodium hydroxide and 0.6 M sodium chloride according to the protocol of Sambrook *et al.* [282]. The filters were hybridized as described for the Northern blots, using exon 10 (v6) or the epican^{U36} (CD44v3-v10) cDNA as probes (Fig. 1). Finally, the membranes were exposed to Kodak X-AR 5 film and autoradiographed for 1–2 hr at room temperature using intensifying screens.

Results

CD44v6 antigen expression in normal oral mucosa and HNSCC: immunohistochemical analysis

Immunohistochemical staining of normal tissues showed that CD44v6 isoforms are highly expressed on the epithelial cells of normal oral mucosa and skin, except for the keratinized squames which were negative (Fig. 2a). Staining of the tumors was equally intense as the normal tissues. In Fig. 2b the MAb U36 staining pattern of a primary HNSCC tumor is shown and in Fig. 2c the staining pattern of an HNSCC metastasis. Please note that in keratinizing areas of primary tumors and metastases a lack of v6-staining can be observed (Fig. 2b). As this is similar in normal mucosa and skin, these keratinized parts were excluded from scoring. The reactivity of MAb U36 and a second anti-v6 MAb designated U39 was analyzed on frozen sections of 277 primary HNSCC tumors. The results of the scoring are summarized in Table 1. In addition, 61 of these sections were stained with a third anti-v6 antibody, MAb VFF18. Very similar results were obtained for the three different anti-CD44v6 antibodies (data not shown). For all antibodies about 97% of the tumors showed a high and homogeneous staining pattern (>50% positive cells).

Table 1 Immunohistochemical staining of primary HNSCC tumors using the anti-CD44v6 MAbs U36 and U39.

positive cells (%) ¹	U36	U39
0-10	3	3
10-50	4	6
50-90	106	104
90-100	164	164
Total number of tumors:	277	277

¹Stained tumors were scored semi-quantitatively by two independent observers. Tumors were classified depending on the percentage of positive cells only, since all positive cells showed a similarly strong staining.

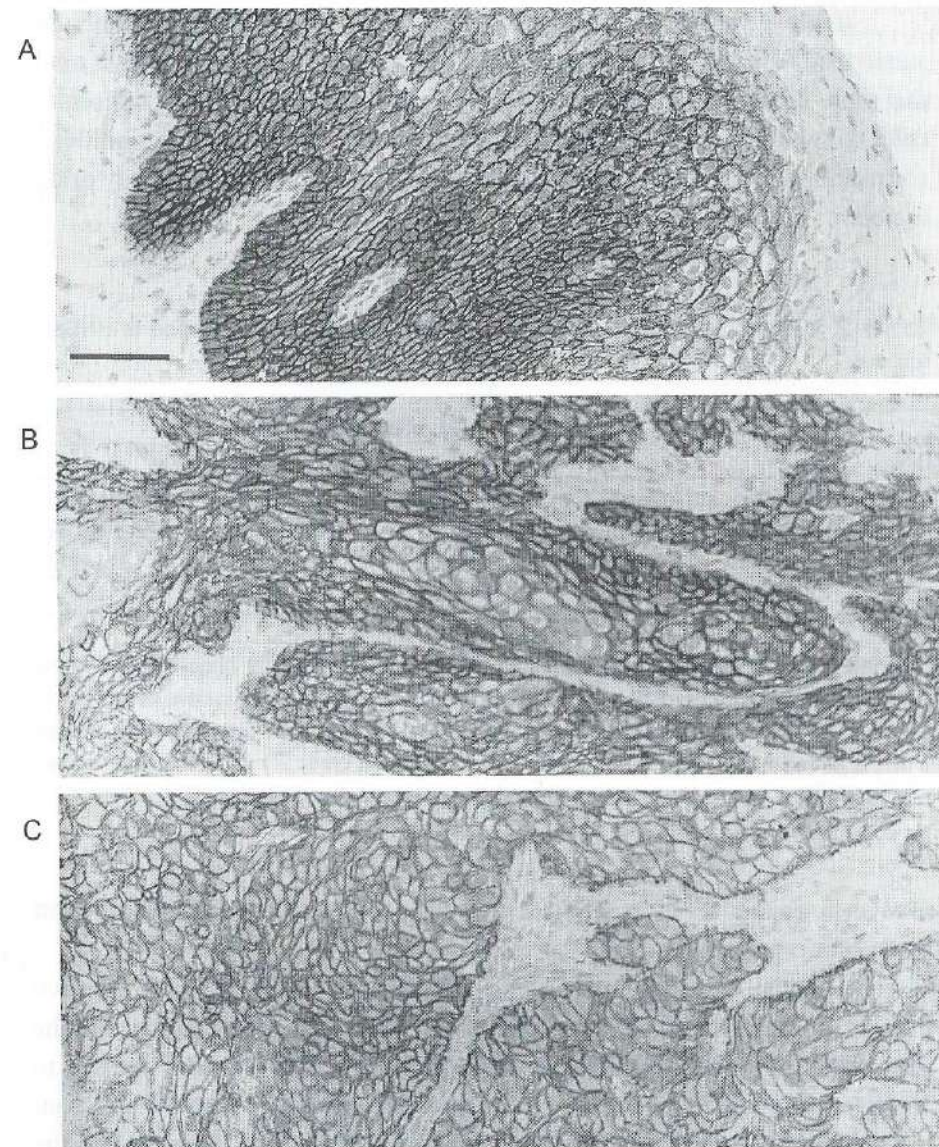


Figure 2 Immunohistochemical staining with anti-CD44v6 MAb U36 on frozen sections of (A) normal oral mucosa, (B) a primary HNSCC tumor and (C) an HNSCC metastasis. HNSCC primary tumors and metastases show an intense and homogeneous staining pattern. For the normal oral mucosa, immunoreactivity is observed in all layers except for the superficial layers, which are negative. Staining results obtained with anti-CD44v6 MAbs VFF18 or U39 were identical. Scale bar represents 50 μ m.

Table 2 shows the staining results of MAb U36 when the tumors are subdivided based on their histological grade. The results indicated a slight trend that more differentiated tumors (grade 1) show a higher percentage of positive cells. However, based on these data we were not able to find a significant correlation between the histological grade and CD44v6 staining intensity of the tumors.

Table 2 Correlation between CD44v6 expression and histological grade of HNSCC tumors

Grade ²	n	MAb U36 staining intensity ¹			
		1	2	3	4
1	22 (100%)	0 (0%)	0 (0%)	4 (18%)	18 (81%)
2	175 (100%)	1 (0.8%)	1 (0.8%)	66 (38%)	107 (61%)
3	80 (100%)	2 (2.5%)	3 (3.8%)	36 (45%)	39 (49%)
total	277	3	4	106	164

¹Stained tumors were scored semi-quantitatively by two independent observers, using the following 4 categories: 1: 0-10%, 2: 10-50%, 3: 50-90% and 4: 90-100% positive cells. Tumors were classified depending on the percentage of positive cells only, since all positive cells showed a similar strong staining. ²grade 1: well differentiated tumors, grade 2: moderately differentiated tumors, grade 3: poorly differentiated or undifferentiated/anaplastic tumors.

CD44v6 expression level in HNSCC cell lines: immunocytochemical and Northern blot analysis

Although almost all tumors show a high and homogeneous CD44v6 expression, we could not exclude that there is a considerable difference in the expression of splice variants encoding this domain. We therefore decided to identify and characterize the splice variants expressed by normal and malignant squamous cells by RNA-based methodologies. Initially, we characterized the CD44v6 transcripts expressed in HNSCC cell lines, in part to enable RNA analysis by Northern blotting and to characterize the splice variants by classical cDNA cloning, and in part to exclude a confounding role of stromal elements or infiltrating lymphocytes in tumors. A panel of cell lines derived from various sources (primary tumors, recurrences and lymph node metastasis) was selected and stained immunocytochemically with the anti CD44v6 MAbs U36 and VFF18. The

staining results were scored semi-quantitatively. Quantitative analysis of antigen expression by fluorescence-activated cell sorting (FACS)-analysis was not possible because *in vitro* cultured HNSCC cells can only be detached by the use of trypsin, which destroys the epitopes of MAb U36 and VFF18. The results of the staining are shown in Table 3. For all HNSCC cell lines, 100% of the cells showed an intense staining pattern. Only a minor variation in staining intensity was observed between the various cell lines. No correlation was found between the staining intensity and the origin of the cell lines (primary tumor, recurrence or metastasis).

To obtain a semi-quantitative estimation of the expression level of the v6-containing CD44 transcripts, a Northern blot of the HNSCC cell lines was hybridized with a specific probe of exon 10 (v6). Quantification of the intensities by phosphor-imaging revealed that from the HNSCC cell lines tested, UM-SCC-14A, UM-SCC-14B and UM-SCC-14C showed the weakest signals on Northern blot, which is consistent with the immunocytochemical results (Table 3). A typical example is shown in Fig. 3. For all HNSCC cell lines, Northern blot analysis showed the presence of three main transcripts of about 2.5, 3.0 and 5.5 kb, respectively, after hybridization with the exon 10 (v6) probe. In addition to these

Table 3 Origin of the HNSCC cell lines, the results of immunocytochemical staining using anti-CD44v6 MAbs U36 and VFF18, and the quantitative results of Northern blot hybridization with the exon 10 (v6) probe.

Cell line ¹	Primary tumor	Specimen site	Staining Intensity ²	Intensity on Northern (%) ³
UM-SCC-14A	floor of the mouth	local recurrence	3	45
UM-SCC-14B	floor of the mouth	local recurrence	3	45
UM-SCC-14C	floor of the mouth	local recurrence	4	45
UM-SCC-22A	hypopharynx	primary tumor	4	50
UM-SCC-22B	hypopharynx	lymph node metastasis	4	100
UM-SCC-11B	hypopharynx	primary tumor	4	85
UM-SCC-35	oropharynx	primary tumor	4	75

¹Characteristics of the tumor cell lines are from Carey *et al.* [300]. ²Staining results with MAb U36 and VFF18 were identical. For all cell lines, 100% of the cells was positively stained. The staining intensity was classified into 5 categories: 0) no staining, 1) weak staining, 2) moderate staining, 3) intense staining and 4) very intense staining. ³Intensity of the signal on Northern blot after hybridization with a specific probe of exon 10 (v6), relative to the UM-SCC-22B signal, as determined by phosphor-imaging.

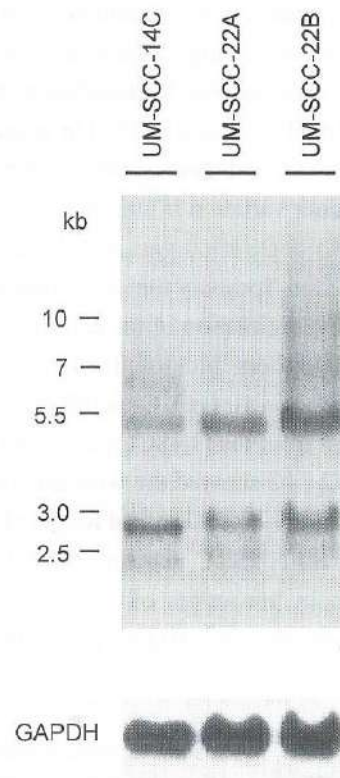


Figure 3 Northern blot analysis of the HNSCC cell lines UM-SCC-14C, UM-SCC-22A and UM-SCC-22B, hybridized with the exon 10 (v6) probe. The cDNA encoding murine GAPDH was used as a probe to check the amount of RNA loaded on the gel. Calculated sizes of the various transcripts are indicated on the left in kb.

three main transcripts, two larger transcripts of about 7 and 10 kb were detected. An identical hybridization pattern was obtained when the isolated epican^{U36} (CD44v3-v10) insert was used as probe, indicating that the HNSCC cell lines mainly express v6-containing transcripts. To confirm that the three mRNA bands resulted from the use of the three different polyadenylation sites that have been described by Shtivelman and Bishop [127] for CD44s, the Northern blot was hybridized with a specific probe derived from the cDNA clone HT5 [127]. This probe, which contains the most 3' end of exon 19, only detected the 5.5 kb transcripts. Based on this observation, we concluded that the differences in

transcript length could indeed be attributed to the differential polyadenylation (data not shown). Due to the relatively small size differences between transcripts encoding different CD44 isoforms, Northern blot analysis does not allow a detailed analysis of the v6-containing CD44 splice variants that are expressed. Therefore, cDNA library screening and RT-PCR were performed in addition.

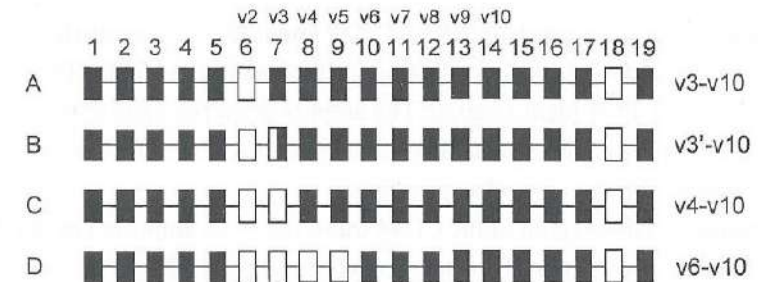


Figure 4 Schematic representation of the CD44 clones isolated by screening the cDNA library of the HNSCC cell line UM-SCC-22A with the ³²P-labeled epican^{U36} (CD44v3-v10) cDNA as probe. The 19 exons of the CD44 gene are indicated by boxes. Open boxes indicate exons that were absent in the various cDNA clones. The cDNA clones were all incomplete clones, starting in exons 1-5.

Molecular cloning of v6-containing CD44 transcripts from HNSCC cell line UM-SCC-22A

Cell line UM-SCC-22A was chosen as a representative HNSCC cell line for identification of CD44 transcripts by cDNA library screening. Several v6-containing CD44 transcripts could be identified (Fig. 4). The cDNA clones were all incomplete clones, missing part of the first exons. A number of cDNA clones were found starting in exon 7 (v3), 10 (v6) or 12 (v8), which could have been derived from several CD44 transcripts. Of the cDNA clones starting in exons 1-5, most clones appeared to contain cDNA inserts with an exon 5 to exon 7 (v3) transition (variant CD44v3-v10; Fig. 4a). In addition, a few other v6-containing cDNA clones were identified. Firstly, clones containing cDNAs spliced from exon 5 to an alternative 3' splice site in exon 7 (v3) were found (variant CD44v3'-v10; Fig. 4b), a variant already described by Screaton *et al.* [115]. Secondly, clones containing cDNAs spliced from exon 5 to exon 8 (v4) were observed (variant CD44v4-v10; Fig. 4c). Moreover, we found clones containing cDNAs with an

alternative splice from exon 5 to exon 10 (v6) (variant CD44v6-v10; Fig. 4d). All these alternatively spliced variants maintained an open reading frame, enabling protein translation in all cases. The clones also varied in the size of the non-coding sequence at the 3' end of exon 19. This variation was also observed on the Northern blots and is due to the presence of three separate polyadenylation sites [127].

V6-containing CD44 transcripts in HNSCC cell lines: RT-PCR analysis

To compare the various v6-containing CD44 transcripts in all HNSCC cell lines, we used RT-PCR identification. The amplification products obtained were compared with the splice variants identified by the cDNA library screening or characterized by subcloning and sequencing.

The complete variable region of the CD44 transcripts was amplified by RT-PCR using a 5s/17as primer pair. To select for v6-containing CD44 transcripts, the obtained amplification products were hybridized with an exon 10 (v6) probe. As shown in Fig. 5a, amplification resulted in products of about 1400 bp and 1000 bp. Subcloning the 1400 bp RT-PCR product from the HNSCC cell line UM-SCC-11B resulted only in fragments containing exons 5 and 7-17 (variant CD44v3-v10, calculated size of the PCR fragment: 1393 bp; Fig. 4a). From the tailing part of the 1400 bp band also a PCR-product containing exon 6 (v2), which is not present in variant CD44v3-v10, was subcloned (variant CD44v2-v10; calculated size of the PCR fragment: 1522 bp). Although not identified by subcloning, we cannot exclude that this 1400 bp band contains several other minor amplification products, (variants CD44v3'-v10 and CD44v4-v10 as identified in the UM-SCC-22A cDNA library summarized in Fig. 4, calculated sizes of these PCR products: 1369 bp and 1267 bp, respectively). The 1000 bp band, which was also intense in all cell lines, is most likely the amplification product spliced from exon 5 to exon 10. Firstly, the calculated size of this transcript is 1036 bp. Secondly, screening of the cDNA library showed that this transcript is indeed expressed in HNSCC cell lines (variant CD44v6-v10; Fig. 4d). Finally, subcloning of an 5s/17as amplification product from the colon carcinoma cell line WiDr, which had exactly the same size on gel, showed that it indeed contained exons 5 and 10-17 (Chapter 5).

For a more refined analysis of the large v6-containing CD44 transcripts resulting in 5s/17as amplification products of about 1400 bp, an additional RT-PCR was performed using a 5s/11as primer pair. Fig. 5b shows the amplification

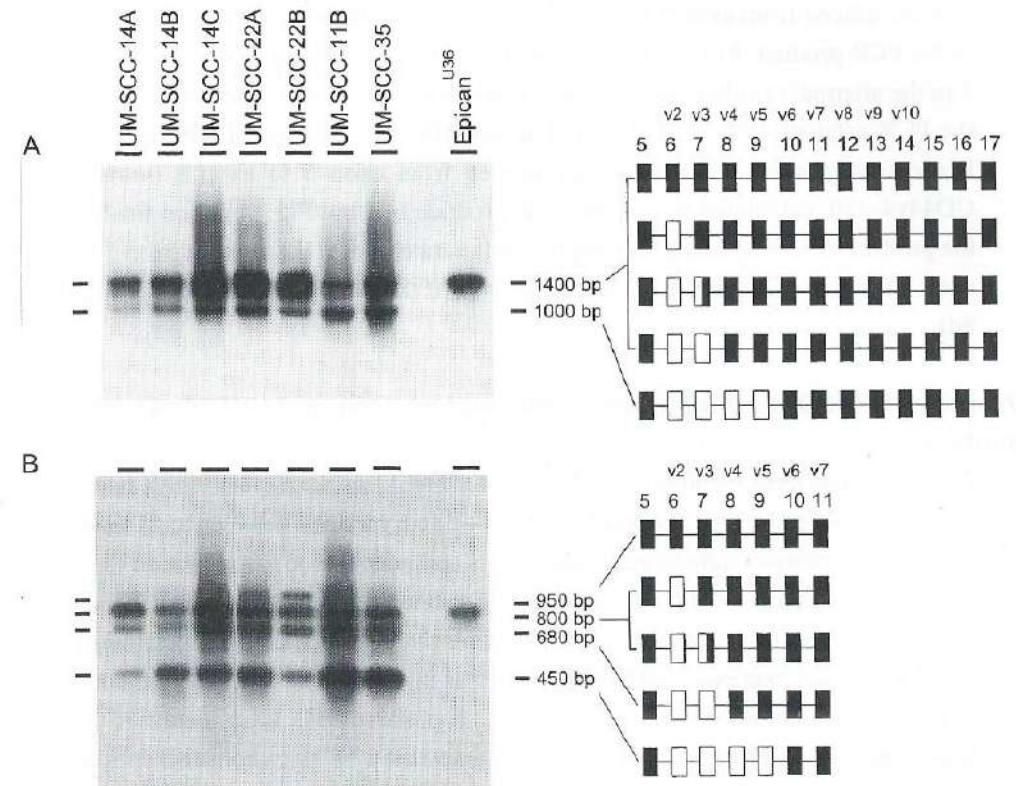


Figure 5 Southern blot analysis of RT-PCR amplification products from HNSCC cell lines using the primer pairs: (A) 5s/17as and (B) 5s/11as. The filters were hybridized with a specific probe of exon 10 (v6). The cell lines are indicated on top. The PCR fragment amplified on the epican^{U36} (CD44v3-v10) clone as template was run in parallel. The various splice variants are indicated on the right.

pattern after hybridization with the exon 10 (v6) probe. In all HNSCC cell lines, four major hybridizing amplification products of 950, 800, 680 and 450 bp were observed. The size of the 950 bp band corresponds to the expected size of an amplification product containing exons 5-11 (variant CD44v2-v10, calculated size of the PCR product: 942 bp), a variant which was already identified by subcloning the >1400 bp 5s/17as amplification product of the cell line UM-SCC-11B. The 800 bp hybridizing fragment is most likely the amplification product of transcripts

that are spliced from exon 5 to exon 7(v3) (variant CD44v3-v10, calculated size of the PCR product: 813 bp; Fig. 4a) and the transcript with the splice from exon 5 to the alternative splice site in exon 7 (variant CD44v3'-v10, calculated size of the PCR product: 789 bp; Fig. 4b). The amplification product of 680 bp most likely corresponds with a transcript spliced from exon 5 to exon 8 (variant CD44v4-v10, calculated size of the PCR product: 687 bp; Fig. 4c). And finally, the product of 450 bp could well represent the transcript splicing from exon 5 to exon 10 (variant CD44v6-v10, calculated size of the PCR product: 456 bp; Fig. 4d).

V6-containing CD44 transcripts in normal oral mucosa and HNSCC: RT-PCR analysis

Summarized, it can be concluded that there is neither a quantitative nor a qualitative difference in the expression of splice variants between cell lines derived from primary tumors, recurrent tumors and lymph node metastasis. In fact, there was no difference with normal primary keratinocytes in culture as well, based on Northern blotting (not shown). Therefore, we characterized the (v6-containing) CD44 transcripts expressed in HNSCC as well as in normal oral mucosa from non-cancer controls by RT-PCR analysis. First, v6 positive cells were identified in frozen sections of normal or malignant squamous tissue by immunohistochemical staining. Then, on a parallel set of frozen sections, microdissection was performed to isolate a pure squamous cell population (estimated to be more than 80%).

Fig. 6a shows the amplification products obtained by RT-PCR using the 5s/17as primer pair after hybridization with the exon 10 (v6) probe. The RT-PCR patterns of the microdissected tumor tissues were similar to that of the HNSCC cell lines, showing a main amplification band of about 1400 bp and a less intense band of 1000 bp. As shown in Fig. 6a normal mucosa, primary tumors and their corresponding metastases showed all identical amplification patterns.

In Fig. 6b, a more refined analysis of the large v6-containing CD44 transcripts in normal oral mucosa and HNSCC tumors is shown, obtained by amplification with the 5s/11as primer pair and hybridization with the exon 10 (v6) probe. The tissue samples showed identical amplification products as the HNSCC tumor cell lines: fragments of 950, 800, 680 and 450 bp. Again no difference was observed between the normal oral mucosa samples and the primary and metastatic tumor samples.

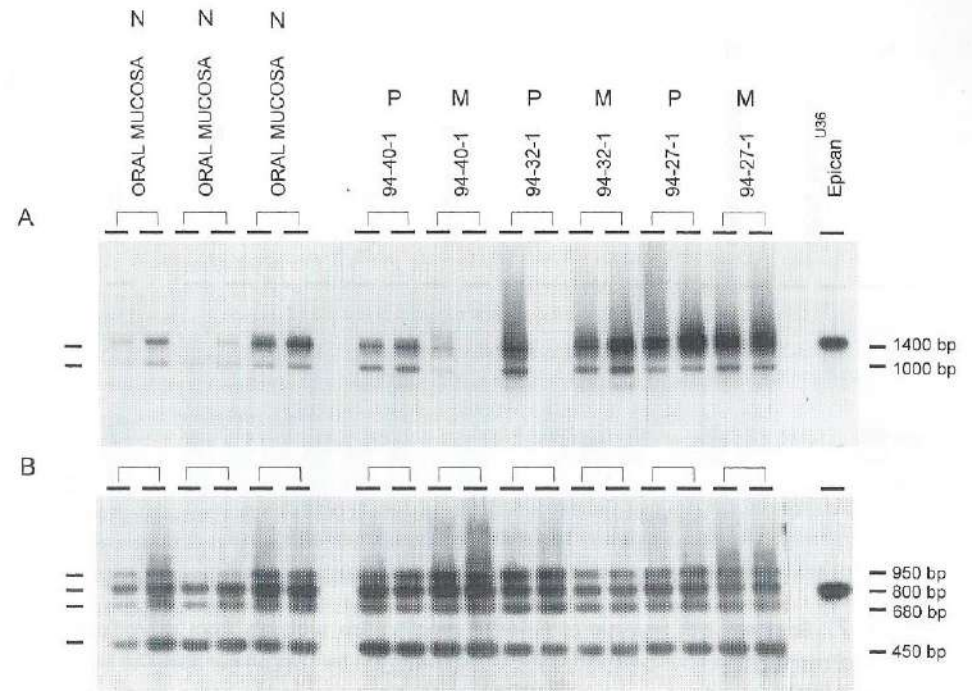


Figure 6 Southern blot analysis of RT-PCR amplification products from microdissected samples of normal squamous cells and HNSCC cells using the primer pairs: (A) 5s/17as and (B) 5s/11as. The filters were hybridized with a specific probe of exon 10 (v6). At the top the patient number and origin of the specimen are given: normal (N), primary tumor (P) or metastasis (M). The RT-PCR results of the microdissected samples differ in intensity due to the variation in the number of microdissected cells. For all samples microdissection and RT-PCR was performed in duplicate.

Other CD44 transcripts in normal oral mucosa and HNSCC: RT-PCR analysis

To make a comparison between all CD44 transcripts expressed in HNSCC and normal oral mucosa, the RT-PCR blots were hybridized with the insert of the epican^{U36} (CD44v3-v10) clone as a probe (Fig. 7). Two additional 5s/17as RT-PCR fragments of 375 and 750 bp did hybridize (Fig. 7a). The PCR product of 375 bp is most likely the amplification product of transcripts encoding the standard form of CD44 (CD44s, calculated size of the PCR product: 379 bp). The PCR product of 750 bp most likely resulted from amplification of transcripts encoding variant CD44v8-v10 (also called CD44E, calculated size of the PCR product: 775 bp). It should be noted, however, that in HNSCC cell lines CD44s transcripts

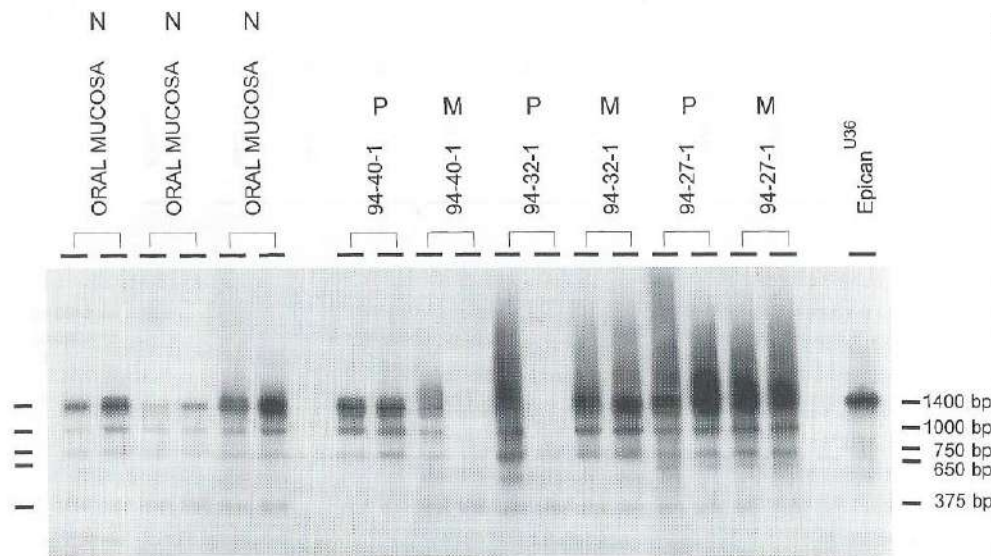


Figure 7 Southern blot analysis of RT-PCR amplification products from microdissected samples of normal squamous cells and HNSCC cells using the 5s/17as primer pair. The filter was hybridized with the insert of the epican^{U36} (CD44v3-v10) clone as a probe. At the top, the patient number and origin of the specimen are given: normal (N), primary tumor (P) or metastasis (M). The RT-PCR results of the microdissected samples differ in intensity due to the variation in the number of microdissected cells. The intensity between bands of the same sample cannot be compared as the epican^{U36} (CD44v3-v10) probe is expected to hybridize much stronger to epican (CD44v3-v10) encoding transcripts than transcripts encoding CD44E (CD44v8-v10) or CD44s. For all samples microdissection and RT-PCR was performed in duplicate.

could not be observed, indicating that the signal in tumors is most likely derived from stromal contamination or infiltrating lymphocytes. The CD44E transcript (CD44v8-v10) was observed in the HNSCC cell lines and is expressed by these cells, but only at a low level. The main transcripts of HNSCC cells, normal and malignant, *in vitro* as well as *in vivo*, contain exon 10 (v6) as indicated above. For one HNSCC patient (patient no. 94-27-1) an additional band of 650 bp was detected, which was not present in the normal oral mucosa samples, but this band was observed in the primary tumor as well as in the metastasis, suggesting that the expression of this CD44 isoform is not associated with the ability of HNSCC to metastasize. After hybridization of the 5s/11as RT-PCR products with the insert of the epican^{U36} (CD44v3-v10) clone as a probe, no additional hybridizing bands were observed (data not shown).

Discussion

CD44 isoforms, in particular isoforms containing the v6 domain, are assumed to play a critical role in the malignant progression of many human tumors, since tumor-specific v6-containing transcripts and CD44v6 overexpression have been observed [233,267-269,297]. Remarkably, recent results of Salmi *et al.* [288], Hudson *et al.* [298] and Soukka *et al.* [299] indicated a downregulation of CD44v6 expression during the malignant transformation of tumors of squamocellular origin. Similar to the CD44v6 dysregulation in other tumor types, the CD44v6 downregulation in squamocellular tumors might be the result of a switch in splice variant expression. However, in contrast to the results of Salmi *et al.* [288] and Soukka *et al.* [299], other reports described an upregulation [303] or no difference [60,304] in CD44v6 expression in malignant squamous tissues. These conflicting data incited us to re-examine the expression of CD44v6 isoforms in normal and malignant squamous tissues. Firstly, the CD44v6 protein levels were compared by immunohistochemistry using three different anti-v6 MAbs. In addition, the v6-containing splice variants in normal and malignant squamous cells were characterized by library screening and RT-PCR, both in tissues and cell lines to exclude contamination with stromal elements or infiltrating lymphocytes.

The immunohistochemical results presented in this Chapter show that the v6 domain of CD44 is highly and homogeneously expressed in the majority of primary HNSCC tumors. In about 97% (U36: 270/277; U39: 268/277) of the primary HNSCC tumors more than 50% of the cells was intensely stained. A significant correlation between CD44v6 expression and the differentiation status of the tumors, as suggested by Soukka *et al.* [299], could not be established. In addition, this Chapter showed that primary HNSCC tumors express similar levels of CD44v6 as normal squamous epithelia, indicating that the level of CD44v6 expression is not correlated with malignant progression in HNSCC.

Not only the level of CD44v6 expression, but also the v6-encoding CD44 splice variants in normal and malignant squamous cells appear to be identical. Even in HNSCC metastases no aberrant v6-containing splice variants could be detected. In total 5 v6-containing CD44 splice variants were detected in normal and malignant squamous tissues as well as in HNSCC cell lines: (a) CD44v2-v10, (b) CD44v3-v10, (c) CD44v3'-v10, (d) CD44v4-v10 and (e) CD44v6-v10. These data are largely in accordance with findings of others, as a number of these transcripts had already been described in normal keratinocytes [110,114,189,190].

Furthermore, our data show that also the expression of other CD44 transcripts is maintained during malignant progression. Besides v6-containing transcripts, which are the main transcripts in squamous cells, CD44v8-v10 (also called CD44E) encoding transcripts were detected by RT-PCR, but only at a low level. The CD44s transcripts observed in squamous tissue appeared to be derived from stromal cell contamination or infiltrating lymphocytes.

The results presented in this Chapter are in agreement with immunohistochemical data published by several other groups [60,304]. However, in contrast to our results, Salmi *et al.* [288] reported that CD44v6 expression was down regulated during the malignant transformation of tissue of squamocellular origin. In a very recent paper, the same group reported on a moderate to strong CD44v6 expression in only 12 out of 49 (24%) primary HNSCC tumors and 19 out of 49 (39%) HNSCC tumors were even completely negative [299]. It should be emphasized that we have found only 3/308 tumors to be negative and our RT-PCR data show that this discrepancy is not caused by a switch in splice variant expression. What is more, the staining intensity of the tissues by three MABs was very similar. Therefore, this difference needs another explanation. Soukka *et al.* [299] as well as our group have used cryosections of snap frozen tissues, indicating that the quality of the available material is comparable. Moreover, the staining methods and scoring methods are largely similar. Therefore, the different results are most likely related to the different anti-v6 antibodies. In this Chapter, we compared the staining pattern of three different anti-v6 MABs (U36, U39 and VFF18), all recognizing different epitopes, on a large number of primary HNSCC tumors. The epitope recognized by each antibody had been mapped by the use of synthetic peptides, and were shown to be directed against linear polypeptide epitopes ('Materials and methods'). Identical staining results were obtained, strongly arguing for the fact that high affinity antibodies directed against linear epitopes in the v6 domain of CD44 all stain similarly on squamous cells. In contrast, Soukka *et al.* [299] used the anti-v6 antibody Var3.1 without including a second anti-v6 antibody to substantiate their conclusions. Several explanations can be given for the aberrant behavior of MAB Var3.1 in comparison to MABs U36, U39 and VFF18. MAB Var3.1 was obtained by immunization with a synthetic peptide derived from the v6 domain that contained an additional cysteine at the -COOH end, whereas MAB VFF18 was obtained by immunization with a glutathione S-transferase fusion protein containing v3-v10, and MABs U36 and U39 by immunization with viable tumor cells [58,60,288]. Firstly, the addition of extra

amino acids to an immunization peptide could result in an antibody with a low affinity for the native antigen. Secondly, addition of a cysteine, which contains a highly reactive thiol-group, gives the synthetic peptide the possibility to form disulphide links with other proteins after injection. Thirdly, a synthetic peptide is able to have conformations that cannot be formed by the native antigen. Finally, it is well possible that MAB Var3.1 recognizes an epitope, which is masked by glycosylation or by the 3-dimensional structure of the native antigen. Epitope mapping of MAB Var3.1 could further elucidate these hypotheses. It has already been shown by the numerous contradictory data reported so far, that the comparison of immunohistochemical staining results is an important issue in the field of CD44. We think that the use of a 'golden standard' is unavoidable when comparing immunohistochemical data. Therefore, we suggest that researchers in the field should always include MAB VFF18 in their experiments, since this antibody is commercially available (Bender MedSystems) and has a well defined epitope.

According to the data obtained by several research groups, there are indications that in squamocellular cancers the CD44v6 expression level is correlated with the histological grade of the tumor. In all cases, a high CD44v6 expression has been associated with a better differentiation [60,190,303,304]. Although it is interesting that they all describe a similar correlation, it should be noted that most of them were just observed trends that were not statistically significant. The staining results with MAB U36 presented in this Chapter also indicated a slight trend towards a higher percentage of positive cells in the more differentiated HNSCC tumors. However, a significant correlation could not be found, probably because only a few HNSCC tumors show a weak MAB U36 staining. Therefore, if such a correlation exists, there will only be a marginal difference between the CD44v6 expression of well and poorly differentiated tumors, varying between 50-95% and 95-100% of strongly positive cells.

In conclusion, the results presented in this Chapter make the existence of abnormal splice variants in malignant squamous cells and their role in the invasive and metastatic behavior of HNSCC doubtful. In contrast to what has been described for other tumor types, v6-containing CD44 splice variants expressed in HNSCC cells do not seem to be correlated with malignant transformation but appear to have an important function in normal squamous cells. Gene targeting experiments should unravel the biological role of this molecule in detail. Recently, Kaya *et al.* [191] published some interesting observations, obtained by antisense

inhibition experiments in a transgenic mouse model. These data indicated that two major functions of CD44 in the murine skin are the regulation of keratinocyte proliferation in response to extracellular stimuli and the maintenance of local hyaluronate homeostasis.

Based on the data presented in this Chapter, we can speculate about the applicability of v6-containing CD44 transcripts and proteins for diagnosis and therapy of HNSCC. With respect to tumor cell detection, it can be concluded that HNSCC cells cannot be distinguished from normal squamous cells based on their v6-containing transcripts. This rules out the possibility to develop a CD44v6-specific RT-PCR method for the detection of HNSCC cells in surgical margins. On the other hand, it might be possible to detect HNSCC cells in blood, bone marrow and lymph nodes, although activated lymphocytes might be a limiting factor in this approach, since these cells have been described to express several v6-containing transcripts [121,137,139]. The value of CD44v6 as a serum marker for HNSCC is described in Chapter 6. In contrast to the limited possibilities as a diagnostic marker, the v6 domain seems to be a good target for antibody-based therapy of HNSCC as described in Chapter 2. Biodistribution studies with ^{99m}Tc-labeled MAb U36 have shown selective tumor targeting, indicating that *in vivo* the uptake of anti-v6 antibodies in normal mucosa and skin is prevented by physiological barriers [79].

Acknowledgements

The authors wish to thank E. Shtivelman for the cDNA clone HT5.

Chapter 5

The role of CD44v6 splice variants in human cancer reconsidered

Nicole L.W. van Hal

Guus A.M.S. van Dongen

Paul van der Valk

Corlinda B.M. ten Brink

Gordon B. Snow

Ruud H. Brakenhoff

Submitted

Abstract

CD44 splice variants, especially those containing the v6 domain, are assumed to play a role in the progression and metastasis of several tumor types, among which colon and breast carcinoma. The biological basis of these hypotheses is formed by (a) the expression of aberrantly spliced CD44v6 variants in tumors, (b) the presence of 'smear-like' reverse transcriptase-polymerase chain reaction (RT-PCR) patterns, and (c) the absence of expression on normal tissues. Our previous observation that normal and malignant squamous tissues express identical v6-encoding CD44 splice variants at a comparable level raised doubts about this interpretation. In this Chapter, we compare the expression of v6-containing CD44 variants in normal and malignant colon, breast and lung cells by immunohistochemistry and RT-PCR analysis on v6 positive cells microdissected from cryosections of normal and malignant tissues. Immunohistochemical staining indicated the presence of a relatively small number of v6 positive cells in all normal tissues. The expression level of these cells was comparable to that of v6 positive cells present in the corresponding malignant tissues. Furthermore, it is shown that there is no difference between the RT-PCR patterns of comparable amounts of microdissected v6 positive normal and malignant cells. Differences were only observed between the various tissue-types (colon, breast or lung). Together, these results argue against a role of v6-containing CD44 splice variants in the malignant progression of cancer. Instead, our data indicate that they should probably be considered as differentiation antigens.

Introduction

CD44 is a large family of transmembrane glycoproteins, generated by alternative splicing. During the last decade, the role of this surface antigen in tumor progression and metastasis became an important direction for research, as it was noted in a rat tumor model that a CD44 isoform containing v4-v7 was able to confer metastatic potential upon a non-metastasizing rat carcinoma cell line [109]. Co-injection of an anti-v6 monoclonal antibody (MAb) with the metastasizing cells led to inhibition of metastatic spread *in vivo* and based on this observation, it was hypothesized that especially v6-containing variants played a crucial role in this process [226,227]. Since then, a lot of effort has been made to identify the CD44 splice variants expressed by human tumors and their metastases. Several tumor types were studied intensively by immunohistochemistry and RT-PCR to find CD44 splice variants that might be involved in metastatic behavior of cells and several follow-up studies were performed to find a correlation between the level of CD44v6 expression and patient-survival. Indeed significant correlations were found in breast [228,268,269], colon [233,234,269], cervix [231,232], and bladder carcinoma [274] as well as aggressive non-Hodgkin lymphoma [139]. Based on these results, clinical applications of tumor-specific CD44 splice variants have been postulated for diagnosis and treatment of human cancer.

One of the fundamentals of these paradigms is the absence of CD44v6 expression in normal human tissues. However, there appears to be a considerable disagreement in this field. Whereas several research groups detect CD44v6 expression in normal colon, breast and lung tissues by immunohistochemistry [122,123,141,142,268,305-308] other groups fail to detect this expression by immunohistochemistry [228,233,235,237,262,309] or even by RT-PCR [264,265,269,309]. In addition, correlations found between the level of CD44v6 expression and tumor progression are in many cases not confirmed by the results of other groups [122,267,307].

These conflicting data and the fact that we could not detect any difference in the CD44v6 expression level or splicing pattern between tumor cells of head and neck squamous cell carcinoma and normal keratinocytes (Chapter 4), raised doubts about the existence of aberrant splicing patterns in other tumor types. The conflicting data that have been published are likely to be explained by differences in methods, antibodies, and/or interpretation of the data. False-negative results can be obtained by immunohistochemistry when low affinity antibodies or anti-

bodies recognizing epitopes that are not accessible on a certain cell type (e.g. due to glycosylation or protein conformation) are used. RT-PCR, although a very sensitive method, is much less sensitive when the fraction of v6-containing CD44 transcripts in the RNA mixture becomes relatively low. When there is a large amount of contaminating stromal elements in the tissue sample, low abundant transcripts could be missed easily. By enrichment of the cell fraction of interest, the chance of artificial results can be reduced.

In this Chapter, we compare the expression of v6-containing CD44 variants in normal and malignant colon, breast and lung tissues. Of each cell type, the CD44v6 expression level of tumor tissues and normal tissues was determined by immunohistochemical staining using two different anti-v6 MAbs. Areas with CD44v6 expressing cells were microdissected from parallel sections, using the immunohistochemically stained sections as a reference. Subsequently, the v6-containing transcripts in microdissected normal and malignant v6 positive cells were compared by RT-PCR analysis. The data were confirmed by using cell lines of the same tumor type to exclude a confounding role of stromal elements or infiltrating lymphocytes.

Materials and methods

Cell culture

Breast carcinoma cell lines (ZR-75: breast carcinoma, MCF7: breast adenocarcinoma, T-47D: ductal breast carcinoma) and colon adenocarcinoma cell lines (WiDr, HT-29, COLO 320, COLO 205, SW1398, LS 174T) were cultured in Dulbecco's modified Eagle's medium (DMEM; Gibco Life Technologies, Breda, The Netherlands) supplemented with 5% fetal calf serum (FCS; Hyclone Laboratories, Logan, UT), 16 mM NaHCO₃, 15 mM HEPES pH 7.4, 2 mM L-glutamine, 1% penicillin, and 1% streptomycin. The lung carcinoma cell lines (H69 and H187: small cell lung carcinoma, H460: large cell lung carcinoma, H522: lung adenocarcinoma, H322: bronchial alveolar carcinoma, GLC-p1 and GLC-p2: lung squamous cell carcinoma) were cultured similarly, but supplemented with 10% FCS (Hyclone Laboratories). All cells were cultured under 5% CO₂ at 37°C.

Cell lines were obtained from dr. E. Boven and dr. G. Giaccone (University Hospital *Vrije Universiteit*, Amsterdam, The Netherlands), except for the lung carcinoma cell lines GLC-p1 and GLC-p2, which were obtained from dr. L. de Ley (Rijksuniversiteit Groningen, Groningen, The Netherlands).

Anti-CD44v6 monoclonal antibodies

Immunohisto(cyto)chemical staining was performed with the anti-CD44v6 monoclonal antibodies U36 and VFF18. MAb U36 was obtained from Centocor (Leiden, The Netherlands) and MAb VFF18 (also called BIWA-1) was obtained from Bender MedSystems (Vienna, Austria). According to the numbering of Kugelman *et al.* [114], the epitope recognized by MAb U36 consists of amino acids 365-376 (Chapter 2) and the epitope recognized by MAb VFF18 consists of amino acids 360-370 [60].

Immunocytochemical staining of carcinoma cell lines

Cells were detached from the culture flask with cell dissociation medium (Sigma, Bornem, Belgium), as the MAb U36 defined epitope is disrupted by trypsinization, and spun on glass slides at a density of 5×10^4 cells/spin. After fixing the cells with freshly prepared 2% paraformaldehyde in phosphate buffered saline (PBS; pH 7.2-7.4) for 10 min, the cells were stained by alkaline-phosphatase anti-alkaline-phosphatase (APAAP) as described previously [281] using the anti-CD44v6 MAbs U36 and VFF18 as first antibody. Endogeneous enzyme activity was inhibited by adding 1 mM levamisole (Sigma) to the substrate. Staining was scored semi-quantitatively by three independent observers. The staining intensity was classified into 4 categories: 0) no staining, 1) weak staining, 2) moderate staining, 3) intense staining.

Immunohistochemical staining of frozen tissue sections

Cryosections of tumors and normal tissues of 4 µm were mounted on glass slides coated with 1 mg/ml poly-L-lysine, air dried for 1 hr and fixed with acetone for 10 min. The sections were rinsed for 5 min with PBS and pre-incubated for 10 min with normal rabbit serum (NRS; DAKO, Glostrup, Denmark) diluted 1:50 in PBS with 1% bovine serum albumin (1% BSA/PBS). Subsequently, the sections were incubated for 1 hr with an anti-CD44v6 specific antibody (MAb U36 or VFF18) diluted to 10 µg/ml in 1% BSA/PBS, biotin-labeled rabbit anti-mouse F(ab')₂ fragments diluted 1:500 in 1% BSA/PBS and

streptavidin-labeled horseradish peroxidase diluted 1:500 in 1% BSA/PBS. Between all incubation steps, the sections were rinsed three times for 5 min with PBS. Finally, the sections were stained with 0.5 mg/ml 3,3-diaminobenzidine tetrahydrochloride/0.01% H₂O₂ in PBS for 3-5 min. After rinsing the sections once with PBS, the nuclei were counterstained with haematoxylin for 45 sec. Finally, the sections were dehydrated and covered with Depex. The staining pattern of the sections was scored semi-quantitatively by two independent observers. Tumors were classified depending on the percentage of positive cells (0-10%, 10-50%, 50-90% or 90-100%) and the staining intensity: 0) no staining, 1) weak staining, 2) moderate staining, 3) intense staining.

Probes

The exon 10 (v6) probe was made by subcloning the polymerase chain reaction (PCR)-product obtained by amplification on chromosomal DNA using a sense primer identical to the sequence of the intron 9/exon 10 boundary (5'-GGA-ATTCTGATATTCTTCTCACAGTCCAGGC-3') and an antisense primer complementary to the sequence of the exon 10/intron 10 boundary (5'-GCTCTA-GACTTGTTAAACCATCCATTACCAGC-3'). The primers contained an additional restriction site (*Eco*RI and *Xba*I, respectively) to facilitate subcloning. A second probe, containing the epican (variant CD44v3-v10) encoding exons, was made by isolation of the *Xho*I restriction fragment containing the full length insert of the epican^{U36} clone (Chapter 4). DNA digests of the clones were run on an NA agarose gel (Pharmacia LKB, Uppsala, Sweden), the insert band was cut out of the gel and frozen. The frozen band was squeezed between parafilm, followed by a phenol/chloroform/isoamyl alcohol (25:24:1) extraction and ethanol precipitation [282]. The isolated insert was labeled with [α -³²P]dCTP by the random primer labeling method [301], using Klenow fragment of DNA polymerase I (Boehringer Mannheim, Almere, The Netherlands).

Microdissection

To allow selection of the v6 positive cells, cryosections of normal and malignant tissues were immunohistochemically stained with anti-v6 MAbs U36 and VFF18. Parallel frozen sections (10 μ m) were stained for 15 sec with a solution containing 1% toluidine blue and 0.2% methylene blue. After rinsing with millipore filtered water, microdissection was carried out immediately, using a Zeiss Stemi SV 11 stereo-microscope. All samples were microdissected in

duplicate. For each sample, 2-5 areas of tumor or normal tissue were dissected, depending on the size of the regions. Microdissected tissue was stored on ice until RNA was isolated.

RNA isolation, RT-reaction and PCR amplification

RNA was extracted from microdissected cryosections or from cultured cells using RNeasy (Qiagen, Crawley, The Netherlands) essentially according to the supplier. For the microdissected cryosections, this procedure was scaled down to a volume of 100 μ l RNeasy. Glycogen (5 μ g) was added as a carrier for the subsequent precipitation. The RNA pellets of the microdissected tissues were dissolved in 25 μ l water. First strand cDNA was synthesized using 5 μ l of the microdissection RNA sample as a template. For the cell lines, first strand cDNA synthesis was carried out with 10 or 100 ng of RNA. The RNA samples were heated for 3 min at 70°C and immediately put on ice. The RNA was reverse transcribed to cDNA by AMV reverse transcriptase (Promega, Leiden, The Netherlands), using an antisense primer located in exon 11 (11as: 5'-CTTCTGCTTGATGACCTCGTCC-3') or exon 17 (17as: 5'-CAAAGCCAAG-GCCAAGAGGGATGC-3'). The reverse transcription reaction was performed for 2 hr at 42°C in a volume of 20 μ l containing 1 mM deoxyribonucleoside triphosphates, 1 mM DTT, 50 mM TRIS-HCl pH 8.3, 60 mM KCl, 3 mM MgCl₂, 1.25 μ M antisense primer, 2 U RNasin (Promega) and 0.75 U AMV reverse transcriptase (Promega).

The obtained cDNA products were used as a template for PCR amplification using the same antisense primer and a sense primer located in exon 5 (5s: 5'-TGTCAGAGAAAGGAGAATACAGAACG-3'). The RT-PCR reactions were performed in a total volume of 50 μ l, using 5 μ l of the cDNA product. The final concentrations in the RT-PCR reactions were: 200 μ M deoxyribonucleoside triphosphates, 0.625 μ M antisense primer, 0.5 μ M sense primer, 10 mM TRIS-HCl pH 8.3, 50 mM KCl and 1.5 mM MgCl₂. To the negative control, water was added instead of RNA-template. As a positive control, PCR-amplification was performed on the epican^{U36} clone (variant CD44v3-v10; 100 pg) using the same primer combinations. To check the quality of the material, an RT-PCR reaction was performed in parallel on 5 μ l of cDNA template using the Abelson primers 1 and 3 [302]. Strict precautions were taken to prevent carry-over contamination. PCR-mix pipetting, RNA isolation/cDNA synthesis and PCR amplification were carried out in three separate laboratories using different pipets for buffers and

samples. The PCR conditions used were as described by Hudson *et al.* [190] with a 'hot start' of 5 min at 95°C and cooling to 72°C. Subsequently, 1 U AmpliTaq DNA polymerase (Perkin Elmer, Gouda, The Netherlands) was added. This was followed by 3 min 57°C, 3 min 72°C, 30 cycles of 1 min 94°C, 1 min 57°C, 2 min 72°C and subsequently a final incubation of 4 min 72°C. PCR amplification was performed on a Hybaid Omnigene thermal cycler (Biozym, Landgraaf, The Netherlands) with paraffin oil to prevent evaporation. Ten μ l of the reaction mixtures was loaded on an 1.5% (5s/11as amplification products) or an 1% (5s/17as amplification products) agarose gel and transferred to a positively charged nylon membrane (Qiabran; Westburg, Leusden, The Netherlands), using a transfer buffer containing 0.4 M sodium hydroxide and 0.6 M sodium chloride according to the protocol of Sambrook *et al.* [282]. The filters were baked for 2 hr at 80°C, prehybridized for 1 hr at 65°C in hybridization mix (0.5 M Na₂HPO₄, 7% sodium dodecyl sulfate (SDS), 1 mM EDTA, pH 7.2) and subsequently hybridized overnight at 65°C after addition of a [α -³²P]dCTP-labeled probe of exon 10 (v6) or the full length insert of the epican^{U36} clone. After 2 washes with a 2 \times saline sodium citrate buffer containing 0.01% SDS (2 \times SSC/0.01% SDS), and 2 washes with 0.2 \times SSC/0.01% SDS at 65°C, the blots were exposed to Kodak X-AR 5 film and autoradiographed for 1-2 hr at room temperature using intensifying screens.

Results

To compare the v6-containing CD44 isoforms expressed by normal tissues and the tumors derived thereof, RT-PCR analysis was performed on v6 positive cells microdissected from cryosections of normal and malignant colon, breast and lung tissues. To allow selection of the v6 positive cells, cryosections were immunohistochemically stained with anti-v6 MAbs U36 and VFF18, which showed similar staining patterns. Examples of immunohistochemical staining with MAb U36 are shown in Fig. 1, 2 and 3 for colon, breast and lung, respectively. Subsequently, the v6 positive areas were microdissected from parallel sections and used for RT-PCR analysis. Since the staining intensity appeared to vary between individual tumors, strong as well as weak staining tumors were selected for this analysis. Interestingly, immunohistochemical staining of the lung carcinomas with anti-v6 MAbs U36 and VFF18 showed a clear

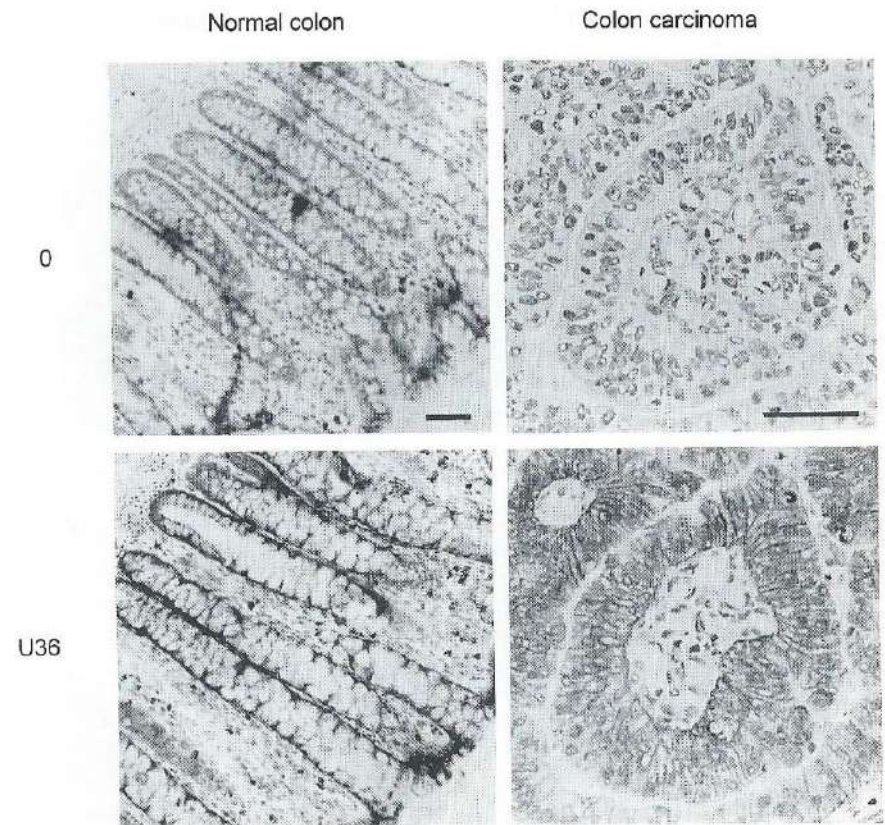


Figure 1 Immunohistochemical staining of cryosections from normal colon tissue and a colon carcinoma with anti-v6 MAb U36 (U36) or without first antibody (0). RT-PCR analysis of v6 positive cells microdissected from these tissues is shown in Fig. 4 (N1 and P1, respectively). Scale bar represents 50 μ m.

difference between adenocarcinomas (heterogeneous and weak) and squamous cell carcinomas (homogeneous and intense). Both types of tumors were analyzed by microdissection of the positive cells, RNA isolation and subsequent RT-PCR analysis.

In all types of normal tissue, v6 positive cells were detected. In normal colon, only the epithelial cells of the crypts were positively stained (Fig. 1). The staining intensity of these cells was comparable to that of colon carcinomas with a high expression level. For RT-PCR analysis, the colonic crypts were micro-

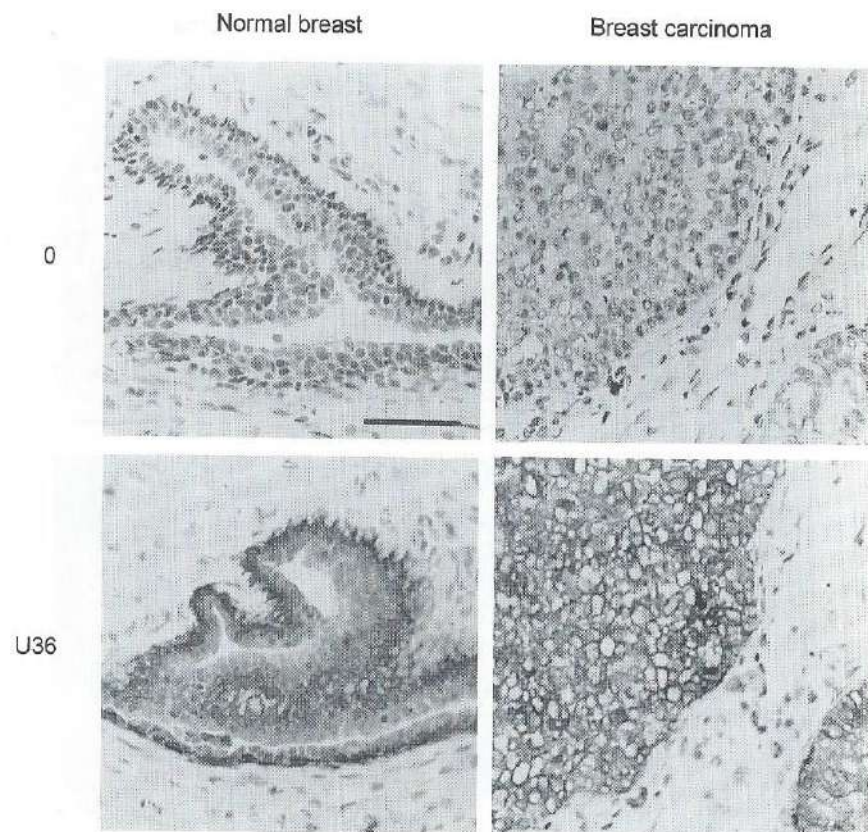


Figure 2 Immunohistochemical staining of cryosections from normal breast tissue and a breast carcinoma with anti-v6 MAb U36 (U36) or without first antibody (0). RT-PCR analysis of v6 positive cells microdissected from these tissues is shown in Fig. 5 (N1 and P2, respectively). Scale bar represents 50 μ m.

dissected from parallel cryosections. In normal breast tissue, the mammary ducts were intensely stained with both anti-v6 MAbs (Fig. 2). For RT-PCR analysis, the mammary ducts were microdissected from parallel tissue cryosections. Finally, in normal lung tissue the basal cells of the respiratory epithelium, glandular ducts, the terminal bronchioli, and the pneumocytes type I were positively stained with MAb U36 and VFF18 (Fig. 3). The staining intensity of these normal cells was comparable to the staining of lung tumors with a high v6 expression level.

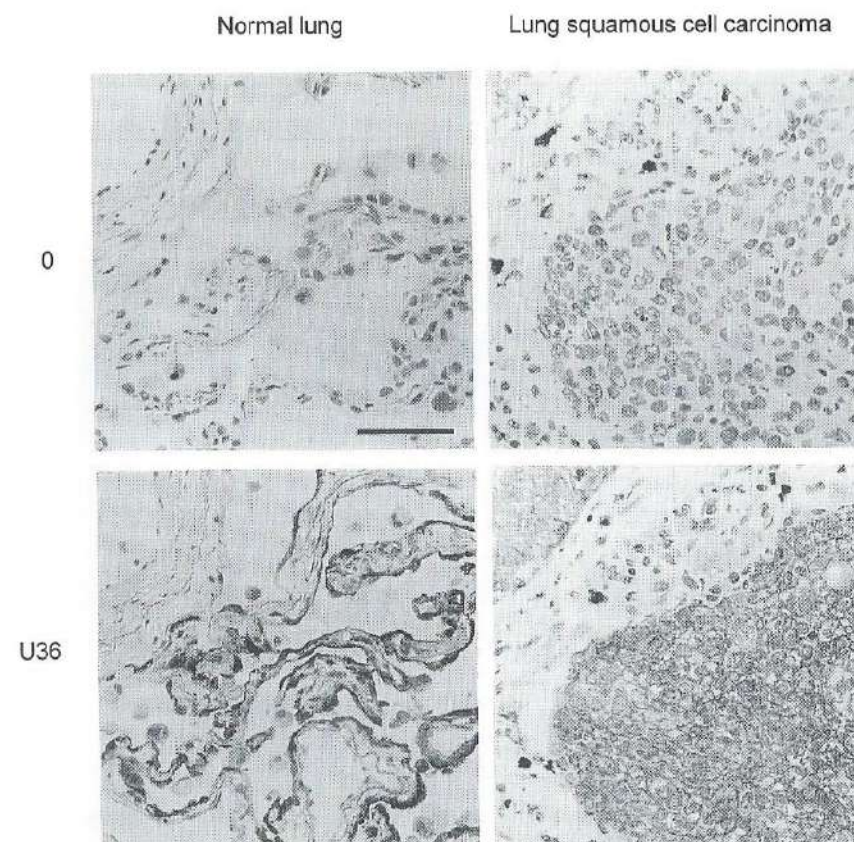


Figure 3 Immunohistochemical staining of cryosections from normal lung tissue and a lung squamous cell carcinoma with anti-v6 MAb U36 (U36) or without first antibody (0). RT-PCR analysis of v6 positive cells microdissected from these tissues is shown in Fig. 6 (N1 and P4, respectively). Scale bar represents 50 μ m.

The RT-PCR results are shown in Fig. 4, 5 and 6 for colon, breast and lung, respectively. On top, the staining results (intensity and percentage of positive cells) of the parallel cryosection is indicated for each individual sample. RT-PCR analysis was performed with two different primer pairs (5s/17as and 5s/11as). RT-PCR with the 5s/17as primer pair was used to amplify the complete variable region of the CD44 mRNA transcripts and for a more refined analysis of the large transcripts an RT-PCR reaction with the 5s/11as primer pair was performed. The v6-containing amplification products were visualized by hybri-

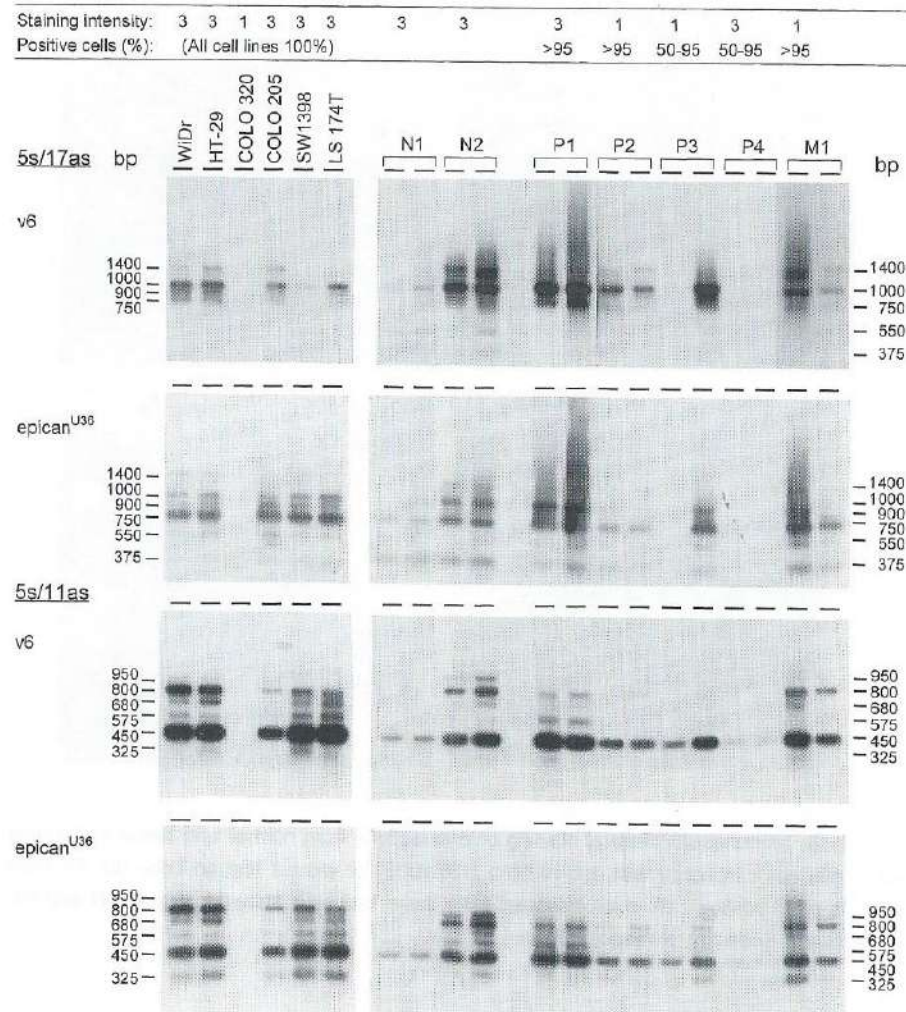


Figure 4 RT-PCR analysis performed on various human colon carcinoma cell lines and on v6 positive cells microdissected from normal colon epithelia (N1 and N2), primary colon carcinomas (P1, P2, P3 and P4) and a colon carcinoma metastasis (M1). For all tissues, microdissection and RT-PCR was performed in duplicate. Primer pairs and hybridizing probes are indicated at the left. At the top, the immunohisto(cyto)chemical staining results are given (for staining examples of N1 and P1, see Fig. 1). The RT-PCR results of the microdissected samples differ in intensity due to the variation in the number of microdissected cells and isolated RNA. For all colon carcinoma cell lines 10 ng of total RNA was used in the RT-reaction.

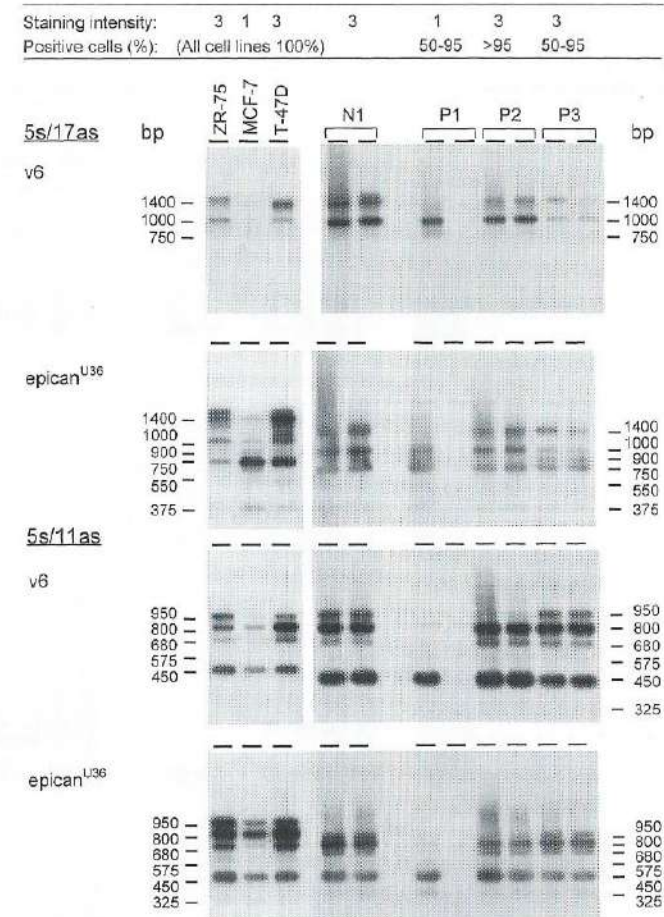


Figure 5 RT-PCR analysis performed on various human breast carcinoma cell lines and on v6 positive cells microdissected from normal ductal epithelium (N1) and primary breast carcinomas (P1, P2 and P3). For all tissues, microdissection and RT-PCR was performed in duplicate. Primer pairs and hybridizing probes are indicated at the left. At the top, the immunohisto(cyto)chemical staining results are given (for staining examples of N1 and P2, see Fig. 2). The RT-PCR results of the microdissected samples differ in intensity due to the variation in the number of microdissected cells and isolated RNA. For all breast carcinoma cell lines 10 ng of total RNA was used in the RT-reaction.

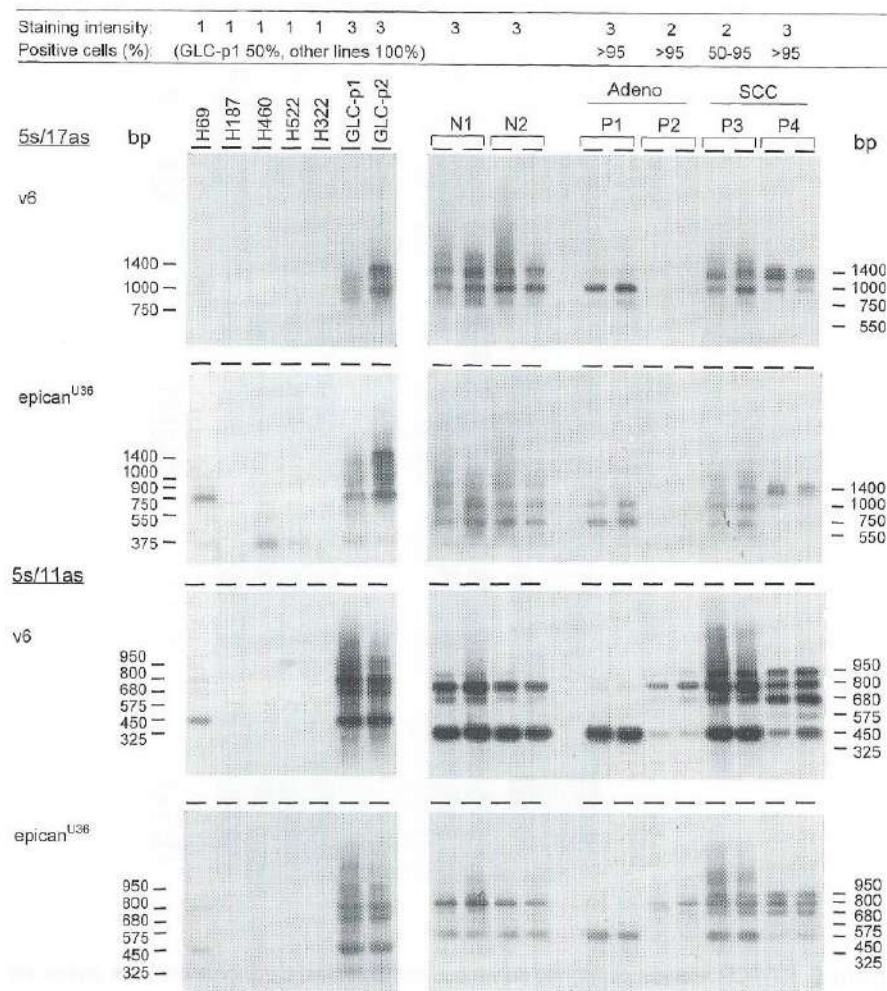


Figure 6 RT-PCR analysis performed on various human lung carcinoma cell lines and on v6 positive cells microdissected from normal lung epithelia (N1 and N2), primary lung adenocarcinomas (P1 and P2) and lung squamous cell carcinomas (P3 and P4). For all tissues, microdissection and RT-PCR was performed in duplicate. Primer pairs and hybridizing probes are indicated at the left. At the top, the immunohisto(cyto)chemical staining results are given (for staining examples of N1 and P4, see Fig. 3). The RT-PCR results of the microdissected samples differ in intensity due to the variation in the number of microdissected cells and isolated RNA. For the cell line GLC-p2, 10 ng of total RNA was used in the RT-reaction, for the other cell lines 100 ng.

dization with an exon 10 (v6) probe. For visualization of all amplification products, hybridization was performed with the insert of the epican^{U36} (variant CD44v3-v10) clone as probe. Besides microdissected v6 positive cells from normal and malignant colon, breast and lung tissues, several tumor cell lines derived from the same tumor types were analyzed as well to exclude a confounding role of stromal elements or infiltrating lymphocytes. The v6 expression level of these cell lines, as determined by immunocytochemical staining, is also given on top of the RT-PCR results (Fig. 4, 5 and 6).

A summary of the RT-PCR results is shown in Fig. 7. The amplification products were identified on basis of their size, known expression patterns, combining the results of the 5s/17as and 5s/11as RT-PCR as well as by subcloning and sequencing. Remarkably, the RT-PCR patterns of the v6 positive cells from normal colon and breast tissues appeared to be similar to those of the corresponding malignant tissues (Fig. 4 and 5). Even after hybridization with the insert of the epican^{U36} clone (encoding variant CD44v3-v10), identical hybridization patterns were observed, indicating the similarity in CD44 expression between normal and malignant cells. In lung, the situation appeared to be more complex, since a clear difference between adenocarcinomas and squamous cell carcinomas was observed. The pattern of normal lung tissue showed some similarity with both of them (Fig. 6). The cell lines showed largely the same RT-PCR patterns as the microdissected samples. Only the appearance of the 375 and 550 bp 5s/17as amplification products was sometimes different between the cell lines and tissues. The aspecific hybridisation of the CD44s derived 375 bp 5s/17as amplification product with the v6 probe, observed in the cells microdissected from colon tissue, might be explained by contamination of the microdissected cells with infiltrating lymphocytes or stromal elements, which express this variant at a much higher level. The intense hybridization of the 375 bp band with the epican^{U36} probe indeed indicates the high abundance of CD44s in the microdissected samples of the colon tissues. A similar aspecific hybridization with the v6 probe was observed in all samples for the variant CD44v8-v10 (CD44E). Incidentally, larger amplification products were observed in tumors (e.g. colon metastasis M1 and breast carcinoma P2, Fig. 4 and 5). After long exposure, however, large amplification products were faintly visible in most other samples as well, both in normal and tumor samples (data not shown).

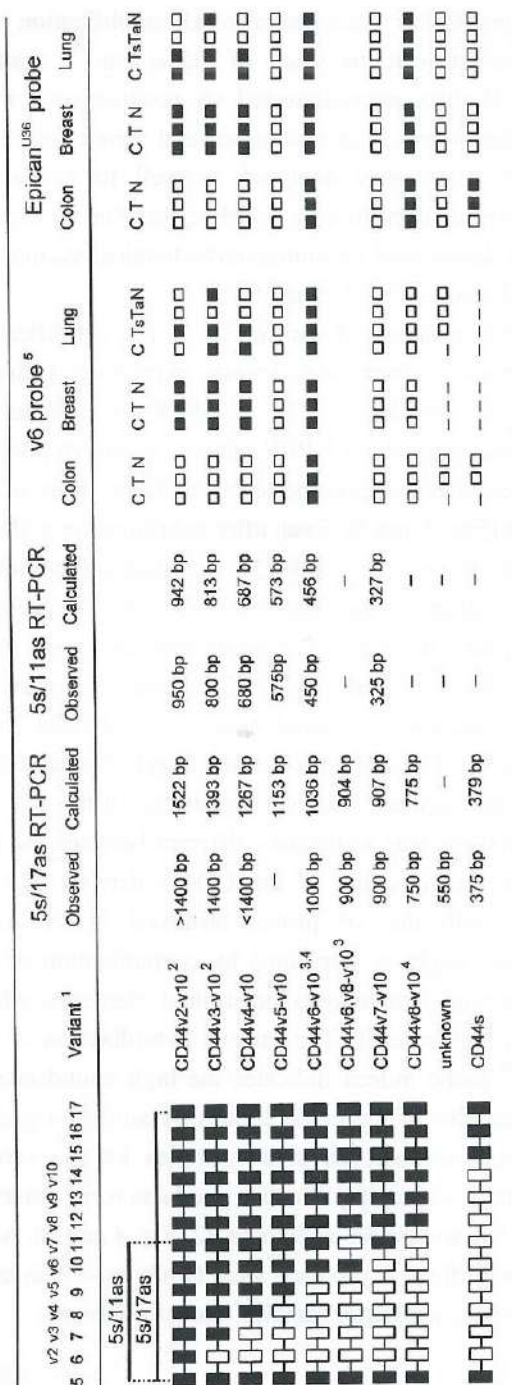


Figure 7 Overview of the 5s/17as and 5s/11as amplification products observed in cell lines (C) and microdissected v6 positive cells from tumors (T) or normal tissues (N) of the colon, breast and lung. Lung tumors are subdivided into squamous cell carcinoma (T_s) and adenocarcinoma (T_a). Lung cell lines only represent the squamous cell lines GLC-p1 and GLC-p2. Bars represent the intensity of the bands hybridizing with either the v6 probe or the epican^{US6} (CD44v3-v10) probe, classified into high (solid squares) or low (open squares) hybridizing signals. A dash indicates a hybridizing band that could not be observed. Observed and calculated sizes of the amplification products and the names of CD44 splice variants from which they most likely originate are indicated. ¹Several of these variants have been detected earlier in colon [141,269,306], breast [122,269,309] or lung tumors [255]. ²Subcloned and sequenced from breast carcinoma cell line ZR-75. ³Subcloned and sequenced from colon carcinoma cell line WiDr. ⁴Subcloned and sequenced from colon carcinoma P1. ⁵The v6 probe showed some aspecific hybridization with variants not containing exon v6.

Although the CD44 variants expressed in normal and malignant cells of the same tissue type appeared to be highly similar, a clear difference in RT-PCR patterns was observed between the colon, breast and lung tissues (Fig. 7). In particular, the pattern of v6-containing transcripts appeared to differ. All colon samples showed a high expression of the v6-containing variant CD44v6-v10 (5s/17as: 1000 bp, 5s/11as: 450 bp; v6 probe). All breast samples showed high expression of the variants CD44v2-v10 (5s/17as: >1400 bp, 5s/11as: 950 bp; v6 probe), CD44v3-v10 (5s/17as: 1400 bp, 5s/11as: 800 bp; v6 probe), CD44v4-v10 (5s/17as: <1400 bp; 5s/11as: 680 bp; v6 probe) and CD44v6-v10 (5s/17as: 1000 bp, 5s/11as: 450 bp; v6 probe), indicating the presence of 4 major v6-containing transcripts in epithelial breast cells. Finally, for the lung a clear difference was found between adenocarcinoma and squamous cell carcinoma. While for lung adenocarcinomas the variant CD44v6-v10 seems to dominate (similar to colon carcinomas), an equal and high expression of the variants CD44v2-v10, CD44v3-v10, CD44v4-v10 and CD44v6-v10 was observed for the lung squamous cell carcinoma samples and the lung squamous cell carcinoma cell lines GLC-p1 and GLC-p2.

Discussion

In this Chapter, we compared the CD44v6 expression in normal and malignant tissues of the colon, breast and lung by immunohistochemistry and RT-PCR analysis on microdissected CD44v6 expressing cells. In contrast to most published data, our results indicate that for none of these tumor types the CD44v6 expression is tumor-specific. There is certainly not a significant gain of novel splice v6-encoding splice variants during malignant progression. This observation makes a role of tumor-specific CD44 splice variants in the process of tumor progression unlikely.

Until now, not much attention has been paid to the few papers that describe comparable RT-PCR patterns for normal and malignant colon [141,306], breast [122] and lung tissues [123]. Based on our data, we conclude that the negative RT-PCR results, which are more often described for normal tissues, are caused by the relatively small fraction of positive cells in the sample. Preselection of v6 positive cells by immunohistochemistry followed by microdissection of these positive cells does result in the detection of v6-encoding transcripts in

normal epithelial cells by RT-PCR. This statement is further supported by a recent publication of Givvehchian *et al.* [306] about colon cancer. The often described enhanced expression of CD44v6 in tumors can probably be attributed to morphological features. Large numbers of tumor cells clustered together appear to have a higher expression than the small positive areas in normal tissues. However, the expression per cell is certainly not higher for tumor cells.

Instead of tumor-specific, our results show that CD44 isoform expression is rather tissue-specific. Although all tissues tested showed expression of the same isoforms (CD44s, CD44v8-v10 (CD44E), CD44v7-v10, CD44v6-v10, CD44v5-v10, CD44v3-v10 and CD44v2-v10), the relative amounts of particularly the v6-containing isoforms depended on the tissue type from which the cells originated. For lung, there appeared to be a difference between adenocarcinomas and squamous cell carcinomas. The main v6-containing splice variants of lung squamous cell carcinomas are identical to those expressed by head and neck squamous cell carcinoma and normal oral mucosa (Chapter 4), indicating that these lung tumor cells have also squamous characteristics on molecular level. The pattern of CD44 splicing might effectively be used to discriminate between adeno-like or squamous-like differentiation of lung carcinomas, when morphological criteria appear to fail.

Based on our results, we do not suppose that the v6-containing CD44 splice variants expressed by tumor cells are a trigger for malignant progression of the cell. On the contrary, the v6 expression of normal cells seems to be retained during malignant transformation. The tissue-specific expression of v6-containing CD44 variants suggests that the molecule should rather be considered as a differentiation antigen.

Acknowledgements

The authors wish to thank P. den Otter for immunohistochemical analysis of the various tumors and normal tissues and T.M. Tadema for making the cryosections that were used for microdissection (both from the Department of Pathology, University Hospital *Vrije Universiteit*, Amsterdam).

Chapter 6

Evaluation of soluble CD44v6 as potential serum marker for head and neck squamous cell carcinoma

Nicole L. W. van Hal

Guus A.M.S. van Dongen

Corlinda B.M. ten Brink

Karl-Heinz Heider

Irene Rech-Weichselbraun

Gordon B. Snow

Ruud H. Brakenhoff

Submitted

Introduction

Abstract

The measurement of soluble CD44 levels in the circulation of patients with malignant diseases has been introduced as a new and simple diagnostic tool for the detection of human cancer. The high CD44v6 expression in head and neck squamous cell carcinoma (HNSCC) justified an evaluation of soluble CD44v6 proteins present in the circulation of HNSCC patients. In this Chapter, we determined CD44v6 plasma levels in healthy volunteers (n=8), non-cancer patients (n=10) and HNSCC patients (n=13) before and after surgical removal of the tumor, using a v6-specific enzyme-linked immunosorbent assay (ELISA). Furthermore, to characterize the soluble v6-containing CD44 proteins present in control and patient plasma in more detail, immunoprecipitation experiments were performed.

No difference could be observed between CD44v6 plasma levels of HNSCC patients and controls. Moreover, surgical removal of the tumor did not result in a reduction of the CD44v6 plasma level. Finally, immunoprecipitation experiments showed that the soluble v6-containing CD44 isoforms in plasma of HNSCC patients are similar to those of healthy controls. Additional experiments to unravel the biological source of these circulating proteins indicated that the v6-containing proteins present in the circulation of healthy individuals are only in part released by activated lymphocytes or other nucleated blood cells. Most circulating CD44v6 proteins seem to be derived from the normal epithelial cell compartments, including breast cells, colon cells and squamous cells. Taken together, these data do not support the use of soluble CD44v6 as tumor marker in HNSCC or any other tumor type derived from cells producing soluble forms.

CD44 is a cell surface glycoprotein expressed by a large variety of tissues. A large family of CD44 isoforms exists, encoded by tissue-specific alternatively spliced transcripts. The CD44 isoforms differ in the size of their extracellular or intracellular domain and their tissue distribution. Multiple functions have been ascribed to CD44, but they appear to be restricted to subsets of the various isoforms. First, CD44 acts as a receptor for the extracellular matrix components hyaluronate [99,148], laminin [166], fibronectin and type I and VI collagen [94]. In addition, CD44 is thought to play a role in several processes that are critical in normal immune system development and functioning, including lymphocyte homing [92,310], hemopoiesis [177] and leukocyte activation [183-185]. Moreover, it can serve as a signaling molecule triggering cytokine release from monocytes [186]. Finally, CD44 molecules containing the v3 domain are able to bind growth factors and might play a role in the control of cell proliferation [171]. Besides their expression on the cell membrane, CD44 proteins are also released from cells and soluble CD44 proteins are detectable in the normal human circulation [81,84,202,311]. The basic level of soluble CD44 in the circulation is thought to have its origin in lymphocytes [205,208,220].

The observation that several human tumors show an overexpression of certain CD44 isoforms and the presence of soluble CD44 isoforms in the circulation, make CD44 a potential serum marker for tumor detection. For several tumor types, elevated CD44 serum levels have indeed been observed using exon-specific ELISA's of CD44s [206,207,213], CD44v5 [210,212] or CD44v6 [206,209,210,212]. Compared to other tumor types, the CD44v6 domain is highly expressed by squamous cell carcinomas of the head and neck (HNSCC), lung, esophagus, cervix and skin. Therefore, this domain seems to be a promising candidate serum marker for squamous cancers like HNSCC.

To evaluate whether plasma levels of soluble CD44v6 have diagnostic significance for HNSCC, a longitudinal study was performed with 13 HNSCC patients. Plasma levels of soluble CD44v6 were measured with a v6-specific ELISA assay before and after surgical removal of the tumor and compared to plasma levels of non-cancer patients and healthy volunteers. To distinguish the various circulating isoforms and to investigate the presence of tumor-derived soluble forms, the spectrum of circulating CD44v6 proteins was assayed by immunoprecipitation experiments on plasma of controls and HNSCC patients.

Finally, the origin of the circulating CD44v6 isoforms was assessed by immunoprecipitation experiments with various anti-CD44 antibodies and model experiments.

Materials and methods

Plasma of HNSCC patients, non-cancer patients and healthy volunteers

Blood was obtained from 13 HNSCC patients (Table 1) and 10 non-cancer patients scheduled for surgery as well as from 8 healthy volunteers using heparin vacutubes (Becton Dickinson Vacutainer Systems Europe, Meylan, France). All patient samples were taken just before surgery from an arterial line. From the HNSCC patients additional blood samples were taken directly after surgical removal of the tumor from the same arterial line and 6 weeks after surgery by venipuncture. Before and during surgery, all patients received comparable amounts of additional fluid by infusion. For a second study, blood samples were taken from a group of 30 other HNSCC patients (characteristics of these patients are available upon request). All blood samples were diluted twice with RPMI 1640 (Bio-Whittaker, Verviers, Belgium) and subsequently spun to remove the cells (30 min, 1400×g, 4°C). Plasma samples were stored at -80°C until analysis. The study was approved by the Medical Ethical Committee of the University Hospital *Vrije Universiteit*.

CD44v6-specific ELISA

A commercially available sandwich-type ELISA, developed by Bender MedSystems (Vienna, Austria) was used for the quantitative measurement of soluble CD44v6 in plasma samples. In this test, a monoclonal antibody specific for an epitope of the CD44 standard molecule is used as capturing antibody adsorbed onto microtiter plates. The anti-v6 antibody VFF18 coupled to horseradish peroxidase serves as tracer antibody with the peroxidase/tetramethylbenzidine substrate system for readout. The ELISA test was performed according to the manufacturer's instructions.

In short, 100 µl of the plasma samples (1:20 diluted in sample diluent), standard solutions and negative controls (sample diluent) were added to the wells, together with 50 µl of the tracer antibody. Subsequently, plates were incubated for 3 hr at room temperature on a rotator platform, allowing the tracer and capture

Table 1 Characteristics of the HNSCC patients.

Nr.	Localization Primary Tumor	cTN/pTN ¹	Stage ²
1	tongue	pT ₃ N ₁	III
2	tonsil	pT ₃ N ₃	IV
3	tonsil	pT ₂ N _{2b}	IV
4	base of tongue	cT ₂ N _{2c}	IV
5	soft palate	pT ₂ N ₀	II
6	piriform sinus	pT ₄ N _{2c}	IV
7	floor of mouth	pT ₄ N ₀	IV
8 ³	dorsal tongue glottic larynx	pT ₂ N ₀ pT ₂ N ₀	II
9	tonsil	pT ₂ N ₀	II
10	hypopharynx	pT ₂ N ₀	II
11 ⁴	base of tongue	pT ₄ N _{2b}	IV
12	piriform sinus	cT ₁ N ₃	IV
13	glottic larynx	pT ₄ N ₁	IV

¹Clinical (c) or pathological (p) stage of the disease, according to the TNM classification of the International Union Against Cancer (Union Internationale contre le Cancer, UICC) [43]. ²Stage grouping according to the UICC [43]. ³Patient with two synchronous primary tumors. ⁴Patient with a second primary tumor.

antibodies to bind simultaneously with CD44 present in the standards and plasma samples. Unbound CD44 and tracer antibody were removed by three washing steps. Then, 100 µl of substrate solution was added for color development. After 15 min, the reaction was terminated by the addition of 100 µl 2 M H₂SO₄ and color intensity was measured at 450 nm (ELISA-reader Anthos ht-II, Anthos Labtec Instruments, Salzburg, Austria). Since the plasma samples were diluted twice with RPMI 1640 (Bio-Whittaker) and RPMI 1640 alone did not give any signal in the assay, the measured CD44v6 levels were multiplied by 2 to calculate the plasma concentration.

Monoclonal antibodies

Anti-CD44 monoclonal antibodies (MAbs) SFF304 (anti-CD44s), VFF 327v3 (anti-CD44v3), VFF8 (anti-CD44v5), VFF18 (anti-CD44v6), VFF9 (anti-CD44v7), VFF17 (anti-CD44v7,8), FW3 11.24 (anti-CD44v9) and VFF14 (anti-CD44v10) were obtained from Bender MedSystems (Vienna, Austria).

Immunoprecipitation of CD44 antigen

CD44 antigen was precipitated with goat anti-mouse IgG-agarose beads (Sigma, Bornem, Belgium) saturated with anti-CD44 MAbs. Before antibody-coupling, anti-mouse IgG agarose was washed twice with phosphate buffered saline (PBS) and blocked with 1% bovine serum albumine (BSA) in PBS (1% BSA/PBS) by overnight incubation at 4°C. For MAbs VFF18 (anti-CD44v6) and SFF304 (anti-CD44s) 50 µl of anti-mouse IgG agarose was used and for MAbs VFF327v3 (anti-CD44v3), VFF8 (anti-CD44v5) and FW3 11.24 (anti-CD44v9) 100 µl. After washing once with PBS, the agarose beads were incubated for 8 hr at 4°C with 5 µg (VFF18, SFF304) or 50 µg (VFF327v3, VFF8, FW3 11.24) tracer MAb, diluted to a final volume of 500 µl 0.01% BSA/PBS. Uncoupled antibody was removed by washing the saturated agarose beads 3 times with PBS. Subsequently, the preformed agarose-MAb complexes were incubated overnight at 4°C with the sample (50 µl human plasma adjusted to a final volume of 500 µl with PBS, 500 µl murine plasma or 1 ml lymphocyte culture medium). Next morning, agarose beads were washed 6 times with PBS and finally 20 µl of sample buffer (50 mM TRIS pH 6.8, 4% sodium dodecyl sulfate (SDS), 12% glycerol, 0.01% bromophenol blue, 5% β-mercaptoethanol) was added. Samples were boiled 5 min before loading on gel. Immunoprecipitations with MAbs VFF17 (anti-CD44v7,8), VFF9 (anti-CD44v7) and VFF14 (anti-CD44v10) were not successful, probably due to the relatively low affinity of these antibodies.

Western blot analysis

Immunoprecipitated proteins were separated by sodium dodecyl sulfate polyacrylamide gel electrophoresis (SDS-PAGE) on a 5% gel and transferred to a nitrocellulose membrane (Schleicher and Schuell, Dassel, Germany). The free binding sites were blocked by incubating the blot overnight with 1% BSA/PBS [282]. The filter was subsequently incubated for 1 hr with 0.75 µCi/ml ¹²⁵I-labeled MAb VFF18 (3.5 µCi/µg MAb) in 1% BSA/PBS [58]. Unbound MAb was re-

moved by washing 3 times for 15 min in PBS with 0.05% Tween-20, and bands were visualized by autoradiography for 48-64 hr at -80°C using intensifying screens.

Analysis of CD44 expression on in vitro stimulated lymphocytes

Blood (30 ml) of a healthy control person was collected in heparin vacutubes (Becton Dickinson Vacutainer Systems Europe). Lymphocytes were isolated by density separation using Lymphoprep (Nycomed, Oslo, Norway). In short, blood was diluted twice with RPMI 1640 (Bio-Whittaker). Subsequently, the diluted blood was carefully applied onto 30 ml Lymphoprep (Nycomed), resulting in two separate phases. After centrifugation (20 min, 900×g), lymphocytes (present at the interface) were collected with a sterile glass pipet and washed twice with RPMI 1640 (Bio-Whittaker). In total 1.1×10^7 lymphocytes were isolated. Half of the cells was resuspended in RPMI 1640 (Bio-Whittaker) supplemented with 10% fetal calf serum (FCS; Hyclone, Logan, UT), 1% penicillin, 1% streptomycin and 2% phytohaemagglutinin (PHA; Gibco Life Technologies, Breda, The Netherlands) to a final concentration of 2.75×10^6 cells/ml, the second half was resuspended to the same concentration in RPMI 1640 (Bio-Whittaker) supplemented with 10% FCS (Hyclone), 1% penicillin and 1% streptomycin. Cells were plated in a 24-wells plate (0.5 ml/well) and cultured under 5% CO₂ at 37°C. After 4 days, the lymphocytes were collected by centrifugation (10 min, 300×g) and washed twice with PBS. Per 1×10^6 lymphocytes, 20 µl icecold lysis buffer (20 mM TRIS-HCl pH 7.5, 140 mM NaCl, 4 mM EDTA, 1% NP-40) with protease inhibitors (10 mM PMSF, 1mM iodoacetamid, 1 µg/ml leupeptin, 1 µg/ml pepstatin and 20 µg/ml trypsin inhibitor) was added. After 30 min incubation on ice, cell debris was removed by centrifugation (30 min, 4°C, 25000×g). Cell lysates were stored at -20°C until use. For Western blotting 15 µl of cell lysate was loaded on the gel. The culture medium of the lymphocytes was spun in an eppendorf centrifuge (1 hr, 4°C, 25000×g) to remove the cell debris and stored at -20°C until immunoprecipitation. For immunoprecipitation of soluble CD44 isoforms, 1 ml conditioned culture medium was used.

Isolation of RNA from nucleated cells present in blood and bone marrow

Blood (7 ml) and bone marrow (1-2 ml) were collected in heparin vacutubes (Becton Dickinson Vacutainer Systems Europe). Blood and bone marrow were diluted twice with RPMI 1640 (Bio-Whittaker) and spun (10 min,

220×g, 4°C). The supernatant was removed and remaining cells were resuspended in 10 ml (blood) or 5 ml (bone marrow) shock buffer (0.16 M NH₄Cl, 10 mM KHCO₃, 0.1 mM EDTA pH 7.4) to lyse the erythrocytes. After a 10-15 min incubation at 4°C the nucleated cells were spun down (5 min, 220×g, 4°C) and washed twice with RPMI 1640 (Bio-Whittaker). Subsequently, RNA was isolated using 1 ml RNazol (Campro scientific, Veenendaal, The Netherlands) according to the supplier.

Isolation of RNA from v6 positive cells of normal oral mucosa and normal colon cryosections

CD44v6 positive cells were microdissected from frozen sections (10 µm) of normal oral mucosa and normal colon cryosections. To allow selection of the v6 positive cells, parallel cryosections were immunohistochemically stained with anti-v6 MAbs U36 and VFF18 using a biotin-streptavidin immunoperoxidase staining technique as described in Chapter 2. For orientation, the sections that were used for microdissection were stained for 15 sec with a solution containing 1% toluidine blue and 0.2% methylene blue. After rinsing with millipore filtered water, microdissection was carried out immediately, using a Zeiss Stemi SV 11 stereo-microscope. For each sample, 2-5 areas of tumor or normal tissue were dissected, depending on the size of the regions. Microdissected tissue was stored on ice until RNA was isolated.

The RNA was extracted with RNazol (Campro Scientific), essentially according to the supplier. The procedure was scaled down to a volume of 100 µl RNazol and glycogen (5 µg) was added as a carrier for the subsequent precipitation. The RNA pellets of the microdissected tissues were dissolved in 25 µl water.

RT-PCR and Southern blot hybridization

First strand cDNA synthesis was carried out using 0.5 µg of total RNA isolated from nucleated cells of blood and bone marrow or 5 µl total RNA isolated from microdissected samples as a template. The RNA samples were heated for 3 min at 70°C and immediately put on ice. The RNA was reverse transcribed to cDNA by AMV reverse transcriptase (Promega, Leiden, The Netherlands), using an antisense primer complementary to a sequence in exon 17 of the CD44 gene (17as: 5'-CAAAGCCAAGGCCAAGAGGGATGC-3'). The reverse transcription reaction was performed in a volume of 20 µl and contained

1 mM deoxynucleotide triphosphates, 1 mM DTT, 50 mM TRIS-HCl pH 8.3, 60 mM KCl, 3 mM MgCl₂, 1.25 µM antisense primer, 2 U RNasin (Promega) and 0.75 U AMV reverse transcriptase (Promega). The reactions were incubated for 2 hr at 42°C.

The obtained cDNA products were used as a template for polymerase chain reaction (PCR) amplification using the antisense primer indicated above and a sense primer identical to a sequence in exon 5 (5s: 5'-TGTCCAGAAAGG-AGAATACAGAACG-3'). The reverse transcriptase-polymerase chain reaction (RT-PCR) was performed in a total volume of 50 µl, using 5 µl of the cDNA product. The final reagent concentrations for RT-PCR were: 200 µM deoxynucleotide triphosphates, 0.625 µM antisense primer, 0.5 µM sense primer, 10 mM TRIS-HCl pH 8.3, 50 mM KCl and 1.5 mM MgCl₂. To the negative control, water was added instead of RNA-template. Strict precautions were taken to prevent carry-over contamination. PCR-mix pipetting, RNA isolation/cDNA synthesis and PCR amplification were carried out in three separate laboratories. The PCR conditions used were as described by Hudson *et al.* [190] with a 'hot start' of 5 min at 95°C and cooling to 72°C. Subsequently, 1 U AmpliTaq DNA polymerase (Perkin Elmer, Gouda, The Netherlands) was added. This was followed by 3 min 57°C, 3 min 72°C, 30 cycles of 1 min 94°C, 1 min 57°C, 2 min 72°C and subsequently a final incubation of 4 min 72°C. PCR amplification was performed on a Hybaid Omnigene thermal cycler (Biozym, Landgraaf, The Netherlands) with paraffin oil to prevent evaporation. Ten µl of the reaction mixtures were loaded on an 1% agarose gel and transferred to a charged nylon membrane (Qiabran: Westburg, Leusden, The Netherlands) using a transfer buffer containing 0.4 M sodium hydroxide and 0.6 M sodium chloride according to the protocol of Sambrook *et al.* [282]. The filters were baked for 2 hr at 80°C, prehybridized for 1 hr at 65°C in hybridization mix (containing 0.5 M Na₂HPO₄ pH 7.2, 7% SDS and 1 mM EDTA) and subsequently hybridized overnight at 65°C after addition of the ³²P-labeled v6 exon as a probe (Chapter 4). After 2 washes with a 2× saline sodium citrate buffer containing 0.01% SDS (2×SSC/0.01% SDS), and 2 washes with 0.2×SSC/0.01% SDS at 65°C, the blot was exposed to Kodak X-AR 5 film and autoradiographed overnight at -80°C, using intensifying screens.

Plasma of (xenograft-bearing) nude mice

The tumor xenograft line HNX-OE was established from a metastasis of a squamous tumor of the oral cavity. Fresh biopsies of the tumor were implanted subcutaneously in the lateral thoracic regions on both sides of athymic nude mice. The xenograft line was maintained by serial subcutaneous transplantation. Blood samples of xenograft-bearing nude mice (tumor size: about 1000 mm³) and control nude mice were taken in heparin vacutubes (Becton Dickinson Vacutainer Systems Europe) and spun (30 min, 1400×g, 4°C). Plasma samples were stored at -80°C until further analysis. For immunoprecipitation, 500 µl murine plasma was used.

Results

Level and spectrum of soluble CD44v6 variants in plasma of HNSCC patients and controls

To study the prognostic value of soluble CD44v6 for HNSCC patients, CD44v6 protein levels were measured by ELISA in plasma of 13 HNSCC patients, 10 non-cancer patients and 8 healthy volunteers (Fig. 1). The 13 HNSCC patients were followed in time. Samples were taken before surgery, directly after surgical removal of the tumor and six weeks after surgery. As indicated in Fig. 1, the CD44v6 plasma levels directly after surgical removal of the tumor (p2; 103 ± 46 ng/ml) were lower than before surgery (p1; 129 ± 37 ng/ml), a difference which appeared to be significant (paired t-test, $p=0.0066$). However, six weeks after surgery the CD44v6 plasma levels had increased (p3; 167 ± 53 ng/ml). This increase appeared to be significant when compared to the initial plasma levels (paired t-test, $p=0.0066$) or to the plasma levels of the samples taken directly after surgery (paired t-test, $p=0.00045$). The changes observed for the 13 HNSCC patients are not related to the presence of tumor as removal of the malignant tissue resulted in an increase in CD44v6 levels. Instead, the changes are most likely caused by dilution of the blood by infusion. This conclusion is substantiated by the observation that plasma levels of HNSCC patients just before surgery (p1; 129 ± 37 ng/ml) were not significantly different (unpaired t-test, $p=0.36$) from those of non-cancer patients that had received comparable volumes of fluid by infusion (cp; 109 ± 62 ng/ml). Similarly, no significant difference (unpaired t-test; $p=0.13$) was found between CD44v6 plasma levels of HNSCC patients

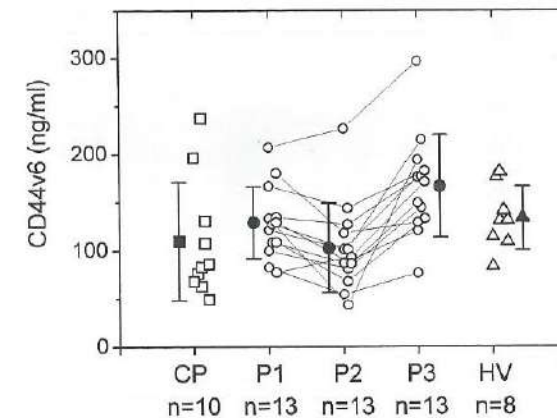


Figure 1 Soluble CD44v6 levels in plasma of 10 non-cancer patients just before surgery (cp), 13 HNSCC patients just before surgery (p1), directly after surgical removal of the tumor (p2) and six weeks after surgery (p3), and 8 healthy volunteers (hv). Plasma levels were determined by ELISA using anti-CD44v6 MAb VFF18.

measured six weeks after surgery (p3; 167 ± 53 ng/ml) and the plasma levels of 8 healthy volunteers (hv; 134 ± 33 ng/ml). Together, these results clearly demonstrate that the CD44v6 plasma levels of HNSCC patients are not related to the presence or absence of tumor, but merely to the physiological conditions during sampling.

Although no significant differences were observed between the absolute CD44v6 plasma levels of HNSCC patients and controls, there could still be a difference in the spectrum of v6-containing CD44 isoforms present in the circulation. It has been suggested earlier that soluble CD44v6 in the circulation of healthy controls originates from activated lymphocytes [208]. Therefore, additional squamous-specific CD44 variants released by HNSCC tumors might be detectable in plasma of HNSCC patients. To compare the v6-containing isoforms present in plasma of non-cancer patients and HNSCC patients, immunoprecipitation experiments were performed (Fig. 2). CD44 isoforms were precipitated with anti-CD44v6 MAb VFF18. Subsequently, a Western blot of the precipitated CD44v6 proteins was incubated with ¹²⁵I-labeled anti-CD44v6 (VFF18) to detect the v6-containing CD44 proteins. Protein bands of about 190, 155, 140, 125 and 95 kDa could be detected in samples of non-cancer patients and HNSCC patients (Fig. 2a and b, respectively). The protein bands of 190 and 155 kDa were clearly

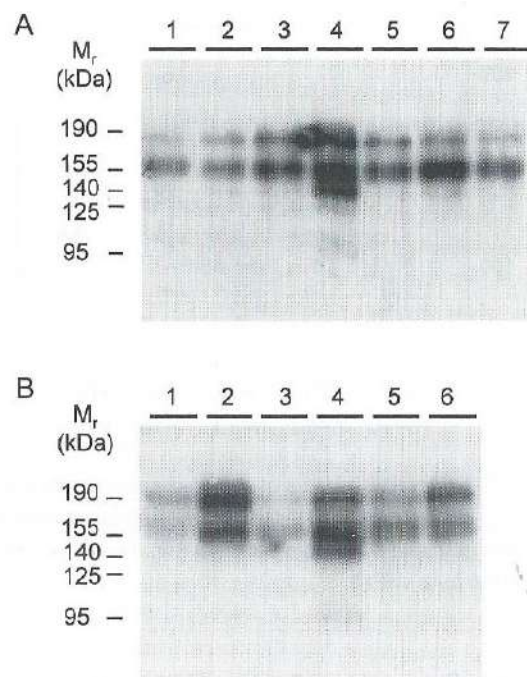


Figure 2 Comparison of soluble CD44v6 proteins in plasma of non-cancer patients and HNSCC patients. CD44v6 proteins in the plasma of 7 non-cancer patients (A) and 6 HNSCC patients (B) were immunoprecipitated with anti-CD44v6 MAb VFF18. Detection of immunoprecipitated CD44 proteins was performed by incubation of the Western blot with 125 I-labeled VFF18.

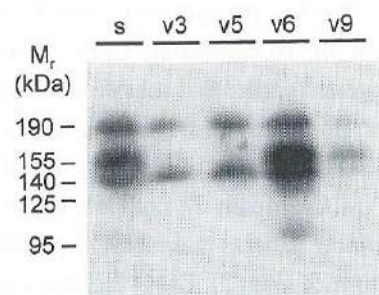


Figure 3 Characterization of the v6-containing soluble proteins in plasma of an HNSCC patient (patient 4, Fig. 2b). Immunoprecipitation was performed with a panel of anti-CD44 MAbs recognizing different variant domains (anti-CD44s, anti-CD44v3, anti-CD44v5, anti-CD44v6 and anti-CD44v9). Detection of immunoprecipitated CD44 proteins was performed by incubation of the Western blot with 125 I-labeled VFF18.

visible for the samples of all non-cancer patients and all HNSCC patients. The protein bands of 140, 125 and 95 kDa differed in intensity between individual samples of both HNSCC patients and non-cancer patients.

To characterize the observed protein bands in more detail, immunoprecipitation was performed with anti-CD44s, anti-CD44v3, anti-CD44v5, anti-CD44v6 and anti-CD44v9. Subsequently, a Western blot of these immunoprecipitates was incubated with 125 I-labeled anti-CD44v6 to detect the proteins containing the v6 domain. Similar results were found for plasma of HNSCC patients and non-cancer patients (not shown), indicating that the soluble CD44v6 variants are indeed identical. A typical example is shown in Fig. 3. The protein bands of 190 and 140 kDa were present after precipitation with antibodies against the standard domain and the variable domains v3, v5, v6 and v9 of CD44. The 155, 125 and 95 kDa protein bands were only precipitated with anti-CD44s, anti-CD44v6 and anti-CD44v9 and not with anti-CD44v3 or anti-CD44v5 antibodies.

Origin of soluble CD44v6 proteins present in normal human plasma

Our results show that soluble CD44v6 proteins cannot be used for tumor detection in HNSCC patients, as controls have similar CD44v6 plasma levels of identical variants. This observation was unexpected as the soluble proteins in normal human plasma were suggested to be derived from activated lymphocytes, thus additional squamous-specific variants in plasma of HNSCC patients were supposed to be present. To investigate whether the CD44 protein released from human lymphocytes can indeed explain the presence of all soluble CD44v6 proteins in human plasma, *in vitro* cultured lymphocytes were studied. Human lymphocytes were isolated from blood of a healthy control person and cultured for 4 days in medium with or without PHA, which activates the lymphocytes. Cell lysates and conditioned culture medium were analyzed for the presence of v6-containing CD44 proteins. Although CD44v6 proteins were clearly upregulated in lymphocytes that had been activated by PHA, soluble CD44v6 proteins could hardly be detected in conditioned culture medium of lymphocytes cultured either in the absence or presence of PHA (data not shown). These data indicate that the release of CD44 from activated lymphocytes *in vitro* is low. However, it cannot be excluded that the release of CD44 isoforms *in vivo* is different.

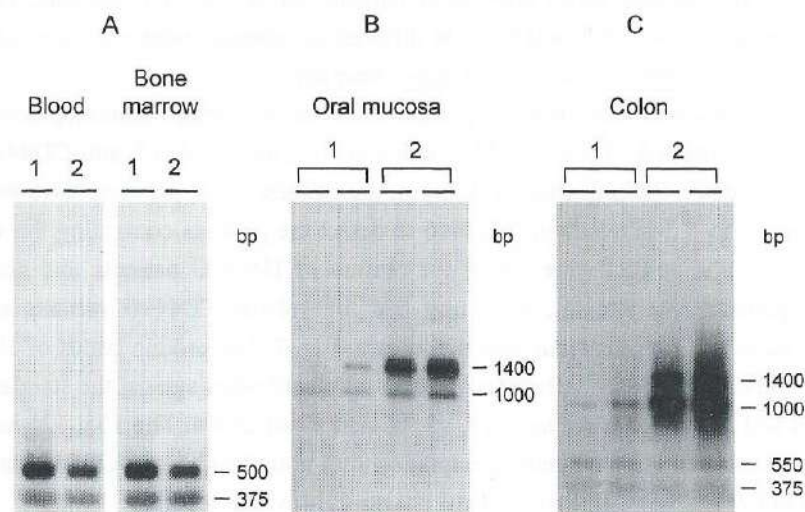


Figure 4 RT-PCR performed on RNA of (A) nucleated cells from blood and bone marrow of two non-cancer patients, (B) v6 positive cells microdissected from cryosections of normal oral mucosa (two non-cancer patients each performed in duplicate), (C) v6 positive cells microdissected from cryosections of normal colon (two non-cancer patients each performed in duplicate). For patient 2 the blot is rather overexposed, the main fragment visible is the amplification product of CD44v6-v10 (1000 bp). Amplification was performed using a sense primer in exon 5 and an antisense primer in exon 17. Amplification products were hybridized with a specific probe of exon v6.

To identify the main v6-containing CD44 proteins expressed by activated lymphocytes and other nucleated blood cells an RT-PCR reaction was performed on RNA isolated from the nucleated cells present in blood and bone marrow of two non-cancer patients. Fig. 4a shows the RT-PCR results when using a sense primer in exon 5 and an antisense primer in exon 17, amplifying all variant exons of CD44. The blot was hybridized with a specific probe of exon v6. In blood and bone marrow samples two main PCR-products were hybridizing, a fragment of 500 bp and a fragment of 375 bp. Subcloning and sequencing revealed that the 500 bp PCR-product resulted from amplification of a CD44 isoform that only contained variant exon v6 (calculated size of the PCR-product: 508 bp). Subcloning and sequencing of the 375 bp PCR-product showed that this fragment originates from CD44s (calculated size of the PCR-product: 379 bp). Therefore,

the positive 375 bp signal on blot appears to be derived from aspecific cross-hybridization, which was apparent on the clones as well. This apparent cross-hybridization could not be explained, as the sequence similarity between CD44s and the probe is only 60% for both the sense and antisense strand. Only the enormous amount of the CD44s derived 375 bp PCR-product, observed on the ethidium bromide gel, could explain this phenomenon. Note that CD44s cross-hybridization is absent in normal oral mucosa and is weak in colon (Fig. 4b and c, respectively). This isoform is hardly expressed in the latter tissue. In addition to the 375 and 500 bp fragments, some larger PCR-products were faintly detectable in the blood and bone marrow samples after long exposure of the blot.

The observation that the soluble CD44 variants which are most abundant in human plasma also contain the domains v3, v5 and v9 (Fig. 3), indicates that activated lymphocytes or other types of nucleated blood cells are not the only source of soluble v6-containing proteins. It appears that also other cell types are involved. Since the v6 domain of CD44 is predominantly expressed by epithelia, like the skin, lungs, oral mucosa, breast and colon [140], epithelial cells are a plausible source of soluble CD44v6 in the circulation. Moreover, large v6-containing transcripts encoding the variants CD44v2-v10, CD44v3-v10, CD44v4-v10 and CD44v6-v10 have been detected in these cells by RT-PCR (Chapters 4 and 5). Fig. 4b shows an example of RT-PCR analysis on v6-positive cells microdissected from normal oral mucosa, when using a sense primer in exon 5 and an antisense primer in exon 17. Two bands were detected after hybridization with a specific probe of exon v6. Firstly, a 1400 bp band which was proven to contain amplification products of the variants CD44v2-v10, CD44v3-v10 and CD44v4-v10. In addition, a 1000 bp band was detected, which was shown to represent the variant CD44v6-v10 (Chapter 4). Normal epithelial cells of the colon were shown to express mainly the variant CD44v6-v10 (Chapter 5). As shown in Fig. 4c, RT-PCR analysis on v6 positive cells microdissected from normal colon mainly resulted in the 1000 bp 5s/17as amplification fragment of the variant CD44v6-v10.

To study the release of CD44v6 from epithelial cells *in vivo*, we used a model of HNSCC xenograft-bearing nude mice. Protein release from HNSCC is expected to be a good representation for the release from normal squamous epithelia, as previous work proved that HNSCC tumors express exactly the same v6-containing CD44 splice variants as normal oral mucosa (Chapter 4). Fig. 5 shows the results of immunoprecipitation experiments on plasma of HNSCC

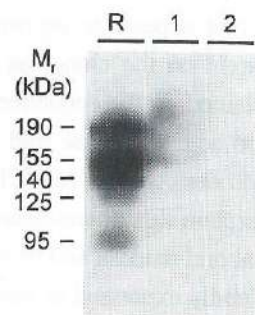


Figure 5 Release of CD44v6 proteins from HNSCC xenografts. CD44v6 proteins present in plasma of an HNSCC xenograft-bearing nude mouse (lane 1) and a control nude mouse (lane 2) were precipitated with anti-v6 MAb VFF18. The immunoprecipitate of patient plasma was added as a reference (lane R). Detection of the precipitated CD44 proteins was performed by incubation of the Western blot with 125 I-labeled VFF18. For immunoprecipitation 50 μ l of human plasma and 500 μ l of murine plasma was used.

xenograft-bearing nude mice and control mice. Proteins were precipitated with anti-CD44v6 and subsequently a Western blot of the precipitated CD44v6 proteins was incubated with 125 I-labeled anti-CD44v6 for detection of the v6-containing CD44 proteins. In plasma of control mice no v6-containing proteins were detectable, which is in agreement with the species-specific recognition of CD44v6 by MAb VFF18. Therefore, the soluble v6-containing proteins that were detected in plasma of the xenograft-bearing mice originated from the human HNSCC xenografts. The protein pattern appeared to be at least in part similar to the pattern observed for normal human plasma (Fig. 5).

Discussion

For several tumor types, elevated CD44 serum levels have been observed using an exon-specific ELISA [206,207,209,210,212,213]. The high expression of v6-containing CD44 isoforms by HNSCC tumors incited us to investigate the diagnostic value of CD44v6 levels in the circulation of HNSCC patients. Surprisingly, no significant difference between CD44v6 plasma levels of HNSCC and non-cancer patients could be observed. What is more, surgical removal of the

tumor did not result in a reduction of the CD44v6 plasma level. Apparently, the release of v6-containing proteins from HNSCC is not high enough to significantly exceed the basic CD44v6 plasma level. This could be attributed to the tumor load of HNSCC patients, which is usually relatively low as compared to other tumor types. Until now, the basic release of CD44 is thought to have its origin in lymphocytes [205,208,220], which would suggest that squamous cell specific variants are present in plasma of HNSCC patients. By introducing immunoprecipitation we expected to detect the squamous-specific isoforms, but surprisingly comparison of the spectrum of v6-containing proteins present in the circulation of HNSCC and non-cancer patients did not reveal any differences as well. Subsequently, we investigated whether the CD44v6 isoform expression and release from human lymphocytes could explain the observed isoforms. In contrast to what has been published by others, our data show that the spectrum of CD44v6 proteins in normal human plasma can only be explained in part by release from lymphocytes or other nucleated blood cells. Immunoprecipitation of v6-containing CD44 proteins from the culture medium of PHA-activated human lymphocytes showed only a low CD44v6 release *in vitro*. What is more, RT-PCR analysis indicated that nucleated blood cells mainly express a small CD44 isoform that, besides exon v6, does not contain any other variant exons. It appeared that mRNA transcripts encoding large v6-containing CD44 isoforms are not expressed by nucleated blood cells, or only at a very low level. However, immunoprecipitation of v6-containing proteins from normal human plasma indicated the presence of relatively large v6-containing proteins. Two protein bands of 190 and 155 kDa were detected in all plasma samples tested. The 190 kDa protein could be precipitated with anti-v3, -v5, -v6 and -v9. Therefore, this protein might be the isoform CD44v2-v10 or CD44v3-v10. The 155 kDa protein band was only detected after precipitation with anti-CD44s, anti-CD44v6 and anti-CD44v9 and not with anti-v3 or anti-v5 and might therefore represent the protein isoform CD44v6-v10.

In contrast to nucleated blood cells, large v6-containing CD44 isoforms are highly expressed by for example normal squamous cells. We recently identified by RT-PCR the v6-containing mRNA transcripts that are expressed by normal oral mucosa (Chapter 4). Four highly expressed v6-containing CD44 splice variants could be identified: (a) CD44v2-v10, (b) CD44v3-v10, (c) CD44v4-v10 and (d) CD44v6-v10. In addition to normal oral mucosa, also epithelial cells from several other tissues, including lung and breast, appear to express these

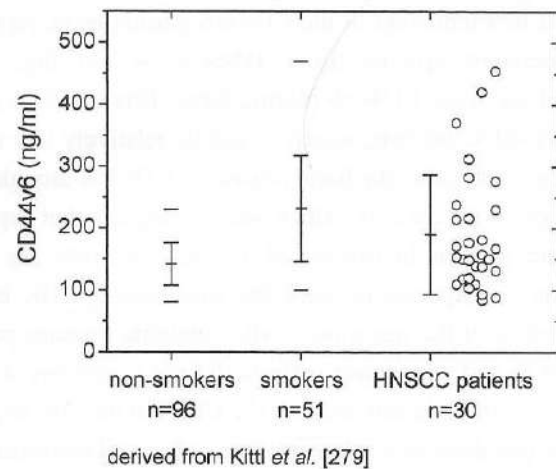


Figure 6 Soluble CD44v6 levels in plasma of 30 HNSCC patients were compared with the levels measured by Kittl *et al.* [279] in plasma samples of 96 non-smoking and 51 smoking healthy volunteers. Plasma levels were determined by exactly the same ELISA assay, using anti-CD44v6 MAb VFF18. The plasma levels of the 30 HNSCC patients were not significantly different from those of the 13 HNSCC patients 6 weeks after surgery (Fig. 1). Minimum and maximum values, mean values and standard deviations published by Kittl *et al.* [279] are indicated.

large v6-containing isoforms. Normal epithelial cells of the colon were shown to express mainly the variant CD44v6-v10 (Chapter 5). We thus postulate that the isoforms CD44v2-v10 and CD44v3-v10 are released by squamous cells of the mucosal linings and the lungs and by breast cells, whereas the v6-v10 isoform is predominantly released by simple epithelia such as colon. Especially CD44v6 protein release from the lungs, which have a large contact surface with the blood circulation, are expected to show a high contribution. This hypothesis is underlined by the earlier observation that heavy smokers have a significantly higher plasma level of soluble CD44v6 isoforms [279]. Originally, this observation was attributed to activated lymphocytes in the lungs, but also the presence of squamous metaplasia or dysplasia of the respiratory epithelium with the concurrent increased v6 expression and v6 release might contribute. In a larger group of HNSCC patients (n=30), almost all smokers, we have indeed incidently observed patients (n=3) with extremely high soluble CD44v6 plasma levels (370-455 ng/ml), similar to what has been described by Kittl *et al.* [279] for smokers

(Fig. 6). Obviously, these comparisons should be interpreted with caution as the assays were performed in different laboratories. Nevertheless, the assay used was exactly the same. Together, these data indicate that there are high levels of CD44v6 variants in normal human plasma, which are at least in part released by epithelial cells. These levels severely hamper the use of soluble CD44v6 as a marker of human malignancies.

Chapter 7

Summary, general discussion and perspectives

Summary

Head and neck squamous cell carcinoma (HNSCC) arises from the mucosa of the upper aerodigestive tract. The patients are treated with surgery and/or radiotherapy, depending on the stage of the disease. Unfortunately, the 5-years survival of HNSCC patients with an advanced stage of the disease is relatively low and patients who received curative treatment have still a high risk to develop locoregional recurrences and distant metastases. These data indicate that the conventional treatment of HNSCC is often insufficient and that small tumor deposits, undetectable by routine diagnostic procedures, remain in the body of the patient, locoregionally as well as at distant sites. An effective systemic adjuvant therapy is urgently needed to treat this minimal residual disease, which is undetectable by routine histopathology. Since the efficacy of chemotherapy for the curative treatment of minimal residual head and neck cancer is limited and this tumor type has an intrinsic sensitivity for radiation, radioimmunotherapy (RIT) appears to be one of the most promising options for adjuvant therapy. At the Department of Otolaryngology/Head and Neck Surgery of the University Hospital *Vrije Universiteit*, a panel of monoclonal antibodies (MAbs) directed against squamous-associated antigens was selected by immunohistochemistry on large series of normal and malignant tissues. Due to its homogeneous and extensive reactivity with squamous tumors, MAb U36 was selected as one of the most promising candidate MAbs to be used for tumor targeting. Subsequently, clinical radioimmunoscinigraphy (RIS) and biodistribution studies showed that MAb U36 is suitable for antibody-based therapy of HNSCC. Furthermore, the selective expression of the MAb U36 defined antigen suggested that it might be a powerful tool for the molecular diagnostics of minimal residual head and neck cancer. These applications demanded further characterization of the MAb U36 defined antigen.

In Chapter 2, it was shown by expression cloning that MAb U36 recognizes the protein CD44v3-v10 (also called epican). CD44 is a heavily glycosylated transmembrane protein with a wide tissue distribution. A large number of CD44 isoforms exists, which are encoded by tissue-specific alternatively spliced transcripts, and CD44v3-v10 is one these. The existence of this large group of splice variants made it necessary to determine the antibody-binding region. The epitope recognized by MAb U36 was mapped and appeared to be located in the v6 domain of CD44.

After the elucidation of the amino acid sequence of the MAb U36 epitope, it appeared that two amino acids differed from the published v6 sequences. Since these sequence variations might interfere with the application of the antibody for tumor targeting, the affinity of MAb U36 for these variant epitopes was investigated in Chapter 3. At one position, the presence of valine instead of glutamic acid resulted in a significant reduction of MAb U36 binding. However, further evaluation showed that the low affinity epitope does not exist *in vivo* and was based on a sequencing artefact published in literature. The other variation, substitution of a lysine by an arginine, appeared to have no influence on the binding of MAb U36. This amino acid variation was based on an allelic polymorphism in the population. In addition, it was analyzed whether this amino acid variation was related to the malignant behavior of tumor cells. No trend was found towards allelic imbalance in tumor cells as compared to normal cells.

As summarized in Chapter 1, many claims have been made with respect to the involvement of CD44 splice variants, in particular isoforms containing the v6 domain, in tumor progression and metastasis formation of several tumor types, including colon and breast carcinoma. It was therefore expected that the v6-containing splice variants expressed on HNSCC tumors were different from those expressed by normal mucosa. These tumor-specific splice variants could be exploited for molecular diagnosis of minimal residual disease in resection margins, bone marrow and/or lymph nodes of HNSCC patients. Therefore, the v6-containing splice variants present on HNSCC tumors were characterized in Chapter 4 and compared to those of normal mucosa. Five putative target antigens of MAb U36 were detected at the mRNA level (CD44v2-v10, CD44v3-v10, CD44v3'-v10, CD44v4-v10 and CD44v6-v10). Surprisingly, in normal oral mucosa the same five v6-containing splice variants were shown to be present at similar levels, suggesting that their expression is not related to the process of squamous carcinogenesis. Despite the presence of these target antigens on malignant cells as well as on normal squamous cells, targeting with MAb U36 had been shown to be tumor-selective [79]. This is most likely due to the fact that normal squamous cells are poorly accessible for intravenously injected immunoglobulins due to the blood-tissue barrier. In tumors, this barrier appears to be defective, which allows MAb U36 to penetrate more readily into the tumor [72].

Since we had not found any differences in the expression of v6-containing CD44 splice variants between normal and malignant squamous cells, doubts arose about their role in the progression of other tumor types. Therefore, in

Chapter 5 a comparison was made between the v6-containing CD44 variants present in normal and malignant colon, breast and lung tissues. Immunohistochemistry showed comparable levels of v6 expression in the malignant as well as in the normal tissues. However, the expression in the normal tissues appeared to be restricted to a small number of cells, in particular subsets of epithelial cells. Reverse transcriptase-polymerase chain reaction (RT-PCR) analysis performed on the CD44v6 expressing cell population, isolated from the tissues by microdissection, showed that normal and malignant v6 positive cells of the same tissue type express identical v6-encoding CD44 mRNA transcripts. These findings contradict the current view of disorganized splicing and elevated CD44v6 protein levels in tumor cells. Instead of a tumor-specific expression pattern, the results rather showed a tissue-specific expression pattern of v6-encoding splice variants, which suggests that the CD44 isoforms should rather be considered as differentiation antigens.

In addition to a transmembrane form, also soluble CD44v6 isoforms exist, which can be detected in the normal human blood circulation. The basic release of these soluble isoforms is thought to have its origin in lymphocytes. For a number of tumor types elevated CD44v6 serum levels have been observed, suggesting its applicability as a diagnostic tool. Since HNSCC show a high expression of the CD44v6 domain, **Chapter 6** focuses on the applicability of a v6-specific ELISA for the detection of HNSCC tumors by measuring the CD44v6 levels in sera of HNSCC patients. Remarkably, HNSCC patients did not show elevated CD44v6 plasma levels when compared to controls and surgical removal of the tumor did not result in a reduction of the CD44v6 plasma level. Further refinement of this analysis by immunoprecipitation experiments showed that not only the levels but also the spectrum of soluble CD44v6 proteins present in plasma of controls and patients is identical. Intriguingly, various additional experiments indicated that the v6-containing CD44 proteins present in the circulation of healthy individuals are largely derived from normal epithelial cells. The presence of these proteins in the circulation of healthy individuals severely hampers the use of soluble CD44v6 as a serum marker of human malignancies.

General discussion and perspectives

Applicability of the MAb U36 defined antigen for HNSCC detection

The possibility to use CD44 for tumor cell detection seems to be limited at first sight. The results presented in Chapter 4 indicate that it will be impossible to detect rare HNSCC cells in surgical margins with the help of a CD44-based detection method as normal and malignant squamous cells show the same level and same spectrum of CD44 variants. Moreover, also the development of a reliable CD44-based method for the detection of disseminated HNSCC cells in lymph nodes, blood and bone marrow appeared to be difficult. To determine the possibility of RT-PCR for the detection of tumor cells in blood, several primer combinations were tested in a model system where HNSCC cells were seeded in 10 ml of blood. With all tested primer combinations positive signals were found in blood, irrespective whether HNSCC cells had been added or not. Apparently, the CD44 splice variants expressed in HNSCC cells are also expressed in (subsets of) blood cells, although at a low level. Due to the high sensitivity of RT-PCR, even these low levels are detectable, a phenomenon which has been described for several other molecular markers as well [312-314]. For most markers, this effect is attributed to illegitimate gene expression but in the case of CD44 this effect might be dependent on the lack of specificity of the splicing mechanism. The existence of CD44v6-mRNA containing hemopoietic cells might also hamper the applicability of immunocytochemistry for the detection of disseminated tumor cells in lymph nodes, blood and bone marrow, although the low level of mRNA expression on (subsets of) these cells not necessarily leads to detectable protein levels. Nevertheless, recent data of Liefers *et al.* [315] show that illegitimate expression of a tumor marker in normal cells is not a restriction for tumor cell detection per se. By using an RT-PCR method for the amplification of carcinoembryonic antigen (CEA) mRNA, they found that the presence of micro-metastasis in lymph nodes of patients with stage II colorectal cancer is associated with a poor prognosis. Although it is well known that CEA mRNA is illegitimately expressed in hemopoietic cells, they were able to make a distinction between tumor-involved and normal lymph nodes, by using an RT-PCR procedure with suboptimal sensitivity. Whether this strategy will also be applicable in case of HNSCC cell detection by CD44v6-based RT-PCR is currently under investigation.

At this moment, several other markers are evaluated that seem to have more potential for HNSCC cell detection in blood, bone marrow and lymph nodes by molecular biological methods. A specific RT-PCR method, based on the squamous cell-associated antigen E48, has been set up for the detection of tumor cells in blood and bone marrow. This method was shown to have a detection level of 1 tumor cell per 2×10^7 white blood cells while in samples from non-cancer controls signal is absent (Brakenhoff *et al.*, submitted). A drawback of this marker is the previously observed heterogeneity of expression in HNSCC tumors, which can reduce the reliability of the assay.

Another diagnostic possibility, the use of soluble CD44v6 in plasma for the detection of minimal residual disease in HNSCC patients, was hampered by the presence of soluble HNSCC-associated CD44v6 variants in the circulation of non-cancer patients and healthy controls. The data presented in Chapter 6 indicated that at least part of the soluble CD44 proteins present in the circulation is derived from epithelial cells, an observation with serious implications for the use of soluble CD44v6 as a marker of other human malignancies as well.

The results presented in this thesis indicate that, despite the intense and homogeneous expression on HNSCC, CD44v6 is currently not the ideal marker for the detection of rare disseminated HNSCC cells or for use as a serum marker. This might be different for the detection of small tumor deposits by imaging procedures. It has been demonstrated that for the detection of primary HNSCC tumors and lymph node metastases the diagnostic value of radioimmuno-scintigraphy with ^{99m}Tc -labeled MAb U36 is comparable to that of palpation, CT and MRI [79]. With these techniques in general tumors with a diameter larger than 1 cm can be detected. However, improvement of the conventional scintigraphy by the current introduction of positron emission tomography (PET) technology might lead to an application of MAb U36 that allows the detection of much smaller tumor cell deposits in HNSCC patients. For application in PET, MAb U36 conjugates containing the positron emitter ^{89}Zr are currently developed at our institute.

Applicability of MAb U36 for treatment of minimal residual disease

The success of antibody-based therapy largely depends on the distribution pattern of the antibody in the patient's body. This might be particularly true when using intrinsically toxic MAb conjugates like in RIT. Moreover, side effects can also occur when the target antigen fulfills a critical physiological function in

normal tissues. On the other hand, antibody binding to the tumor may also cause negative effects, for example when tumor cell dissemination is induced. Finally, soluble v6-containing variants in the blood circulation form a potential impediment for the development of a successful MAb-based therapy.

Until now, preclinical and clinical data indicate that MAb U36 may be well suited for the treatment of minimal residual disease in HNSCC patients by RIT. RIT with MAb U36 was shown to be curative in xenograft-bearing nude mice with small tumors (100 mm^3). In addition, clinical studies in HNSCC patients indicated that intravenous injection of the antibody leads to selective accumulation in the tumor ($20.4 \pm 12.4 \% \text{ ID/kg}$), although some accumulation was observed in the normal oral mucosa, thyroid gland and in bone marrow as well. The maximum dose of ^{186}Re -labeled MAb U36 that can be applied to patients and the effectiveness of this dose are currently investigated in a phase I/II clinical trial.

The soluble CD44v6 protein present in the circulation of HNSCC patients appears not to be a serious problem for tumor targeting with MAb U36. Although complex formation has indeed been observed in blood samples of patients that were injected with MAb U36, the total amount of CD44v6 protein in the circulation (less than 1 mg) is relatively small compared to the amount of antibody injected. No evidence was found for sequestration of MAb-antigen complexes into the liver or any other organ.

The effect of RIT on CD44v6 positive cells that are present in several normal tissues, *e.g.* the skin, normal oral mucosa, thyroid gland, colon, breast and lung (see Chapters 1 and 5), is unknown. Functional characterization of v6-containing CD44 proteins might give more insight into these questions. During this PhD period, a number of experiments was performed elucidate the function of CD44v6 proteins. By antisense cDNA transfection as well as by gene targeting strategies we tried to generate cells with downregulated levels of CD44 expression. Subsequently, these CD44 negative cell lines might be used to re-express specific CD44 variants by cDNA transfection to study the variants *in vitro* with the help of functional assays. At this moment, there are no indications that MAb U36 has a large impact on the physiology of CD44v6 positive cells in normal tissues as concentrations up to 53 mg of trace-labeled MAb U36 did not cause any adverse reactions in HNSCC patients.

Finally, there are also no indications at this moment that binding of MAb U36 to CD44v6 positive cells has a large impact on the physiology of squamous tumors. First, administration of up to 400 μg MAb U36 to HNSCC-xenograft bearing nude mice, resulting in antigen saturation, did not result in a change in growth rate or induce metastasis. Second, culturing of HNSCC cell lines in the presence of MAb U36 (up to 100 $\mu\text{g/ml}$), did neither influence cell proliferation, as determined by sulphorhodamine B assay, nor cell morphology. Finally, binding of MAb U36 to cultured HNSCC cells did not result in an alteration of gene expression as assessed by differential display.

Taken together, data obtained so far indicate that MAb U36-based RIT is a promising option for the treatment of minimal residual disease of HNSCC. Due to their high level of CD44v6 expression, this might also be true for SCC of other origin as well as for breast and bladder carcinoma (see Chapter 2). If the ongoing phase I/II clinical trials confirm these expectations this will be an important breakthrough in the treatment of cancer.

Samenvatting, algemene discussie en perspectieven

Samenvatting

Plaveiselcelcarcinomen in het hoofd-halsgebied (HHPCC) ontstaan uit het slijmvlies van de bovenste lucht- en voedselweg. De behandeling van patiënten met dit type tumoren is afhankelijk van het tumorstadium en bestaat uit chirurgie en/of radiotherapie. Helaas is de vijfjaarsoverleving van HHPCC-patiënten met een vergevorderd tumorstadium relatief laag en bestaat er voor deze groep, die met curatieve intentie behandeld worden, nog steeds een groot risico op de ontwikkeling van locoregionale recidieven en afstandsmetastasen. Dit geeft aan dat de huidige behandeling van HHPCC voor een groot aantal patiënten niet voldoende is. Zowel locoregionaal als op afstand blijven tumorcellen achter, die met routinediagnostiek niet gedetecteerd worden. Er is daarom een grote behoefte aan een systemische adjuvante therapie om ook deze laatste tumorcellen, aangeduid als 'minimal residual disease', effectief te kunnen bestrijden. Omdat de effectiviteit van chemotherapie tot nu toe beperkt lijkt en HHPCC een intrinsieke gevoeligheid heeft voor bestraling, lijkt radio-immunotherapie (RIT) als adjuvante therapie een veelbelovende optie te zijn. Derhalve is op onze afdeling Keel- Neus- en Oorheilkunde van de Vrije Universiteit te Amsterdam een panel monoclonale antilichamen (MAbs) geselecteerd, gericht tegen plaveiselepitheel-geassocieerde antigenen. De eerste selectie vond plaats op basis van immunohistochemische kleuring van een groot aantal normale en maligne weefsels. Vanwege zijn intense en homogene reactiviteit met plaveiselcelcarcinomen werd MAb U36 geselecteerd als één van de geschiktste kandidaten voor RIT. Vervolgens werd door middel van radioimmunoscintigrafie en biodistributiestudies in HHPCC patiënten aangetoond dat MAb U36 inderdaad een geschikt antilichaam is voor selectieve 'tumor targeting'. Daarnaast suggereerde de selectieve expressie van het door MAb U36 herkende antigeen, dat deze marker mogelijk gebruikt zal kunnen worden voor de detectie van 'minimal residual disease'. Deze potentiële toepassingen maakten een verdere karakterisatie van het antigeen dat door MAb U36 wordt herkend gewenst.

In hoofdstuk 2 werd door middel van expressie-clonering aangetoond dat MAb U36 het eiwit CD44v3-v10 herkent, ook wel epican genoemd. CD44 is een sterk geglycosyleerd transmembraaneiwit dat in een groot aantal weefsels tot expressie komt. Er bestaat een grote variëteit aan CD44-isovormen, die

ontstaan door weefsel-specifieke alternatieve splicing, en CD44v3-v10 is daar één van. Het bestaan van deze grote groep van splicevarianten maakte het noodzakelijk om het antilichaambindende domein, de epitoot, in kaart te brengen. Deze epitoot werd bepaald met behulp van een zogenaamde 'pepscan' en bleek in het v6-domein van CD44 te liggen.

Na opheldering van de aminozuurvolgorde van de MAb U36 epitoot, bleek dat deze in twee aminozuren verschilde van sequenties die al eerder in de literatuur waren beschreven. Omdat deze sequentievariëaties een belemmering konden vormen voor 'tumor targeting' met MAb U36, werd in hoofdstuk 3 de affiniteit van MAb U36 voor deze epitootvarianten onderzocht. Op één positie leidde de aanwezigheid van een valine in plaats van een glutaminezuur tot een significant lagere binding van MAb U36. Verdere evaluatie liet echter zien dat deze lage-affiniteitsepitoot *in vivo* niet bestaat, en dat de in de literatuur gepubliceerde sequentie gebaseerd is op een artefact. De andere variatie, de substitutie van een lysine door een arginine, had geen invloed op de binding van MAb U36. Deze aminozuur variatie bleek gebaseerd te zijn op een allelisch polymorfisme in de populatie. Vervolgens werd onderzocht of deze aminozuur-variëatie gerelateerd is aan de maligne progressie van tumorcellen. Er werden echter geen aanwijzingen gevonden dat de allelische variatie uit balans is in tumorcellen.

Zoals reeds beschreven in hoofdstuk 1, worden CD44-splicevarianten (en v6 bevattende varianten in het bijzonder) verondersteld een rol te spelen in de progressie en metastasering van verschillende tumortypen, waaronder dikke-darmkanker en borstkanker. Het was daarom te verwachten dat de v6 bevattende splicevarianten op HHPCC anders waren dan die op normale mucosa. Daarmee zouden deze splicevarianten goede tumorspecifieke markers zijn voor de moleculaire diagnostiek van tumorcellen in chirurgische resectie randen, beenmerg, bloed en lymfeklieren. Daarom werd in hoofdstuk 4 geanalyseerd welke v6 bevattende CD44-splicevarianten er in HHPCC-tumoren tot expressie komen. Om de tumorspecifieke splicevarianten te kunnen identificeren werden deze vergeleken met de varianten die in normale mucosa tot expressie komen. In HHPCC werden op mRNA-niveau vijf mogelijke doelwitantigenen van MAb U36 aangetoond (CD44v2-v10, CD44v3-v10, CD44v3'-v10, CD44v4-v10 en CD44v6-v10). In normale mucosa uit de mondholte bleken exact dezelfde vijf v6 bevattende splicevarianten op een vergelijkbaar niveau tot expressie te komen, hetgeen erop duidt dat in plaveiselcellen de expressie van

deze varianten niet gerelateerd is aan het proces van carcinogenese. Niettemin was al eerder aangetoond dat MAb U36, ondanks de aanwezigheid van deze doelwitantigenen op zowel normale als maligne plaveiselcellen, *in vivo* tumorselectief is [79]. Dit is waarschijnlijk te danken aan het feit dat normale plaveiselcellen moeilijk bereikbaar zijn voor intraveneus toegediende immunoglobulinen door de hoge bloed-weefsel barrière. Het tumorweefsel wordt echter gekenmerkt door defecten in deze barrière, waardoor MAb U36 makkelijker in de tumor kan binnendringen [72].

Aangezien we geen verschil in de expressie van v6 bevattende CD44-splicevarianten konden aantonen tussen normale en maligne plaveiselcellen, rezen er twijfels over hun rol in de progressie van andere typen tumoren. Daarom is in **hoofdstuk 5** een vergelijking gemaakt tussen de v6 bevattende CD44-varianten in normaal en maligne weefsel van dikke darm, borst en long. Immunohistochemische aankleuringen lieten zien dat het v6-domein in vergelijkbare mate tot expressie komt in normale en maligne weefsels. Echter, in de normale weefsels bleek de expressie zich te beperken tot subgroepen van epitheliale cellen. 'Reverse transcriptase-polymerase chain reaction' (RT-PCR) analyses die werden uitgevoerd op de v6-positieve cellen (geïsoleerd via microdissectie) lieten zien dat normale en maligne v6-positieve cellen van hetzelfde weefseltype identieke v6 coderende CD44 mRNA transcripten tot expressie brengen. Deze bevindingen zijn in tegenspraak met de huidige visie dat tumorcellen een ontregelde splicing en verhoogde CD44v6-eiwitniveaus vertonen. In plaats van tumorspecifiek bleek de expressie van v6 coderende splicevarianten eerder weefsel specifiek te zijn, hetgeen suggereert dat ze als differentiatie-antigenen beschouwd moeten worden.

Zoals in **hoofdstuk 1** beschreven werd, zijn er naast de transmembraan-eiwitten ook oplosbare CD44v6-isovormen, die in de normale humane bloedsomloop circuleren. Men denkt dat deze oplosbare isovormen voornamelijk afkomstig zijn van lymfocyten. Voor een aantal typen tumoren zijn verhoogde CD44v6-serumniveaus beschreven, hetgeen toepassing in de diagnostiek mogelijk maakt. Aangezien HHPCC's het CD44v6-domein erg hoog tot expressie brengen, is in **hoofdstuk 6** onderzocht of het bepalen van CD44v6-spiegels in het serum van HHPCC-patiënten, via een v6-specifieke ELISA, gebruikt kan worden voor het opsporen van HHPCC-tumoren of het meten van behandelingsresultaten. Wij konden in HHPCC-patiënten echter geen verhoogde plasma-niveaus meten ten opzichte van controles en bovendien leidde opera-

tieve verwijdering van de tumor niet tot een afname van de CD44v6-spiegel. Immunoprecipitatie-experimenten toonden vervolgens aan dat niet alleen het niveau, maar ook het spectrum van oplosbare CD44v6-eiwitten in plasma van controles en patiënten identiek is. Deze gegevens duiden erop dat de CD44v6-eiwitspiegel in de bloedcirculatie van HHPCC-patiënten niet bruikbaar is voor de diagnostiek. Uit aanvullende experimenten bleek verder dat de v6 bevattende CD44-eiwitten in de circulatie van gezonde individuen grotendeels van normale epitheliale cellen afkomstig zijn. De aanwezigheid van deze eiwitten in de bloedcirculatie van gezonde personen zal het gebruik van CD44v6 als serummarker voor de detectie van andere humane maligniteiten ook aanzienlijk bemoeilijken, zo niet onmogelijk maken.

Algemene discussie en perspectieven

De toepasbaarheid van het MAb U36 antigeen voor HHPCC-detectie

Op het eerste gezicht lijken de mogelijkheden voor de toepassing van CD44 voor tumorceldetectie beperkt. De resultaten uit hoofdstuk 4 laten zien dat het onmogelijk zal zijn om tumorcellen die in de chirurgische snijranden zijn achtergebleven aan te tonen met een op CD44 gebaseerde detectiemethode. De achterliggende reden hiervoor is dat zowel normale als maligne plaveiselcellen hetzelfde niveau en hetzelfde spectrum aan CD44-varianten laten zien. Ook de ontwikkeling van een betrouwbare, op CD44 gebaseerde methode voor de detectie van tumorcellen in lymfeklieren, bloed en beenmerg lijkt moeilijk te zijn. Om de mogelijkheden van RT-PCR voor tumorceldetectie in bloed te onderzoeken, werden verschillende primercombinaties getest in een modelsysteem waarbij HHPCC-cellen werden gezaaid in 10 ml bloed. Alle geteste primercombinaties bleken echter ook een positief signaal te geven voor bloed waarin geen tumorcellen waren gezaaid. Blijkbaar worden alle CD44-splicevarianten die in HHPCC tot expressie komen ook op een zeer laag niveau in (bepaalde) bloedcellen tot expressie gebracht. Vanwege de hoge gevoeligheid van RT-PCR zijn deze lage niveaus detecteerbaar, een fenomeen dat ook voor verschillende andere moleculaire markers is beschreven [312-314]. Voor de meeste markers is dit effect toe te schrijven aan het 'leken' van het gen, maar in het geval van CD44 is dit mogelijk het gevolg van een gebrek aan specificiteit van het splicingmechanisme. Hemopoëtische cellen die CD44v6 tot

expressie brengen, kunnen ook een belemmering vormen voor de toepasbaarheid van immunocytochemie voor de detectie van tumorcellen in lymfeklieren, bloed en beenmerg, ofschoon de lage mRNA expressie in deze cellen niet hoeft te leiden tot detecteerbare hoeveelheden v6-eiwit. Desondanks laten recente gegevens van Liefers *et al.* [315] zien dat achtergrondexpressie van een tumormarker in normale cellen niet noodzakelijk een beperking voor tumorcel-detectie hoeft te zijn. Met behulp van een RT-PCR methode voor de amplificatie van het 'carcinoembryonisch antigen' (CEA) mRNA werd gevonden dat in patiënten met stadium II colorectaalcarcinoom de aanwezigheid van micro-metastasen in lymfeklieren geassocieerd is met een slechte prognose. Hoewel het bekend is dat CEA mRNA ook aanwezig is in hemopoëtische cellen, was het toch mogelijk om een onderscheid te maken tussen lymfeklieren met en zonder tumorcellen door gebruik te maken van een RT-PCR methode met een verlaagde gevoeligheid. Of deze strategie ook toepasbaar zal zijn voor HHPCC-detectie met behulp van een op CD44v6 gebaseerde RT-PCR, wordt op dit moment op ons laboratorium onderzocht.

Op dit moment worden er verschillende andere markers onderzocht die meer mogelijkheden lijken te hebben voor detectie van HHPCC-cellen met behulp van moleculair-biologische methodes in bloed, beenmerg en lymfeklieren. Met behulp van een specifieke RT-PCR methode, gebaseerd op het plaveiselcel-geassocieerde antigeen E48, blijkt het mogelijk om 1 tumorcel te detecteren in een omgeving van ongeveer 2×10^7 witte bloedcellen. Deze marker blijkt ook niet tot expressie te komen op hemopoëtische cellen bij gezonde controles (Brakenhoff *et al.*, submitted). Een nadeel van deze marker is de heterogene expressie in HHPCC-tumoren, hetgeen de betrouwbaarheid van de test kan verminderen.

Een andere toepassing voor diagnostiek, het gebruik van oplosbaar CD44v6 in plasma voor de detectie van 'minimal residual disease' in HHPCC-patiënten, werd belemmerd door de aanwezigheid van HHPCC-geassocieerde CD44v6-varianten in de normale humane bloedcirculatie. De gegevens in hoofdstuk 6 laten zien dat tenminste een deel van de oplosbare CD44-eiwitten in het bloed afkomstig is van epitheliale cellen, een waarneming die belangrijke implicaties heeft voor het gebruik van oplosbaar CD44v6 als marker voor de detectie van andere maligniteiten.

De resultaten die in dit proefschrift worden gepresenteerd laten zien dat, ondanks de hoge en homogene expressie op HHPCC, CD44v6 niet de ideale marker is voor detectie van de na conventionele behandeling achtergebleven tumorcellen of voor het gebruik als serummarker. Dit zou anders kunnen liggen voor de detectie van kleine tumorhaarden door middel van 'imaging' procedures. Voor de detectie van primaire HHPCC-tumoren en lymfeklier-metastasen is inmiddels aangetoond dat de diagnostische waarde van radio-immunoscintigrafie met ^{99m}Tc -gelabeld MAb U36 vergelijkbaar is met palpatie, CT en MRI [79]. Met deze technieken kunnen over het algemeen tumoren met een diameter groter dan 1 cm gedetecteerd worden. De conventionele scintigrafie wordt momenteel verder verbeterd door de introductie van positronemissietomografie (PET), wat het detecteren van veel kleinere tumoren mogelijk zou kunnen maken. Voor de toepassing van PET worden er momenteel op ons instituut MAb U36 conjugaten ontwikkeld die de positronemitter ^{89}Zr bevatten.

Toepasbaarheid van MAb U36 voor de behandeling van 'minimal residual disease'

Het succes van een op antilichamen gebaseerde therapie is voor een groot deel afhankelijk van het distributiepatroon van het antilichaam in het lichaam van de patiënt. Dit kan met name een rol spelen als intrinsiek toxische MAb conjugaten gebruikt worden, zoals bij RIT. Indien het doelwitantigeen in normale weefsels een belangrijke fysiologische functie vervult, bestaat eveneens de kans dat er neveneffecten optreden. Daarnaast kan ook de binding van het antilichaam aan de tumor tot negatieve bijwerkingen leiden, bijvoorbeeld als metastasering wordt geïnduceerd. Ook de aanwezigheid van oplosbare v6 bevattende varianten in de bloedcirculatie vormt een mogelijke belemmering voor de ontwikkeling van een succesvolle op MAb U36 gebaseerde therapie.

Tot nu toe laten preklinische en klinische gegevens zien dat MAb U36 waarschijnlijk zeer geschikt is voor de behandeling van 'minimal residual disease' in HHPCC-patiënten met behulp van RIT. RIT met MAb U36 bleek curatief in HHPCC-dragende naakte muizen met kleine tumoren (100 mm^3). Bovendien hebben klinische studies in HHPCC-patiënten laten zien dat intraveneuze injectie van antilichaam leidt tot selectieve ophoping in de tumor ($20.4 \pm 12.4 \% \text{ ID/kg}$), hoewel er ook enige ophoping in de normale mucosa uit de mond, schildklier en in beenmerg werd gevonden. De maximale dosis voor ^{186}Re -gelabeld MAb U36 die aan patiënten kan worden toegediend en de thera-

peutische effectiviteit van deze dosis worden momenteel bepaald in een fase I/II klinische studie.

Het oplosbare CD44v6 dat in de bloedsomloop van HHPCC-patiënten aanwezig is, vormt waarschijnlijk geen serieuze belemmering voor 'tumor targeting' met MAb U36. Complexvorming is inderdaad waar te nemen in bloedmonsters van patiënten die zijn geïnjecteerd met MAb U36, maar de totale hoeveelheid CD44v6-eiwit in de circulatie (minder dan 1 mg) is relatief klein ten opzichte van de hoeveelheid antilichaam die wordt geïnjecteerd. Er zijn geen aanwijzingen gevonden voor een ophoping van MAb-antigeencomplexen in de lever of andere organen.

Het effect van RIT op CD44v6-positieve cellen die in verschillende normale weefsels aanwezig zijn, zoals in huid, slijmvliezen, schildklier, dikke darm, borst en long (zie hoofdstukken 1 en 5), is niet bekend. Kennis over de functie van v6 bevattende CD44-eiwitten in deze weefsels zal hier mogelijk meer inzicht in kunnen geven. Tijdens dit promotie-onderzoek is eveneens onderzoek gedaan om de functie van de CD44v6-eiwitten op plaveiselcellen op te helderen. Door middel van zowel anti-sense cDNA transfectie als door 'gene targeting'-methoden werden pogingen gedaan om cellen te genereren met een sterk verlaagde CD44-expressie. Van deze CD44-negatieve cellijnen kan vervolgens geanalyseerd worden welke functie ontbreekt en of functioneel verlies weer hersteld kan worden na herintroductie van specifieke splice-varianten. Dit deel van het onderzoek heeft echter (nog) niet tot duidelijke resultaten geleid en is verder buiten beschouwing gelaten in dit proefschrift. Op dit moment zijn er in ieder geval geen aanwijzingen dat MAb U36 een grote invloed heeft op de fysiologie van CD44v6-positieve cellen in normale weefsels, aangezien concentraties tot 53 mg MAb U36 geen negatieve bijwerkingen lieten zien in HHPCC-patiënten.

Eveneens zijn er op dit moment ook geen indicaties dat de binding van MAb U36 aan CD44v6-positieve tumorcellen een grote invloed heeft op de fysiologie van de tumorcellen. Ten eerste leidde de toediening van hoeveelheden tot 400 µg MAb U36 aan HHPCC-dragende naakte muizen, wat resulteert in verzadiging van het antigeen, niet tot een verandering in de groeisnelheid van de tumor of een metastatisch gedrag. Ten tweede had het kweken van HHPCC-cellijnen in de aanwezigheid van MAb U36 (tot 100 µg/ml) noch invloed op de celproliferatie (gemeten met behulp van de sulphorhodamine B bepaling), noch op de celmorfologie. Tot slot liet 'differen-

tial display' zien dat binding van MAb U36 aan gekweekte HHPCC-cellen niet resulteert in een verandering van het gen-expressiepatroon.

Alles samengevat wijst het onderzoek tot nu toe uit dat het U36-antigeen (CD44v6), ondanks de tot nu toe beperkte diagnostische mogelijkheden, een veelbelovend doelwitmolecuul is voor de behandeling van 'minimal residual disease' van HHPCC. Omdat naast HHPCC ook andere typen plaveiselcelcarcinomen en een deel van de borst- en blaascarcinomen een hoge CD44v6-expressie laten zien, zou een op MAb U36 gebaseerde RIT mogelijk ook voor deze tumoren toepasbaar zijn (hoofdstuk 2). Als de fase I/II klinische studies die momenteel aan de gang zijn deze verwachtingen kunnen bevestigen, dan zou dat een belangrijke doorbraak betekenen op het gebied van de behandeling van kanker.

161

1. Zarbo RJ and Crissman JD. The surgical pathology of head and neck cancer. *Sem. Oncol.* 15:10-19 (1988)
2. Vokes EE, Weichselbaum RR, Lippman SM and Hong WK. Head and neck cancer. *N. Engl. J. Med.* 328:184-194 (1993)
3. Muir C and Weiland L. Upper aerodigestive tract cancers. *Cancer* 75 (Suppl.):147-153 (1995)
4. Blitzer PH. Epidemiology of head and neck cancer. *Sem. Oncol.* 15:2-9 (1988)
5. Choi SY and Kahyo H. Effect of cigarette smoking and alcohol consumption in the aetiology of cancer of the oral cavity, pharynx and larynx. *Int. J. Epidemiol.* 20:878-885 (1991)
6. Boffetta P, Mashberg A, Winkelmann R and Garfinkel L. Carcinogenic effect of tobacco smoking and alcohol drinking on anatomic sites of the oral cavity and oropharynx. *Int. J. Cancer* 52:530-533 (1992)
7. Christen AG. The impact of tobacco use and cessation on oral and dental diseases and conditions. *Am. J. Med.* 93 (Suppl 1A):25S-31S (1992)
8. Mashberg A, Boffetta P, Winkelmann R and Garfinkel L. Tobacco smoking, alcohol drinking, and cancer of the oral cavity and oropharynx among U.S. veterans. *Cancer* 72:1369-1375 (1993)
9. Field JK, Spandidos DA, Malliri A, Gosney JR, Yiagnisis M and Stell PM. Elevated p53 expression correlates with history of heavy smoking in squamous cell carcinoma of the head and neck. *Br. J. Cancer* 64:573-577 (1991)
10. Hollstein M, Sidransky D, Vogelstein B and Harris CC. p53 Mutations in human cancers. *Science* 253:49-53 (1991)
11. Boyle JO, Hakim J, Koch W, Van der Riet P, Hruban RH, Roa A, Correo R, Eby YJ, Ruppert JM and Sidransky D. The incidence of p53 mutations increases with progression of head and neck cancer. *Cancer Res.* 53:4477-4480 (1993)
12. Brennan JA, Boyle JO, Koch WM, Goodman SN, Hruban RH, Eby YJ, Couch MJ, Forastiere AA and Sidransky D. Association between cigarette smoking and mutation of the p53 gene in squamous-cell carcinoma of the head and neck. *N. Engl. J. Med.* 332:712-717 (1995)
13. Snijders PJF, Steenbergen RDM, Top B, Scott SD, Meijer CJLM and Walboomers JMM. Analysis of p53 status in tonsillar carcinomas associated with human papillomavirus. *J. Gen. Virol.* 75:2769-2775 (1994)
14. Ishitoya J, Toriyama M, Oguchi N, Kitamura K, Ohshima M, Asano K and Yamamoto T. Gene amplification and overexpression of EGF receptor in squamous cell carcinomas of the head and neck. *Br. J. Cancer* 59:559-562 (1989)
15. Weichselbaum RR, Dunphy EJ, Beckett MA, Tybor AG, Moran WJ, Goldman ME, Vokes EE and Panje WR. Epidermal growth factor receptor gene amplification and expression in head and neck cancer cell lines. *Head Neck* 11:437-442 (1989)
16. Kijianenko J, Bianchi AB, Cvitkovic E, Janot F, Lubinski B and Conti CJ. Unexpected *Prad-1* amplification in multiple simultaneous localisations of squamous cell carcinoma of the head and neck. *Eur. J. Cancer* 29A:653-654 (1993)

17. Callender T, El-Naggar AK, Lee MS, Frankenthaler R, Luna MA and Batsakis JG. PRAD-1 (CCND1)/Cyclin D1 oncogene amplification in primary head and neck squamous cell carcinoma. *Cancer* 74:152-158 (1994)
18. Jares P, Fernández PL, Campo E, Nadal A, Bosch F, Aiza G, Nayach I, Traserra J and Cardesa A. *PRAD-1/Cyclin D1* gene amplification correlates with messenger RNA overexpression and tumor progression in human laryngeal carcinomas. *Cancer Res.* 54:4813-4817 (1994)
19. Nawroz H, Van der Riet P, Hruban RH, Koch W, Ruppert JM and Sidransky D. Allelotype of head and neck squamous cell carcinoma. *Cancer Res.* 54:1152-1155 (1994)
20. Van der Riet P, Nawroz H, Hruban RH, Corio R, Tokino K, Koch W and Sidransky D. Frequent loss of chromosome 9p21-22 early in head and neck cancer. *Cancer Res.* 54:1156-1158 (1994)
21. Califano J, Van der Riet P, Westra W, Nawroz H, Clayman G, Plantadosi S, Corio R, Lee D, Greenberg B, Koch W and Sidransky D. Genetic progression model for head and neck cancer: implications for field cancerization. *Cancer Res.* 56:2488-2492 (1996)
22. Mao L, Lee JS, Fan YH, Ro JY, Batsakis JG, Lippman S, Hittelman W and Hong WK. Frequent microsatellite alterations at chromosomes 9p21 and 3p14 in oral premalignant lesions and their value in cancer risk assessment. *Nature Med.* 2:682-685 (1996)
23. Mao L, Fan Y-H, Lotan R and Hong WK. Frequent abnormalities of *FHIT*, a candidate tumor suppressor gene, in head and neck cancer cell lines. *Cancer Res.* 56:5128-5131 (1996)
24. Nawroz H, Koch W, Anker P, Stroun M and Sidransky D. Microsatellite alterations in serum DNA of head and neck cancer patients. *Nature Med.* 2:1035-1037 (1996)
25. Reed AL, Califano J, Cairns P, Westra WH, Jones RM, Koch W, Ahrendt S, Eby Y, Sewell D, Nawroz H, Bartek J and Sidransky D. High frequency of *p16 (CDKN2/MTS-1/INK4A)* inactivation in head and neck squamous cell carcinoma. *Cancer Res.* 56:3630-3633 (1996)
26. Virgilio L, Shuster M, Gollin SM, Veronese ML, Ohta M, Huebner K and Croce CM. *FHIT* gene alterations in head and neck squamous cell carcinomas. *Proc. Natl. Acad. Sci. USA* 93:9770-9775 (1996)
27. Papadimitrakopoulou V, Izzo J, Lippman SM, Lee JS, Fan YH, Clayman G, Ro JY, Hittelman WN, Lotan R, Hong WK and Mao L. Frequent inactivation of *p16^{INK4a}* in oral premalignant lesions. *Oncogene* 14:1799-1803 (1997)
28. Rawnsley JD, Srivatsan ES, Chakrabarti R, Billings KR and Wang MB. Deletion analysis of the *p16/CDKN2* gene in head and neck squamous cell carcinoma using quantitative polymerase chain reaction method. *Arch. Otolaryngol. Head Neck Surg.* 123:863-867 (1997)
29. Waber P, Dlugosz S, Cheng Q-C, Truelson J and Nisen PD. Genetic alterations of chromosome band 9p21-22 in head and neck cancer are not restricted to *p16^{INK4a}*. *Oncogene* 15:1699-1704 (1997)
30. Lydiatt WM, Davidson BJ, Schantz SP, Caruana S and Chaganti RS. 9p21 deletion correlates with recurrence in head and neck cancer. *Head Neck* 20:113-118 (1998)
31. Cloos J, Braakhuis BJM, Steen I, Copper MP, De Vries N, Nauta JJP and Snow GB. Increased mutagen sensitivity in head and neck squamous cell carcinoma patients, particularly those with multiple primary tumors. *Int. J. Cancer* 56: 816-819 (1994)

32. Cloos J, Spitz MR, Schantz SP, Hsu TC, Zhang Z-F, Tobi H, Braakhuis BJM and Snow GB. Genetic susceptibility to head and neck squamous cell carcinoma. *J. Natl. Cancer Inst.* **88**:530-535 (1996)
33. Snow GB, Patel P, Leemans CR and Tiwari R. Management of cervical lymph nodes in patients with head and neck cancer. *Eur. Arch. Otorhinolaryngol.* **249**:187-194 (1992)
34. Berger DS and Fletcher GH. Distant metastases following local control of squamous-cell carcinoma of the nasopharynx, tonsillar fossa and base of the tongue. *Radiology* **100**:141-143 (1971)
35. Merino OR, Lindberg RD and Fletcher GH. An analysis of distant metastases from squamous cell carcinoma of the upper respiratory and digestive tracts. *Cancer* **40**:145-151 (1977)
36. Wolf G, Vikram B, Jacobs C and Makuch R. Adjuvant chemotherapy for advanced head and neck squamous carcinoma. Final report of the head and neck contracts program. *Cancer* **60**:301-311 (1987)
37. Vikram B, Stong EW, Shah JP and Spiro R. Failure at distant sites following multimodality treatment for advanced head and neck cancer. *Head Neck Surg.* **6**:730-733 (1984)
38. Leemans CR, Tiwari R, Nauta JJP, Van der Waal I and Snow GB. Regional lymph node involvement and its significance in the development of distant metastases in head and neck carcinoma. *Cancer* **71**:452-456 (1993)
39. Zbären P and Lehmann W. Frequency and sites of distant metastases in head and neck squamous cell carcinoma. An analysis of 101 cases at autopsy. *Arch. Otolaryngol. Head Neck Surg.* **113**:762-764 (1987)
40. Nishijima W, Takooda S, Tokita N, Takayama S and Sakura M. Analysis of distant metastases in squamous cell carcinoma of the head and neck and lesions above the clavicle at autopsy. *Arch. Otolaryngol. Head Neck Surg.* **119**:65-68 (1993)
41. Leemans CR, Tiwari R, Nauta JJP, Van der Waal I and Snow GB. Recurrence at the primary site in head and neck cancer and the significance of neck lymph node metastases as a prognostic factor. *Cancer* **73**:187-190 (1994)
42. Harmer MH (Ed.). TNM classification of malignant tumors. International Union Against Cancer, 3rd ed., Geneva (1978)
43. Hermanek P and Sobin LH (Eds.). International Union Against Cancer. TNM classification of malignant tumours, 4th ed., Springer Verlag, New York (1987)
44. Vernham GA and Crowther JA. Head and neck carcinoma - stage at presentation. *Clin. Otolaryngol.* **19**:120-124 (1994)
45. Choksi AJ, Dimery IW and Hong WK. Adjuvant chemotherapy of head and neck cancer: the past, the present and the future. *Semin. Oncol.* **15**: 45-59 (1988)
46. Stell PM and Rawson NSB. Adjuvant chemotherapy in head and neck cancer. *Br. J. Cancer* **61**:779-787 (1990)
47. Jassem J and Bartelink H. Chemotherapy in locally advanced head and neck cancer: a critical reappraisal. *Cancer Treat. Rev.* **21**:447-462 (1995)

48. El-Sayed S and Nelson N. Adjuvant and adjunctive chemotherapy in the management of squamous cell carcinoma of the head and neck region: a meta-analysis of prospective and randomized trials. *J. Clin. Oncol.* **14**:838-847 (1996)
49. Brennan JA, Mao L, Hruban RH, Boyle JO, Eby YJ, Koch WM, Goodman SN and Sidransky D. Molecular assessment of histopathological staging in squamous-cell carcinoma of the head and neck. *N. Engl. J. Med.* **332**:429-435 (1995)
50. Galh HJ, Heissler E, Hell B, Bier J, Riettmüller G and Pantel K. Immunocytologic detection of isolated tumor cells in bone marrow of patients with squamous cell carcinomas of the head and neck region. *Int. J. Oral Maxillofac. Surg.* **24**:351-355 (1995)
51. Maestro R, Dolcetti R, Gasparotto D, Doglioni C, Pelucchi S, Barzan L, Grandi E and Boiocchi M. High frequency of p53 gene alterations associated with protein overexpression in human squamous cell carcinoma of the larynx. *Oncogene* **7**:1159-1166 (1992)
52. Wollenberg B, Ollesch A, Maag K, Funke I and Wilmes E. Mikrometastasen im knochenmark von patienten mit karzinomen des kopf-hals-bereiches. *Laryngo-Rhino-Otol.* **73**:88-93 (1994)
53. Van Dongen GAMS, Brakenhoff RH, Ten Brink C, Van Gog FB, De Bree R, Quak JJ and Snow GB. Squamous cell carcinoma-associated antigens used in novel strategies for the detection and treatment of minimal residual head and neck cancer. *Anticancer Res.* **16**:2409-2413 (1996)
54. Pelkey TJ, Frierson HF and Bruns DE. Molecular and immunological detection of circulating tumor cells and micrometastases from solid tumors. *Clin. Chem.* **42**:1369-1381 (1996)
55. Samuel J, Noujaim AA, Willans DJ, Brzezinska GS, Haines DM and Longenecker BM. A novel marker for basal (stem) cells of mammalian stratified squamous epithelia and squamous cell carcinoma. *Cancer Res.* **49**:2465-2470 (1989)
56. Quak JJ, Van Dongen GAMS, Balm AJM, Brakkee JPG, Scheper RJ, Snow GB and Meijer CJLM. A 22-kDa surface antigen detected by monoclonal antibody E48 is exclusively expressed in stratified squamous and transitional epithelia. *Am. J. Pathol.* **136**:191-197 (1990)
57. Inoue M, Nakanishi K, Sasagawa T, Tanizawa O, Inoue H, and Hakura A. A novel monoclonal antibody against squamous cell carcinoma. *Jpn. J. Cancer Res.* **81**:176-182 (1990)
58. Schrijvers AHGJ, Quak JJ, Uytendinck AM, Van Walsum M, Meijer CJLM, Snow GB, and Van Dongen GAMS. MAb U36, a novel monoclonal antibody successful in immunotargeting of squamous cell carcinoma of the head and neck. *Cancer Res.* **53**:4383-4390 (1993)
59. Yoshiura M, Murakami H, Tashiro H and Kurisu K. Production of a human monoclonal antibody to normal basal and squamous cell carcinoma-associated antigen. *J. Oral Pathol. Med.* **22**:451-458 (1993)
60. Heider K-H, Sproll M, Susani S, Patzelt E, Beaumier P, Ostermann E, Ahorn H and Adolf GR. Characterization of a high-affinity monoclonal antibody specific for CD44v6 as candidate for immunotherapy of squamous cell carcinomas. *Cancer Immunol. Immunother.* **43**:245-253 (1996)
61. Boeheim K, Speak JA, Frei E and Bernal SD. SQM1 antibody defines a surface membrane antigen in squamous carcinoma of the head and neck. *Int. J. Cancer* **36**:137-142 (1985)
62. Kimmel KA and Carey TE. Altered expression in squamous cells of an orientation restricted epithelial antigen detected by monoclonal antibody A9. *Cancer Res.* **46**:3614-3623 (1986)

63. Myoken Y, Moroyama T, Miyauchi S, Takada K and Namba M. Monoclonal antibodies against human oral squamous cell carcinoma reacting with keratin proteins. *Cancer* 60:2927-2937 (1987)
64. Murthy U, Basu A, Rodeck U, Herlyn M, Ross AH and Das M. Binding of an antagonistic monoclonal antibody to an intact and fragmented EGF-receptor polypeptide. *Arch. Biochem. Biophys.* 252:549-560 (1987)
65. Quak JJ, Van Dongen GAMS, Gerretsen M, Hayashida D, Balm AJM, Brakkee JGP, Snow GB and Meijer CJLM. Production of monoclonal antibody (K931) to a squamous cell carcinoma antigen identified as the 17-1A antigen. *Hybridoma* 9:377-387 (1990)
66. Divgi CR, Welt S, Kris M, Real FX, Yeh SDJ, Gralla R, Merchant B, Schweighart S, Unger M, Larson SM and Mendelsohn J. Phase I and imaging trial of Indium-111-labeled anti-epidermal growth factor receptor monoclonal antibody 225 in patients with squamous cell lung carcinoma. *J. Natl. Cancer Inst.* 83:97-104 (1991)
67. Quak JJ, Schrijvers AHGJ, Brakkee JGP, Davis HD, Scheper RJ, Balm AJM, Meijer CJLM, Snow GB and Van Dongen GAMS. Expression and characterization of two differentiation antigens in stratified squamous epithelia and carcinomas. *Int. J. Cancer* 50:507-513 (1992)
68. Balm AJM, Hageman PC, Mulder CJ and Hilken J. Carcinoma-associated monoclonal antibodies in head and neck carcinoma: immunohistochemistry and biodistribution of monoclonal antibodies 175F4 and 175F11. *Eur. Arch. Otorhinolaryngol.* 249:237-242 (1992)
69. Chang K, Pastan I and Willingham MC. Frequent expression of the tumor antigen CAK1 in squamous-cell carcinomas. *Int. J. Cancer* 51:548-554 (1992)
70. Maraveyas A, Stafford N, Rowlinson-Busza G, Stewart JSW and Epenetos AA. Pharmacokinetics, biodistribution, and dosimetry of specific and control radiolabeled monoclonal antibodies in patients with primary head and neck squamous cell carcinoma. *Cancer Res.* 55:1060-1069 (1995)
71. De Bree R, Roos JC, Quak JJ, Den Hollander W, Snow GB and Van Dongen GAMS. Clinical screening of monoclonal antibodies 323/A3, cSF-25, and K928 for suitability of targeting tumours in the upper aerodigestive and respiratory tract. *Nucl. Med. Commun.* 15:613-627 (1994)
72. Cobb LM. Intratumour factors influencing the access of antibody to tumour cells. *Cancer Immunol. Immunother.* 28:235-240 (1989)
73. Wessels BW and Rogus RD. Radionuclide selection and model absorbed dose calculations for radiolabeled tumor associated antibodies. *Med. Phys.* 11:638-645 (1984)
74. Goldenberg DM. Monoclonal antibodies in cancer detection and therapy. *Am. J. Med.* 94:297-312 (1993)
75. Van Dongen GAMS, Brakenhoff RH, De Bree R, Gerretsen M, Quak JJ and Snow GB. Progress in radioimmunotherapy of head and neck cancer (review). *Oncol. Rep.* 1:259-264 (1994)
76. Van Gog FB, Visser GWM, Klok R, Van der Schors R, Snow GB and Van Dongen GAMS. Monoclonal antibodies labeled with Rhenium-186 using the MAG3 chelate: relationship between the number of chelated groups and biodistribution characteristics. *J. Nucl. Med.* 37:352-362 (1996)
77. Van Gog FB, Brakenhoff RH, Stichter-van Walsum M, Snow GB and Van Dongen GAMS. Perspectives of combined radioimmunotherapy and anti-EGFR antibody therapy for the treatment of residual head and neck cancer. *Int. J. Cancer* 77:13-18 (1998)

78. Gerretsen M, Visser GWM, Brakenhoff RH, Van Walsum M, Snow GB and Van Dongen GAMS. Complete ablation of small squamous cell carcinoma xenografts with ¹⁸⁶Re-labeled monoclonal antibody E48. *Cell Biophys.* 24-25:135-142 (1994)
79. De Bree R, Roos JC, Quak JJ, Den Hollander W, Snow GB and Van Dongen GAMS. Radioimmunoscintigraphy and biodistribution of Technetium-99m-labeled monoclonal antibody U36 in patients with head and neck cancer. *Clin. Cancer Res.* 1:591-598 (1995)
80. De Bree R, Roos JC, Plaizier MABD, Quak JJ, Van Kamp GJ, Den Hollander W, Snow GB and Van Dongen GAMS. Selection of monoclonal antibody E48 IgG or U36 IgG for adjuvant radioimmunotherapy in head and neck cancer patients. *Br. J. Cancer* 75:1049-1060 (1997)
81. Dalchau R, Kirkley J and Fabre JW. Monoclonal antibody to a human brain-granulocyte-T lymphocyte antigen probably homologous to the W 3/13 antigen of the rat. *Eur. J. Immunol.* 10:745-749 (1980)
82. Trowbridge IS, Lesley J, Schulte R, Hyman R and Trotter J. Biochemical characterization and cellular distribution of a polymorphic, murine cell-surface glycoprotein expressed on lymphoid tissues. *Immunogenetics* 15:299-312 (1982)
83. Hughes EN, Mengod G and August JT. Murine cell surface glycoproteins. Characterisation of a major component of 80,000 daltons as a polymorphic differentiation antigen of mesenchymal cells. *J. Biol. Chem.* 256:7023-7027 (1981)
84. Telen MJ, Eisenbarth GS and Haynes BF. Human erythrocyte antigens. Regulation of expression of a novel erythrocyte surface antigen by the inhibitor Lutheran *In(Lu)* gene. *J. Clin. Invest.* 71:1878-1886 (1983)
85. Haynes BF, Harden EA, Telen MJ, Hemler ME, Strominger JL, Palker TJ, Searce RM and Eisenbarth GS. Differentiation of human T lymphocytes. I. Acquisition of a novel human cell surface protein (p80) during normal intrathymic T cell maturation. *J. Immunol.* 131:1195-1200 (1983)
86. Tarone G, Ferracini R, Galeto G and Comoglio P. A cell surface integral membrane glycoprotein of 85,000 mol wt (gp85) associated with triton X-100-insoluble cell skeleton. *J. Cell Biol.* 99:512-519 (1984)
87. Letarte M, Iturbe S and Quackenbush J. A glycoprotein of molecular weight 85,000 on human cells of B-lineage: detection with a family of monoclonal antibodies. *Mol. Immunol.* 22:113-124 (1985)
88. Underhill CB, Thurn AL and Lacy BE. Characterization and identification of the hyaluronate binding site from membranes of SV-3T3 cells. *J. Biol. Chem.* 260:8128-8133 (1985)
89. Underhill CB, Green SJ, Comoglio PM and Tarone G. The hyaluronate receptor is identical to a glycoprotein of M_r 85,000 (gp85) as shown by a monoclonal antibody that interferes with binding activity. *J. Biol. Chem.* 262:13142-13146 (1987)
90. Isacke CM, Sauvage CA, Hyman R, Lesley J, Schulte R and Trowbridge IS. Identification and characterization of the human Pgp-1 glycoprotein. *Immunogenetics* 23:326-332 (1986)

91. Jalkanen ST, Bargatze RF, Herron LR and Butcher EC. A lymphoid cell surface glycoprotein involved in endothelial cell recognition and lymphocyte homing in man. *Eur. J. Immunol.* **16**:1195-1202 (1986)
92. Jalkanen S, Bargatze RF, De los Toyos J and Butcher EC. Lymphocyte recognition of high endothelium: antibodies to distinct epitopes of an 85-95-kD glycoprotein antigen differentially inhibit lymphocyte binding to lymph node, mucosal, or synovial endothelial cells. *J. Cell Biol.* **105**:983-990 (1987)
93. Gallatin WM, Wayner EA, Hoffman PA, St John T, Butcher EC and Carter WG. Structural homology between lymphocyte receptors for high endothelium and class III extracellular matrix receptor. *Proc. Natl. Acad. Sci. USA* **86**:4654-4658 (1989)
94. Carter WG and Wayner EA. Characterization of the class III collagen receptor, a phosphorylated, transmembrane glycoprotein expressed in nucleated human cells. *J. Biol. Chem.* **263**:4193-4201 (1988)
95. Wayner EA and Carter WG. Identification of multiple cell adhesion receptors for collagen and fibronectin in human fibrosarcoma cells possessing unique α and common β subunits. *J. Cell Biol.* **105**:1873-1884 (1987)
96. Letarte M. Human p85 glycoprotein bears three distinct epitopes defined by several monoclonal antibodies. *Mol. Immunol.* **23**:639-644 (1986)
97. Omary MB, Trowbridge IS, Letarte M, Kagnoff MF and Isacke CM. Structural heterogeneity of human Pgp-1 and its relationship with p85. *Immunogenetics* **27**:460-464 (1988)
98. Picker LJ, Nakache M and Butcher EC. Monoclonal antibodies to human lymphocyte homing receptors define a novel class of adhesion molecules on diverse cell types. *J. Cell Biol.* **109**:927-937 (1989)
99. Aruffo A, Stamenkovic I, Melnick M, Underhill CB and Seed B. CD44 is the principal cell surface receptor for hyaluronate. *Cell* **61**:1303-1313 (1990)
100. Culty M, Miyake K, Kincade PW, Silorski E, Butcher EC and Underhill C. The hyaluronate receptor is a member of the CD44 (H-CAM) family of cell surface glycoproteins. *J. Cell Biol.* **111**:2765-2774 (1990)
101. Cobbold S, Hale G and Waldman H. Non-lineage, LFA-1 family and leukocyte common antigens: new and previously defined clusters. In: *Leukocyte Typing III: White Cell Differentiation Antigens*. McMichael AJ (Ed.), Oxford University, Oxford, 788-803 (1987)
102. Goldstein LA, Zhou DFH, Picker LJ, Minty CN, Bargatze RF, Ding JF and Butcher EC. A human lymphocyte homing receptor, the Hermes antigen, is related to cartilage proteoglycan core and link proteins. *Cell* **56**:1063-1072 (1989)
103. Idzerda RL, Carter WG, Nottenburg C, Wayner EA, Gallatin WM and St John T. Isolation and DNA sequence of a cDNA clone encoding a lymphocyte adhesion receptor for high endothelium. *Proc. Natl. Acad. Sci. USA* **86**:4659-4663 (1989)
104. Stamenkovic I, Amiot M, Pasando JM and Seed B. A lymphocyte molecule implicated in lymph node homing is a member of the cartilage link protein family. *Cell* **56**:1057-1062 (1989)

105. Zhou DFH, Ding JF, Picker LJ, Bargatze RF, Butcher EC and Goeddel DV. Molecular cloning and expression of Pgp-1. The mouse homolog of the human H-CAM (Hermes) lymphocyte homing receptor. *J. Immunol.* **143**:3390-3395 (1989)
106. Wolffe EJ, Gause WC, Pelfrey CM, Holland SM, Steinberg AD and August JT. The cDNA sequence of mouse Pgp-1 and homology to human CD44 cell surface antigen and proteoglycan core/link proteins. *J. Biol. Chem.* **265**:341-347 (1990)
107. Brown TA, Bouchard T, St John T, Wayner E and Carter WG. Human keratinocytes express a new CD44 core protein (CD44E) as a heparan-sulfate intrinsic membrane proteoglycan with additional exons. *J. Cell Biol.* **113**:207-221 (1991)
108. Dougherty GJ, Lansdorp PM, Cooper DL and Humphries RK. Molecular cloning of CD44R1 and CD44R2, two novel isoforms of the human CD44 lymphocyte "homing" receptor expressed by hemopoietic cells. *J. Exp. Med.* **174**:1-5 (1991)
109. Günthert U, Hofmann M, Rudy W, Reber S, Zöller M, Haussmann I, Matzku S, Wenzel A, Ponta H and Herrlich P. A new variant of glycoprotein CD44 confers metastatic potential to rat carcinoma cells. *Cell* **65**:13-24 (1991)
110. Hofmann M, Rudy W, Zöller M, Tölg C, Ponta H, Herrlich P and Günthert U. CD44 splice variants confer metastatic behavior in rats: homologous sequences are expressed in human tumor cell lines. *Cancer Res.* **51**:5292-5297 (1991)
111. Cooper DL, Dougherty G, Harn H-J, Jackson S, Baptist EW, Byers J, Datta A, Phillips G and Isola NR. The complex CD44 transcriptional unit: alternative splicing of three internal exons generates the epithelial form of CD44. *Biochem. Biophys. Res. Commun.* **182**:569-578 (1992)
112. He Q, Lesley J, Hyman R, Ishihara K and Kincade PW. Molecular isoforms of murine CD44 and evidence that the membrane proximal domain is not critical for hyaluronate recognition. *J. Cell Biol.* **119**:1711-1719 (1992)
113. Jackson DG, Buckley J and Bell JI. Multiple variants of the human lymphocyte homing receptor CD44 generated by insertions at a single site in the extracellular domain. *J. Biol. Chem.* **267**:4732-4739 (1992)
114. Kugelman LC, Ganguly S, Haggerty JG, Weissman SM and Milstone LM. The core protein of epican, a heparan sulfate proteoglycan on keratinocytes, is an alternative form of CD44. *J. Invest. Dermatol.* **99**:886-891 (1992)
115. Sreaton GR, Bell MV, Jackson DG, Cornelis FB, Gerth U and Bell JI. Genomic structure of DNA encoding the lymphocyte homing receptor CD44 reveals at least 12 alternatively spliced exons. *Proc. Natl. Acad. Sci. USA* **89**:12160-12164 (1992)
116. Rudy W, Hofmann M, Schwartz-Albiez R, Zöller M, Heider K-H, Ponta H and Herrlich P. The two major CD44 proteins expressed on a metastatic rat tumor cell line are derived from different splice variants: each one individually suffices to confer metastatic behavior. *Cancer Res.* **53**:1262-1268 (1993)
117. Goodfellow PN, Banting G, Wiles MV, Tunnacliffe A, Parkar M, Solomon E, Dalchau R and Fabre JW. The gene, MIC4, which controls expression of the antigen defined by monoclonal antibody F10.44.2, is on human chromosome 11. *Eur. J. Immunol.* **12**:659-663 (1982)

118. Von Heijne G. A new method for predicting signal sequence cleavage sites. *Nucl. Acids Res.* 14:4683-4690 (1986)
119. Tölg C, Hofmann M, Herrlich P and Ponta H. Splicing choice from ten variant exons establishes CD44 variability. *Nucl. Acids Res.* 21:1225-1229 (1993)
120. Screaton GR, Bell MV, Bell JI and Jackson DG. The identification of a new alternative exon with highly restricted tissue expression in transcripts encoding the mouse Pgp-1 (CD44) homing receptor. *J. Biol. Chem.* 268:12235-12238 (1993)
121. Arch R, Wirth K, Hofmann M, Ponta H, Matzku S, Herrlich P and Zöller M. Participation in normal immune responses of a metastasis-inducing splice variant of CD44. *Science* 257:682-685 (1992)
122. Friedrichs K, Franke F, Lisboa B-W, Kügler G, Gille I, Terpe H-J, Hölzel F, Maass H and Günther U. CD44 isoforms correlate with cellular differentiation but not with prognosis in human breast cancer. *Cancer Res.* 55:5424-5433 (1995)
123. Givchian M, Woerner SM, Lacroix J, Zöller M, Drings P, Becker H, Kayser K, Ridder R and Von Knebel Doeberitz M. Expression of CD44 splice variants in normal respiratory epithelium and bronchial carcinomas: no evidence for altered CD44 splicing in metastasis. *Oncogene* 12:1137-1144 (1996)
124. Goldstein LA and Butcher EC. Identification of mRNA that encodes an alternative form of H-CAM(CD44) in lymphoid and nonlymphoid tissues. *Immunogenetics* 32:389-397 (1990)
125. Stamenkovic I, Aruffo A, Amiot M and Seed B. The hematopoietic and epithelial forms of CD44 are distinct polypeptides with different adhesion potentials for hyaluronate-bearing cells. *EMBO J.* 10:343-348 (1991)
126. Harn H-J, Isola N and Cooper DL. The multispecific cell adhesion molecule CD44 is represented in reticulocyte cDNA. *Biochem. Biophys. Res. Comm.* 178:1127-1134 (1991)
127. Shlivelman E and Bishop JM. Expression of CD44 is repressed in neuroblastoma cells. *Mol. Cell Biol.* 11:5446-5453 (1991)
128. Matsumura Y, Sugiyama M, Matsumura S, Hayle AJ, Robinson P, Smith JC and Tarin D. Unusual retention of introns in CD44 gene transcripts in bladder cancer provides new diagnostic and clinical oncological opportunities. *J. Pathol.* 177:11-20 (1995)
129. Yoshida K, Bolodeoku J, Sugino T, Goodison S, Matsumura Y, Warren BF, Toge T, Tahara E and Tarin D. Abnormal retention of intron 9 in CD44 gene transcripts in human gastrointestinal tumors. *Cancer Res.* 55:4273-4277 (1995)
130. Neame SJ and Isacke CM. Phosphorylation of CD44 *in vivo* requires both Ser323 and Ser325, but does not regulate membrane localization or cytoskeletal interaction in epithelial cells. *EMBO J.* 11:4733-4738 (1992)
131. Puré E, Camp RL, Peritt D, Panettieri RA Jr, Lazaar AL and Nayak S. Defective phosphorylation and hyaluronate binding of CD44 with point mutations in the cytoplasmic domain. *J. Exp. Med.* 181:55-62 (1995)
132. Nottenburg C, Rees G and St John T. Isolation of mouse CD44 cDNA: Structural features are distinct from the primate cDNA. *Proc. Natl. Acad. Sci. USA* 86:8521-8525 (1989)

133. Lokeshwar VB and Bourguignon LYW. Post-translational protein modification and expression of ankyrin-binding site(s) in GP85 (Pgp-1/CD44) and its biosynthetic precursors during T-lymphoma membrane biosynthesis. *J. Biol. Chem.* 266:17983-17989 (1991)
134. Jalkanen S, Jalkanen M, Bargatze R, Tammi M and Butcher EC. Biochemical properties of glycoproteins involved in lymphocyte recognition of high endothelial venules in man. *J. Immunol.* 141:1615-1623 (1988)
135. Flanagan BF, Dalchau R, Allen AK, Daar AS and Fabre JW. Chemical composition and tissue distribution of the human CDw44 glycoprotein. *Immunol.* 67:167-175 (1989)
136. Fox SB, Fawcett J, Jackson DG, Collins I, Gatter KC, Harris AL, Gearing A and Simmons DL. Normal human tissues, in addition to some tumors, express multiple different CD44 isoforms. *Cancer Res.* 54:4539-4546 (1994)
137. Mackay CR, Terpe H-J, Stauder R, Marston WL, Stark H and Günther U. Expression and modulation of CD44 variant isoforms in humans. *J. Cell Biol.* 124:71-82 (1994)
138. Stauder R, Eisterer W, Thaler J and Günther U. CD44 variant isoforms in non-Hodgkin's lymphoma: a new independent prognostic factor. *Blood* 85:2885-2899 (1995)
139. Koopman G, Heider K-H, Horst E, Adolf GR, Van den Berg F, Ponta H, Herrlich P and Pals ST. Activated human lymphocytes and aggressive non-Hodgkin's lymphomas express a homologue of the rat metastasis-associated variant of CD44. *J. Exp. Med.* 177:897-904 (1993)
140. Terpe H-J, Stark H, Prehm P and Günther U. CD44 variant isoforms are preferentially expressed in basal epithelia of non-malignant human fetal and adult tissues. *Histochem.* 101:79-89 (1994)
141. Gotley DC, Fawcett J, Walsh MD, Reeder JA, Simmons DL and Antalis TM. Alternatively spliced variants of the cell adhesion molecule CD44 and tumour progression in colorectal cancer. *Br. J. Cancer* 74:342-351 (1996)
142. Woodman AC, Sugiyama M, Yoshida K, Sugino T, Borgya A, Goodison S, Matsumura Y and Tarin D. Analysis of anomalous CD44 gene expression in human breast, bladder, and colon cancer and correlation of observed mRNA and protein isoforms. *Am. J. Pathol.* 149:1519-1530 (1996)
143. Bourguignon LYW, Walker G, Suchard SJ and Balazovich K. A lymphoma plasma membrane-associated protein with ankyrin-like properties. *J. Cell Biol.* 102:2115-2124 (1986)
144. Kalomiris EL and Bourguignon LYW. Mouse T lymphoma cells contain a transmembrane glycoprotein (GP85) that binds ankyrin. *J. Cell Biol.* 106:319-327 (1988)
145. Lokeshwar VB, Fregien N and Bourguignon LYW. Ankyrin-binding domain of CD44(GP85) is required for the expression of hyaluronic acid-mediated adhesion function. *J. Cell Biol.* 126:1099-1199 (1994)
146. Lacy BE and Underhill CB. The hyaluronate receptor is associated with actin filaments. *J. Cell Biol.* 105:1395-1404 (1987)
147. Tsukita S, Oishi K, Sato N, Sagara J, Kawai A and Tsukita S. ERM family members as molecular linkers between the cell surface glycoprotein CD44 and actin-based cytoskeletons. *J. Cell Biol.* 126:391-401 (1994)

148. Miyake K, Underhill CB, Lesley J and Kincade PW. Hyaluronate can function as a cell adhesion molecule and CD44 participates in hyaluronate recognition. *J. Exp. Med.* **172**:69-75 (1990)
149. Neame PJ and Barry FP. The link proteins. *Experientia* **49**:393-402 (1993)
150. Peach RJ, Hollenbaugh D, Stamenkovic I and Aruffo A. Identification of hyaluronic acid binding sites in the extracellular domain of CD44. *J. Cell Biol.* **122**:257-264 (1993)
151. Yang B, Yang BL, Savani RC and Turley EA. Identification of a common hyaluronan binding motif in the hyaluronan binding proteins RHAMM, CD44 and link protein. *EMBO J.* **13**:286-296 (1994)
152. Hardingham TE and Fosang AJ. Proteoglycans: many forms and many functions. *FASEB J.* **6**:861-870 (1992)
153. Van der Voort R, Manten-Horst E, Smit L, Ostermann E, Van den Berg F and Pals ST. Binding of cell-surface expressed CD44 to hyaluronate is dependent on splicing and cell type. *Biochem. Biophys. Res. Comm.* **214**:137-144 (1995)
154. Sleeman J, Rudy W, Hofmann M, Moll J, Herrlich P and Ponta H. Regulated clustering of variant CD44 proteins increases their hyaluronate binding capacity. *J. Cell Biol.* **135**:1139-1150 (1996)
155. Lesley J, He Q, Miyake K, Hamann A, Hyman R and Kincade PW. Requirements for hyaluronic acid binding by CD44: a role for the cytoplasmic domain and activation by antibody. *J. Exp. Med.* **175**:257-266 (1992)
156. Lesley J, Kincade PW and Hyman R. Antibody-induced activation of the hyaluronan receptor function of CD44 requires multivalent binding by antibody. *Eur. J. Immunol.* **23**:1902-1909 (1993)
157. Perschl A, Lesley J, English N, Trowbridge I and Hyman R. Role of CD44 cytoplasmic domain in hyaluronan binding. *Eur. J. Immunol.* **25**:495-501 (1995)
158. Underhill CB and Toole BP. Physical characteristics of hyaluronate binding to the surface of simian virus 40-transformed 3T3 cells. *J. Biol. Chem.* **255**:4544-4549 (1980)
159. Underhill CB, Chi-Rosso G and Toole BP. Effects of detergent solubilization on the hyaluronate-binding protein from membranes of simian virus 40-transformed 3T3 cells. *J. Biol. Chem.* **258**:8086-8091 (1983)
160. Liao H-X, Levesque MC, Patton K, Bergamo B, Jones D, Moody MA, Telen MJ and Haynes BF. Regulation of human CD44H and CD44E isoform binding to hyaluronan by phorbol myristate acetate and anti-CD44 monoclonal and polyclonal antibodies. *J. Immunol.* **151**:6490-6499 (1993)
161. Bourguignon LYW, Lokeshwar VB, Chen X and Kerrick WGL. Hyaluronic acid-induced lymphocyte signal transduction and HA receptor (GP85/CD44)-cytoskeleton interaction. *J. Immunol.* **151**:6634-6644 (1993)
162. Bennett KL, Modrell B, Greenfield B, Bartolazzi A, Stamenkovic I, Peach R, Jackson DG, Spring F and Aruffo A. Regulation of CD44 binding to hyaluronan by glycosylation of variable spliced exons. *J. Cell Biol.* **131**:1623-1633 (1995)
163. Katoh S, Zheng Z, Oritani K, Shimozato T and Kincade PW. Glycosylation of CD44 negatively regulates its recognition of hyaluronan. *J. Exp. Med.* **182**:419-429 (1995)

164. Lesley J, English N, Perschl A, Gregoroff J and Hyman R. Variant cell lines selected for alterations in the function of the hyaluronan receptor CD44 show differences in glycosylation. *J. Exp. Med.* **182**:431-437 (1995)
165. Bartolazzi A, Nocks A, Aruffo A, Spring F and Stamenkovic I. Glycosylation of CD44 is implicated in CD44-mediated cell adhesion to hyaluronan. *J. Cell Biol.* **132**:1199-1208 (1996)
166. Jalkanen S and Jalkanen M. Lymphocyte CD44 binds the COOH-terminal heparin-binding domain of fibronectin. *J. Cell Biol.* **116**:817-825 (1992)
167. Faassen AE, Schragar JA, Klein DJ, Oegema TR, Couchman JR and McCarthy JB. A cell surface chondroitin sulfate proteoglycan, immunologically related to CD44, is involved in type I collagen-mediated melanoma cell motility and invasion. *J. Cell Biol.* **116**:521-531 (1992)
168. Streefer PR, Berg EL, Rouse BT, Bargatze RF and Butcher EC. A tissue-specific endothelial cell molecule involved in lymphocyte homing. *Nature* **331**:41-46 (1988)
169. Nakache M, Berg EL, Streefer PR and Butcher EC. The mucosal vascular addressin is a tissue-specific endothelial cell adhesion molecule for circulating lymphocytes. *Nature* **337**:179-181 (1989)
170. Berg EL, Goldstein LA, Jutila MA, Nakache M, Picker LJ, Streefer PR, Wu NW, Zhou D and Butcher EC. Homing receptors and vascular addressins: cell adhesion molecules that direct lymphocyte traffic. *Immunol. Rev.* **108**:5-18 (1989)
171. Bennett KL, Jackson DG, Simon JC, Tanczos E, Peach R, Modrell B, Stamenkovic I, Plowman G and Aruffo A. CD44 isoforms containing exon v3 are responsible for the presentation of heparin-binding growth factor. *J. Cell Biol.* **128**:687-698 (1995)
172. Toyama-Sorimachi N, Sorimachi H, Tobita Y, Kitamura F, Yagita H, Suzuki K and Miyasaka M. A novel ligand for CD44 is serglycin, a hematopoietic cell lineage-specific proteoglycan. *J. Biol. Chem.* **270**:7437-7444 (1995)
173. Naujokas MF, Morin M, Anderson MS, Peterson M and Miller J. The chondroitin sulfate form of Invariant Chain can enhance stimulation of T cell responses through interaction with CD44. *Cell* **74**:257-268 (1993)
174. Weber GF, Ashkar S, Glimcher MJ and Cantor H. Receptor-ligand interaction between CD44 and Osteopontin (Eta-1). *Science* **271**:509-512 (1996)
175. Horst E, Meijer CJ, Redaskiewicz T, Van Dongen JJ, Pleters R, Figdor CG, Hooffman A and Pals ST. Expression of a human homing receptor (CD44) in lymphoid malignancies and related stages of lymphoid development. *Leukemia* **4**:383-389 (1990)
176. Horst E, Meijer CJLM, Duijvestijn AM, Hartwig N, Van der Harten HJ and Pals ST. The ontogeny of human lymphocyte recirculation: high endothelial cell antigen (HECA-452) and CD44 homing receptor expression in the development of the immune system. *Eur. J. Immunol.* **20**:1483-1489 (1990)
177. Miyake K, Medina KL, Hayashi S-I, Ono S, Hamaoka T and Kincade PW. Monoclonal antibodies to Pgp-1/CD44 block lympho-hemopoiesis in long-term bone marrow cultures. *J. Exp. Med.* **171**:477-488 (1990)

178. Butcher EC, Scollay RG and Weissman IL. Organ specificity of lymphocyte migration: mediation by highly selective lymphocyte interaction with organ-specific determinants on high endothelial venules. *Eur. J. Immunol.* 10:556-561 (1980)
179. Butcher EC. The regulation of lymphocyte traffic. *Curr. Top. Microbiol. Immunol.* 128:85-122 (1986)
180. Jalkanen S, Steere AC, Fox RI and Butcher EC. A distinct endothelial cell recognition system that controls lymphocyte traffic into inflamed synovium. *Science* 233:556-558 (1986)
181. Stoolman LM and Ebling H. Adhesion molecules of cultured hematopoietic malignancies. A calcium-dependent lectin is the principle mediator of binding to the high endothelial venule of lymph nodes. *J. Clin. Invest.* 84:1196-1205 (1989)
182. Green SJ, Tarone G and Underhill CB. Aggregation of macrophages and fibroblasts is inhibited by a monoclonal antibody to the hyaluronate receptor. *Exp. Cell Res.* 178:224-232 (1988)
183. Huef S, Groux H, Caillou B, Valentin H, Prieur A-M and Bernard A. CD44 contributes to T cell activation. *J. Immunol.* 143:798-801 (1989)
184. Shimizu Y, Van Seventer GA, Siraganian R, Wahl L and Shaw S. Dual role of the CD44 molecule in T cell adhesion and activation. *J. Immunol.* 143:2457-2463 (1989)
185. Denning SM, Le PT, Singer KH and Haynes BF. Antibodies against the CD44 p80, lymphocyte homing receptor molecule augment human peripheral blood T cell activation. *J. Immunol.* 144:7-15 (1990)
186. Webb DSA, Shimizu Y, Van Seventer GA, Shaw S and Gerrard TL. LFA-3, CD44 and CD45: Physiologic triggers of human monocyte TNF and IL-1 release. *Science* 249:1295-1297 (1990)
187. Galandrin R, Galluzzo E, Albi N, Grossi CE and Velardi A. Hyaluronate is costimulatory for human T cell effector functions and binds to CD44 on activated T cells. *J. Immunol.* 153:21-31 (1994)
188. Moll J, Schmidt A, Van der Putten H, Plug R, Ponta H, Herrlich P and Zöller M. Accelerated immune response in transgenic mice expressing rat CD44v4-v7 on T cells. *J. Immunol.* 156:2085-2094 (1996)
189. Günthert U. CD44: A multitude of isoforms with diverse functions. *Curr. Top. Microbiol. Immunol.* 184:47-63 (1993)
190. Hudson DL, Sleeman J and Watt FM. CD44 is the major peanut lectin-binding glycoprotein of human epidermal keratinocytes and plays a role in intercellular adhesion. *J. Cell Sci.* 108:1959-1970 (1995)
191. Kaya G, Rodriguez I, Jorcano JL, Vassalli P and Stamenkovic I. Selective suppression of CD44 in keratinocytes of mice bearing an antisense CD44 transgene driven by a tissue-specific promoter disrupts hyaluronated metabolism in the skin and impairs keratinocyte proliferation. *Genes Dev.* 11:996-1007 (1997)
192. Culty M, Nguyen HA and Underhill CB. The hyaluronan receptor (CD44) participates in the uptake and degradation of hyaluronan. *J. Cell Biol.* 116:1055-1062 (1992)
193. Oksala O, Salo T, Tammi R, Häkkinen L, Jalkanen M, Inki P and Larjava H. Expression of proteoglycans and hyaluronan during wound healing. *J. Histochem. Cytochem.* 43:125-135 (1995)

194. Jacobson K, O'Dell D, Hollfield B, Murphy TL and August JT. Redistribution of a major cell surface glycoprotein during cell movement. *J. Cell Biol.* 99:1613-1623 (1984)
195. Jacobson K, O'Dell D and August JT. Lateral diffusion of an 80,000-dalton glycoprotein in the plasma membrane of murine fibroblasts: relationships to cell structure and function. *J. Cell Biol.* 99:1624-1633 (1984)
196. Thomas L, Byers HR, Vink J and Stamenkovic I. CD44H regulates tumor cell migration on hyaluronate-coated substrate. *J. Cell Biol.* 118:971-977 (1992)
197. Herbst TJ, McCarthy JB, Tsilibary EC and Furcht LT. Differential effects of laminin, intact type IV collagen, and specific domains of type IV collagen on endothelial cell adhesion and migration. *J. Cell Biol.* 106:1365-1373 (1988)
198. Chelberg MK, Tsilibary EC, Hauser AR and McCarthy JB. Type IV collagen-mediated melanoma cell adhesion and migration: Involvement of multiple, distinct domains of the collagen molecule. *Cancer Res.* 49:4796-4802 (1989)
199. Faassen AE, Mooradian DL, Tranquillo RT, Dickinson RB, Letourneau PC, Oegema TR and McCarthy JB. Cell surface CD44-related chondroitin sulfate proteoglycan is required for transforming growth- β -stimulated mouse melanoma cell motility and invasive behavior on type I collagen. *J. Cell Sci.* 105:501-511 (1993)
200. Underhill C. CD44: The hyaluronan receptor. *J. Cell Sci.* 103:293-298 (1992)
201. Milstone LM, Hough-Monroe L, Kugelman LC, Bender JR and Haggerty JG. Epican, a heparan/chondroitin sulfate proteoglycan form of CD44, mediates cell-cell adhesion. *J. Cell Sci.* 107:3183-3190 (1994)
202. Lucas MG, Green AM and Telen MJ. Characterization of the serum *In(Lu)*-related antigen: identification of a serum protein related to erythrocyte p80. *Blood* 73:596-600 (1989)
203. Haynes BF, Hale LP, Patton KL, Martin ME and McCallum RM. Measurement of an adhesion molecule as an indicator of inflammatory disease activity. *Arthr. Rheum.* 34:1434-1443 (1991)
204. Ristamäki R, Joensuu H, Grön-Virta K, Salmi M and Jalkanen S. Origin and function of circulating CD44 in non-Hodgkin's lymphoma. *J. Immunol.* 158:3000-3008 (1997)
205. Bazil V and Horejší V. Shedding of the CD44 adhesion molecule from leukocytes induced by anti-CD44 monoclonal antibody simulating the effect of a natural receptor ligand. *J. Immunol.* 149:747-753 (1992)
206. Ristamäki R, Joensuu H, Salmi M and Jalkanen S. Serum CD44 in malignant lymphoma: an association with treatment response. *Blood* 84:238-243 (1994)
207. De Rossi G, Marroni P, Paganuzzi M, Mauro FR, Tenca C, Zarcone D, Velardi A, Molica S and Grossi CE. Increased serum levels of soluble CD44 standard, but not of variant isoforms v5 and v6, in B cell chronic lymphocytic leukemia. *Leukemia* 11:134-141 (1997)
208. Gansauge F, Gansauge S, Rau B, Scheiblich A, Poch B, Schoenberg MH and Beger HG. Low serum levels of soluble CD44 variant 6 are significantly associated with poor prognosis in patients with pancreatic carcinoma. *Cancer* 80:1733-1739 (1997)
209. Kainz C, Tempfer C, Winkler S, Sliutz G, Koelbl H and Reinthaller A. Serum CD44 splice variants in cervical cancer patients. *Cancer Letters* 90:231-234 (1995)

210. **Han H-J, Ho L-I, Shyu R-Y, Yuan J-S, Lin F-G, Young T-H, Liu C-A, Tang H-S and Lee W-H.** Soluble CD44 isoforms in serum as potential markers of metastatic gastric carcinoma. *J. Clin. Gastroenterol.* **22**:107-110 (1996)
211. **Lein M, Weiss S, Jung K, Schnorr D and Loening S.** Soluble CD44 variants in serum of patients with prostate cancer and other urological malignancies. *The Prostate* **29**:334-335 (1996)
212. **Martin S, Jansen F, Bokelmann J and Kolb H.** Soluble CD44 splice variants in metastasizing human breast cancer. *Int. J. Cancer (Pred. Oncol.)* **74**:443-445 (1997)
213. **Guo Y-J, Liu G, Wang X, Jin D, Wu M, Ma J and Sy M-S.** Potential use of soluble CD44 in serum as indicator of tumor burden and metastasis in patients with gastric or colon cancer. *Cancer Res.* **54**:422-426 (1994)
214. **Slutz G, Tempfer C, Winkler S, Kohlberger P, Reinthaller A and Kainz C.** Immunohistochemical and serological evaluation of CD44 splice variants in human ovarian cancer. *Br. J. Cancer* **72**:1494-1497 (1995)
215. **Gearing AJH and Newman W.** Circulating adhesion molecules in disease. *Immunol. Today* **14**:506-512 (1993)
216. **Katoh S, McCarty JB and Kincade PW.** Characterization of soluble CD44 in the circulation of mice. Levels are affected by immune activity and tumor growth. *J. Immunol.* **153**:3440-3449 (1994)
217. **Yu Q and Toole BP.** A new alternatively spliced exon between v9 and v10 provides a molecular basis for synthesis of soluble CD44. *J. Biol. Chem.* **271**:20603-20607 (1996)
218. **Campanero MR, Pulido R, Alonso JL, Pivel JP, Pimentel-Muñoz FX, Fresno M and Sánchez-Madrid F.** Down-regulation by tumor necrosis factor- α of neutrophil cell surface expression of the sialoprotein CD43 and the hyaluronate receptor CD44 through a proteolytic mechanism. *Eur. J. Immunol.* **21**:3045-3048 (1991)
219. **Bazil V and Strominger JL.** Metalloprotease and serine protease are involved in cleavage of CD43, CD44 and CD16 from stimulated human granulocytes. Induction of cleavage of L-selectin via CD16. *J. Immunol.* **152**:1314-1322 (1994)
220. **Ristamäki R, Joensuu H and Jalkanen S.** Does soluble CD44 reflect the clinical behavior of human cancer? *Curr. Topics Microbiol. Immunol.* **213**:155-166 (1996)
221. **Camp RL, Scheynius A, Johansson C and Puré E.** CD44 is necessary for optimal contact allergic responses but is not required for normal leukocyte extravasation. *J. Exp. Med.* **178**:497-507 (1993)
222. **Willerford DM, Hoffman PA and Gallatin WM.** Expression of lymphocyte receptors for high endothelium in primates. Anatomic partitioning and linkage to activation. *J. Immunol.* **142**:3416-3422 (1989)
223. **Gamble JR, Skinner MP, Berndt MC and Vadas MA.** Prevention of activated neutrophil adhesion to endothelium by soluble adhesion protein GMP140. *Science* **249**:414-417 (1990)
224. **Schleiffenbaum B, Sperlini O and Tedder TF.** Soluble L-selectin is present in human plasma at high levels and retains functional activity. *J. Cell Biol.* **119**:229-238 (1992)

225. **Matzku S, Wenzel A, Liu S and Zöller M.** Antigenic differences between metastatic and nonmetastatic BSp73 rat tumor variants characterized by monoclonal antibodies. *Cancer Res.* **49**:1294-1299 (1989)
226. **Reber S, Matzku S, Günther U, Ponta H, Herrlich P and Zöller M.** Retardation of metastatic tumor growth after immunization with metastasis-specific monoclonal antibodies. *Int. J. Cancer* **46**:919-927 (1990)
227. **Seifer S, Arch R, Reber S, Komitowski D, Hofmann M, Ponta H, Herrlich P, Matzku S and Zöller M.** Prevention of tumor metastasis formation by anti-variant CD44. *J. Exp. Med.* **177**:443-445 (1993)
228. **Kaufmann M, Heider K-H, Sinn H-P, Von Minckwitz G, Ponta H and Herrlich P.** CD44 variant exon epitopes in primary breast cancer and length of survival. *Lancet* **345**:615-619 (1995)
229. **Tempfer C, Lösch A, Heinzl H, Häusler G, Kölbl H, Breitenacker G and Kainz C.** Prognostic value of immunohistochemically detected CD44 isoforms CD44v5, CD44v6 and CD44v7-8 in human breast cancer. *Eur. J. Cancer* **32A**:2023-2025 (1996)
230. **Kainz C, Kohlberger P, Slutz G, Tempfer C, Heinzl H, Reinthaller A, Breitenacker G and Kölbl H.** Splice variants of CD44 in human cervical cancer stage IB to IIB. *Gynecol. Oncol.* **57**:383-387 (1995)
231. **Kainz C, Kohlberger P, Tempfer C, Slutz G, Glitsch G, Reinthaller A and Breitenacker G.** Prognostic value of CD44 splice variants in human stage III cervical cancer. *Eur. J. Cancer* **31A**:1706-1709 (1995)
232. **Dall P, Heider K-H, Hekele A, Von Minckwitz G, Kaufmann M, Ponta H and Herrlich P.** Surface protein expression and messenger RNA-splicing analysis of CD44 in uterine cervical cancer and normal cervical epithelium. *Cancer Res.* **54**:3337-3341 (1994)
233. **Wielenga VJM, Heider K-H, Offerhaus JA, Adolf GR, Van den Berg FM, Ponta H, Herrlich P and Pals ST.** Expression of CD44 variant proteins in human colorectal cancer is related to tumor progression. *Cancer Res.* **53**:4754-4756 (1993)
234. **Mulder J-WR, Kruij PM, Sewnath M, Oosting J, Seldenrijk CA, Weldema WF, Offerhaus GJA, Pals ST.** Colorectal cancer prognosis and expression of exon-v6-containing CD44 proteins. *Lancet* **344**:1470-1472 (1994)
235. **Finke LH, Terpe H-J, Zöhr C, Haensch W and Schlag PM.** Colorectal cancer prognosis and expression of exon-v6-containing CD44 proteins. *Lancet* **345**:583 (1995)
236. **Nihei Z, Ichikawa W, Kojima K, Togo S, Miyanaga T, Hirayama R and Mishima Y.** The positive relationship between the expression of CD44 variant 6 and prognosis in colorectal cancer. *Surg. Today* **26**:760-761 (1996)
237. **Orzechowski H-D, Beckenbach C, Herbst H, Stölzel U, Riecken E-O and Stallmach A.** Expression of CD44v6 is associated with cellular dysplasia in colorectal epithelial cells. *Eur. J. Cancer* **31A**:2073-2079 (1995)
238. **Heider K-H, Hofmann M, Horst E, Van den Berg F, Ponta H, Herrlich P and Pals ST.** A human homologue of the rat metastasis-associated variant of CD44 is expressed in colorectal carcinomas and adenomatous polyps. *J. Cell Biol.* **120**:227-233 (1993)

239. Fujita N, Yaegashi N, Ide Y, Sato S, Nakamura M, Ishiwata I and Yajima A. Expression of CD44 in normal human *versus* tumor endometrial tissues: possible implication of reduced expression of CD44 in lymph-vascular space involvement of cancer cells. *Cancer Res.* 54:3922-3928 (1994)
240. Heider K-H, Dämmrich J, Skroch-Angel P, Müller-Hermelink H-K, Vollmers HP, Herrlich P and Ponta H. Differential expression of CD44 splice variants in intestinal- and diffuse-type human gastric carcinomas and normal gastric mucosa. *Cancer Res.* 53: 4197-4203 (1993)
241. Dämmrich J, Vollmers HP, Heider K-H and Müller-Hermelink H-K. Importance of different CD44v6 expression in human gastric intestinal and diffuse type cancers for metastatic lymphogenic spreading. *J. Mol. Med.* 73:395-401 (1995)
242. Harn H-J, Ho L-I, Chang J-Y, Wu C-W, Jiang S-Y, Lee H-S and Lee W-H. Differential expression of the human metastasis adhesion molecule CD44v in normal and carcinomatous stomach mucosa of chinese subjects. *Cancer* 75:1065-1071 (1995)
243. Hong R-L, Lee W-J, Shun C-T, Chu J-S, Chen Y-C. Expression of CD44 and its clinical implication in diffuse-type and intestinal-type gastric adenocarcinomas. *Oncology.* 52:334-339 (1995)
244. Fan X, Long A, Goggins M, Fan X, Keeling PWN and Kelleher D. Expression of CD44 and its variants on gastric epithelial cells of patients with *Helicobacter pylori* colonisation. *Gut* 38:507-512 (1996)
245. Mayer B, Jauch KW, Günther U, Figdor CG, Schildberg FW, Funke I and Johnson JP. De-novo expression of CD44 and survival in gastric cancer. *Lancet* 342:1019-1022 (1993)
246. Terpe H-J, Storkel S, Zimmer U, Anquez V, Fischer C, Pantel K and Günther U. Expression of CD44 isoforms in renal cell tumors. Positive correlation to tumor differentiation. *Am. J. Pathol.* 148:453-463 (1996)
247. Kan M, Aki M, Akiyama K, Naruo S, Kanayama H and Kagawa S. High-level expression of the CD44 variant sharing exon v10 in renal cancer. *Jap. J. Cancer Res.* 86:847-53 (1995)
248. Terpe H-J, Koopman R, Imhof BA and Günther U. Expression of integrins and CD44 isoforms in non-Hodgkin's lymphomas: CD44 variant isoforms are preferentially expressed in high-grade malignant lymphomas. *J. Pathol.* 174:89-100 (1994)
249. Ristamäki R, Joensuu H, Söderström K-O and Jalkanen S. CD44v6 expression in non-Hodgkin's lymphoma: an association with low histological grade and poor prognosis. *J. Pathol.* 176:259-267 (1995)
250. Manten-Horst E, Danen EHJ, Smiit L, Snoek M, Le Poole IC, Van Muijnen GNP, Pals ST and Ruifer DJ. Expression of CD44 splice variants in human cutaneous melanoma and melanoma cell lines is related to tumor progression and metastatic potential. *Int. J. Cancer (Pred. Oncol.)* 64:182-188 (1995)
251. Stauder R, Van Driel M, Schwärzler C, Thaler J, Lokhorst HM, Kreuser ED, Bloem AC, Günther U and Eisterer W. Different CD44 splicing patterns define prognostic subgroups in multiple myeloma. *Blood* 88:3101-3108 (1996)

252. Gross N, Beretta C, Peruisseau G, Jackson D, Simmons D and Beck D. CD44H expression by human neuroblastoma cells: relation to *MYCN* amplification and lineage differentiation. *Cancer Res.* 54:4238-4242 (1994)
253. Gansauge F, Gansauge S, Zobywalski A, Scharnweber C, Link KH, Nussler AK and Beger HG. Differential expression of CD44 splice variants in human pancreatic adenocarcinoma and in normal pancreas. *Cancer Res.* 55:5499-5503 (1995)
254. Kallakury BVS, Yang F, Figge J, Smith KE, Kausik SJ, Tacy NJ, Fisher HAG, Kaufman R, Figge H and Ross JS. Decreased levels of CD44 protein and mRNA in prostate carcinoma. Correlation with tumor grade and ploidy. *Cancer* 78:1461-1469 (1996)
255. Jackson DG, Schenker T, Waibel R, Bell JI and Stahel RA. Expression of alternatively spliced forms of the CD44 extracellular-matrix receptor on human lung carcinomas. *Int. J. Cancer* 8 (Suppl.):110-115 (1994)
256. Penno MB, August JT, Baylin SB, Mabry M, Linnoila I, Lee VS, Croteau D, Yang XL and Rosada C. Expression of CD44 in human lung tumors. *Cancer Res.* 54:1381-1387 (1994)
257. Teder P, Bergh J and Heldin P. Functional hyaluronan receptors are expressed on a squamous cell lung carcinoma line but not on other lung carcinoma cell lines. *Cancer Res.* 55:3908-3914 (1995)
258. Hong R-L, Pu Y-S, Hsieh T-S, Chu J-S and Lee W-J. Expressions of E-cadherin and exon v6-containing isoforms of CD44 and their prognostic values in human transitional cell carcinoma. *J. Urol.* 153:2025-2028 (1995)
259. Southgate J, Trejdosiewicz LK, Smith B and Selby PJ. Patterns of splice variant CD44 expression by normal human urothelium *in situ* and *in vitro* and by bladder-carcinoma cell lines. *Int. J. Cancer* 62:449-456 (1995)
260. Sugino T, Gorham H, Yoshida K, Bolodeoku J, Nargund V, Cranston D, Goodison S and Tarin D. Progressive loss of CD44 gene expression in invasive bladder cancer. *Am. J. Pathol.* 149:873-882 (1996)
261. Tempfer C, Gitsch G, Haeusler G, Reinthaller A, Koelbl H and Kainz C. Prognostic value of immunohistochemically detected CD44 expression in patients with carcinoma of the vulva. *Cancer* 78:273-277 (1996)
262. Mulder J-WR, Wielenga VJM, Polak MM, Van den Berg FM, Adolf GR, Herrlich P, Pals ST and Offerhaus GJA. Expression of mutant p53 protein and CD44 variant proteins in colorectal tumorigenesis. *Gut* 36:76-80 (1995)
263. Kim H, Yang X-L, Rosada C, Hamilton SR and August JT. CD44 expression in colorectal adenomas is an early event occurring prior to K-ras and p53 gene mutation. *Arch. Biochem. Biophys.* 310:504-507 (1994)
264. Imazeki F, Yokosuka O, Yamaguchi T, Ohto M, Isono K and Omata M. Expression of variant CD44-messenger RNA in colorectal adenocarcinomas and adenomatous polyps in humans. *Gastroenterol.* 110:362-368 (1996)
265. Koretz K, Möller P, Lehnert T, Hinz U, Otto HF and Herfarth C. Effect of CD44v6 on survival in colorectal carcinoma. *Lancet* 345:327-328 (1995)

266. Charpin C, Garcia S, Bouvier C, Devictor B, Andrac L, Choux R, Lavaut M-N and Allasia C. Automated and quantitative immunocytochemical assays of CD44v6 in breast carcinomas. *Human Pathol.* **28**:289-296 (1997)
267. Matsumura Y and Tarin D. Significance of CD44 gene products for cancer diagnosis and disease evaluation. *Lancet* **340**:1053-1058 (1992)
268. Dall P, Heider K-H, Sinn H-P, Skroch-Angel P, Adolf G, Kaufmann M, Herrlich P and Ponta H. Comparison of immunohistochemistry and RT-PCR for detection of CD44v-expression, a new prognostic factor in human breast cancer. *Int. J. Cancer* **60**:471-477 (1995)
269. Rodriguez C, Monges G, Rouanet P, Dutrillaux B, Lefrançois D and Theillet C. CD44 expression patterns in breast and colon tumors: a PCR-based study of splice variants. *Int. J. Cancer (Pred. Oncol.)* **64**:347-354 (1995)
270. Finn L, Dougherty G, Finley G, Meisler A, Becich M and Cooper DL. Alternative splicing of CD44 pre-mRNA in human colorectal tumors. *Biochem. Biophys. Res. Commun.* **200**:1015-1022 (1994)
271. Goodison S, Yoshida K, Sugino T, Woodman A, Gorham H, Bolodeoku J, Kaufmann M and Tarin D. Rapid analysis of distinctive CD44 RNA splicing preferences that characterize colonic tumors. *Cancer Res.* **57**:3140-3144 (1997)
272. Wong LS, Cantrill JE, Morris AG and Fraser IA. Expression of CD44 splice variants in colorectal cancer. *Br. J. Surgery* **84**:363-367 (1997)
273. Yokozaki H, Ito R, Nakayama H, Kuniyasu H, Taniyama K and Tahara E. Expression of CD44 abnormal transcripts in human gastric carcinomas. *Cancer Letters* **83**:229-234 (1994)
274. Matsumura Y, Hanbury D, Smith J and Tarin D. Non-invasive detection of malignancy by identification of unusual CD44 gene activity in exfoliated cancer cells. *Br. Med. J.* **308**:619-624 (1994)
275. Kan M, Furukawa A, Aki M, Kanayama H and Kagawa S. Expression of CD44 splice variants in bladder cancer. *Int. J. of Urol.* **2**:295-301 (1995)
276. Higashikawa K, Yokozaki H, Ue T, Taniyama K, Ishikawa T, Tarin D and Tahara E. Evaluation of CD44 transcription variants in human digestive tract carcinomas and normal tissues. *Int. J. Cancer* **66**:11-17 (1996)
277. Yoshida K, Sugino T, Bolodeoku J, Warren BF, Goodison S, Woodman A, Toge T, Tahara E and Tarin D. Detection of exfoliated carcinoma cells in colonic luminal washings by identification of deranged patterns of expression of the CD44 gene. *J. Clin. Pathol.* **49**:300-305 (1996)
278. Jung K, Lein M, Weiss S, Schnorr D, Henke W and Loening S. Soluble CD44 molecules in serum of patients with prostate cancer and benign prostatic hyperplasia. *Eur. J. Cancer* **32A**:627-630 (1996)
279. Kihl EM, Ruckser R, Rech-Weichselbraun I, Hinterberger W and Bauer K. Significant elevation of tumour-associated isoforms of soluble CD44 in serum of normal individuals caused by cigarette smoking. *Eur. J. Clin. Chem. Clin. Biochem.* **35**:81-84 (1997)
280. Guo MML and Hildreth JEK. HIV-induced loss of CD44 expression in monocytic cell lines. *J. Immunol.* **151**:2225-2236 (1993)

281. Brakenhoff RH, Gerretsen M, Knippels PMC, Van Dijk M, Van Essen H, Olde Weghuis D, Sinke RJ, Snow GB and Van Dongen GAMS. The human E48 antigen, highly homologous to the murine Ly-6 antigen ThB, is a GPI-anchored molecule apparently involved in keratinocyte cell-cell adhesion. *J. Cell Biol.* **129**:1677-1689 (1995)
282. Sambrook J, Fritsch EF and Maniatis T. *Molecular Cloning: A Laboratory Manual*. Cold Spring Harbor Laboratory, New York (1989)
283. Studier FW, Rosenberg AH, Dunn JJ and Dubendorff JW. Use of T7 RNA polymerase to direct expression of cloned genes. *Methods Enzymol.* **185**: 60-89 (1990)
284. Geysen HM, Rodda SJ, Mason TJ, Tribbick G and Schoofs PG. Strategies for epitope analysis using peptide synthesis. *J. Immunol. Methods* **102**:259-274 (1987)
285. Lindmo T, Boven E, Luffita F, Fedorko J and Bunn Jr PA. Determination of the immunoreactive fraction of radiolabeled monoclonal antibodies by linear extrapolation to binding at infinite antigen excess. *J. Immunol. Methods* **72**:77-89 (1984)
286. Barker HM, Craig SP, Spurr NK and Cohen PTW. Sequence of human protein serine/threonine phosphatase 1 gamma and localization of the gene (PPP1CC) encoding it to chromosome bands 12q24.1-q24.2. *Biochim. Biophys. Acta* **1178**:228-233 (1993)
287. Friedrichs K, Kügler G, Franke F, Terpe HJ, Artl J, Regidor PA and Günther U. CD44 isoforms in prognosis of breast cancer. *Lancet* **345**:1237 (1995)
288. Salmi M, Grön-Virta K, Sointu P, Grenman R, Kalimo H and Jalkanen S. Regulated expression of exon v6 containing isoforms of CD44 in man: downregulation during malignant transformation of tumors of squamocellular origin. *J. Cell Biol.* **122**:431-442 (1993)
289. Kievit E, Pinedo HM, Schlüper HMM, Haisma HJ and Boven E. Comparison of the monoclonal antibodies 17-1A and 323/A3: the influence of the affinity on tumour uptake and efficacy of radioimmunotherapy in human ovarian cancer xenografts. *Br. J. Cancer* **73**: 457-463 (1996)
290. Wei AP and Herron JN. Use of Synthetic peptides as tracer antigens in fluorescence polarization immunoassays of high molecular weight analytes. *Anal. Chem.* **65**: 3372-3377(1993)
291. Farghaly SA. Tumor markers in gynecologic cancer. *Gynecol. Obstet. Invest.* **34**:65-72 (1992)
292. Herbst, AL. The epidemiology of ovarian carcinoma and the current status of tumor markers to detect disease. *Am. J. Obstet. Gynecol.* **170**:1099-1105 (1994)
293. Jacobson DR, Fishman CL and Mills NE. Molecular genetic tumor markers in the early diagnosis and screening of non-small-cell lung cancer. *Annals Oncol.* **6** (Suppl. 3):S3-8 (1995)
294. Gao X, Porter AT, Grignon DJ, Pontes JE and Honn KV. Diagnostic and prognostic markers for human prostate cancer. *Prostate* **31**:264-281 (1997)
295. Partin AW and Oesterling JE. The clinical usefulness of prostate specific antigen: update 1994. *J. Urol.* **152**:1358-1368 (1994)
296. Northover J. The use of prognostic markers in surgery for colorectal cancer. *Eur. J. Cancer* **31A**:1207-1209 (1995)
297. Tanabe KK, Ellis LM and Saya H. Expression of CD44R1 adhesion molecule in colon carcinomas and metastases. *Lancet* **341**:725-726 (1993)

298. Hudson DL, Speight PM and Watt FM. Altered expression of CD44 isoforms in squamous-cell carcinomas and cell lines derived from them. *Int. J. Cancer* 66:457-463 (1996)
299. Soukka T, Salmi M, Joensuu H, Häkkinen L, Sointu P, Koulou L, Kalimo K, Klemi P, Grénman R and Jalkanen S. Regulation of CD44v6-containing isoforms during proliferation of normal and malignant epithelial cells. *Cancer Res.* 57:2281-2289 (1997)
300. Carey TE, Wolf GT, Baker SR and Krause CJ. Cell surface antigen expression and prognosis. In: *Head and Neck Cancer*. Fee WE, Goepfert H, Johns ME, Strong EW, Ward PH (Eds.), Decker, Philadelphia, vol 2, 77-82 (1990)
301. Feinberg AP and Vogelstein B. A technique for radiolabeling DNA restriction endonuclease fragments to high specific activity. *Anal. Biochem.* 132:6-13 (1983)
302. Martiat P, Maisin D, Philippe M, Ferrant A, Michaux JL, Cassiman JJ, Van den Berghe H and Sokal G. Detection of residual BCR/ABL transcripts in chronic myeloid leukaemia patients in complete remission using the polymerase chain reaction and nested primers. *Br. J. Haematol.* 75:355-358 (1990)
303. Roye GD, Myers RB, Brown D, Poczaitek R, Beenken SW and Grizzle WE. CD44 expression in dysplastic epithelium and squamous-cell carcinoma of the esophagus. *Int. J. Cancer* 69:254-258 (1996)
304. Herold-Mende C, Seiter S, Born AI, Patzelt E, Schupp M, Zöller J, Bosch FX and Zöller M. Expression of CD44 splice variants in squamous epithelia and squamous cell carcinomas of the head and neck. *J. Pathol.* 179:66-73 (1996)
305. Ariza A, Mate JL, Isamat M, López D, Von Uexküll-Güldenband C, Rosell R, Fernández-vasalo and Navas-palacios JJ. Standard and variant CD44 isoforms are commonly expressed in lung cancer of the non-small cell type but not of the small cell type. *J. Pathol.* 177:363-368 (1995)
306. Givchian M, Wörner S, Sträter J, Zöller M, Heuschen U, Heuschen G, Lehnert T, Herfarth C and Von Knebel Doeberitz M. No evidence for cancer-related CD44 splice variants in primary and metastatic colorectal cancer. *Eur. J. Cancer* 34:1099-1104 (1998)
307. Regidor P-A, Callies R, Regidor M, Günther U, Zöller M and Schindler AE. Expression of the CD44 variant isoforms 6 and 4/5 in breast cancer. Correlation with established prognostic parameters. *Arch. Gynecol. Obstet.* 258:125-135 (1996)
308. Seelentag WKF, Komminoth P, Saremaslani P, Heltz PU and Roth J. CD44 isoform expression in the diffuse neuroendocrine system. I. Normal cells and hyperplasia. *Histochem. Cell. Biol.* 106:543-550 (1996)
309. Iida N and Bourguignon LYW. New CD44 splice variants associated with human breast cancers. *J. Cell. Biol.* 162:127-133 (1995)
310. Haynes BF, Telen MJ, Hale LP and Dennings SM. CD44, a molecule involved in leukocyte adherence and T-cell activation. *Immunol. Today* 10:423-428 (1989)
311. Picker LJ, De los Toyos J, Telen MJ, Haynes BF and Butcher EC. Monoclonal antibodies against the CD44 [Ln/Lu]-related p80, and Pgp-1 antigens in man recognize the Hermes class of lymphocyte homing receptors. *J. Immunol.* 142:2046-2051 (1989)

312. Schoenfeld A, Luqmani Y, Smidt D, O'Reilly S, Shousha S, Sinnott HD and Coombes RC. Detection of breast cancer micrometastases in axillary lymph nodes by using polymerase chain reaction. *Cancer Res.* 54:2986-2990 (1994)
313. Dingemans AM, Brakenhoff RH, Postmus PE and Giaccone G. Detection of cytokeratin-19 transcripts by reverse transcriptase-polymerase chain reaction in lung cancer cell lines and blood of lung cancer patients. *Lab. Invest.* 77:213-220 (1997)
314. Zippelius A, Kufer P, Honold G, Kollermann MW, Oberneder R, Schlimok G, Riethmüller G and Pantel K. Limitations of reverse-transcriptase polymerase chain reaction analyses for detection of micrometastatic epithelial cancer cells in bone marrow. *J. Clin. Oncol.* 15:2701-2708 (1997)
315. Liefers G-J, Cleton-Jansen A-M, Van de Velde CJH, Hermans J, Van Krieken HJM, Cornelisse CJ, Tollenaar AEM. Micrometastases and survival in stage II colorectal cancer. *N. Engl. J. Med.* 339:223-228 (1998)

Curriculum vitae

Nicole van Hal werd op 27 maart 1970 geboren te Boxmeer. In 1988 behaalde zij haar VWO diploma aan het Eemland College Noord te Amersfoort. In datzelfde jaar begon zij met de studie Scheikunde aan de Universiteit Utrecht. Tijdens de doctoraal fase deed zij drie keuzevakken. Het eerste keuzevak deed zij in het Wilhelmina Kinderziekenhuis bij het Laboratorium Metabole Stoorissen (prof.dr. R. Berger). Hier heeft ze gewerkt aan het opzetten van een 'High Performance Liquid Chromatography' methode voor de bepaling van het acylcarnitine-gehalte in plasma en urine van patiënten met een acyl-CoA dehydrogenase deficiëntie. Een tweede keuzevak werd gevolgd bij de vakgroep Moleculaire Genetica van de Faculteit Biologie (prof.dr. P.J. Weisbeek). Met behulp van recombinant DNA technieken heeft zij hier onderzoek verricht aan licht-gereguleerde transcriptiefactoren in planten. Het derde keuzevak was Chemische Informatica (dr. A.M.F. Hezemans) bij de Faculteit Scheikunde en omvatte een cursus programmeren in Turbo Pascal voor gevorderden. Haar hoofdvak deed ze bij de vakgroep Biochemie van Lipiden (prof.dr. K.W.A. Wirtz), waar zij aan de hand van biochemische technieken onderzoek deed aan het fosfatidylinositol transporteiwit in gecloneerde *Xenopus laevis* cellijnen. In augustus 1993 werd de Scheikunde studie afgerond. In september van datzelfde jaar werd zij Assistent in Opleiding bij de vakgroep Keel-, Neus- en Oorheelkunde van de Vrije Universiteit te Amsterdam (prof.dr. G.B. Snow). De resultaten van het onderzoek dat zij daar heeft verricht zijn beschreven in dit proefschrift. Sinds juli 1998 is zij werkzaam als post-doc bij de afdeling Veiligheid en Gezondheid van Voeding van het RIKILT-DLO te Wageningen alwaar zij een 'microarray' detectiemethode aan het opzetten is.

List of publications

1. Van Hal NLW, Van Dongen GAMS, Rood-Knippels EMC, Van der Valk P, Snow GB and Brakenhoff RH. Monoclonal antibody U36, a suitable candidate for clinical immunotherapy of squamous-cell carcinoma, recognizes a CD44 isoform. *Int. J. Cancer* 68:520-527 (1996)
2. Van Hal NLW, Van Dongen GAMS, Snow GB and Brakenhoff RH. Applicability of anti-CD44v6 antibody U36 for immunotherapy of squamous cell carcinoma. *Proc. Am. Assoc. Cancer Res.* 38:403, #2704 (1997)
3. Van Hal NLW, Van Dongen GAMS, Ten Brink CBM, Herron JN, Snow GB and Brakenhoff RH. Sequence variation in the monoclonal-antibody-U36-defined CD44v6 epitope. *Cancer Immunol. Immunother.* 45:88-92 (1997)
4. Van Hal NLW, Van Dongen GAMS, Stigter-van Walsum M, Snow GB and Brakenhoff RH. Characterization of CD44v6 isoforms in head and neck squamous cell carcinoma. (Submitted)
5. Van Hal NLW, Van Dongen GAMS, Van der Valk P, Ten Brink CBM, Snow GB and Brakenhoff RH. The role of CD44v6 splice variants in human cancer reconsidered. (Submitted)
6. Van Hal NLW, Van Dongen GAMS, Ten Brink CBM, Helder K-H, Rech-Wechselbraun I, Snow GB and Brakenhoff RH. Evaluation of soluble CD44v6 as potential serum marker for head and neck squamous cell carcinoma. (Submitted)

Dankwoord

Het onderzoek is gedaan, het proefschrift is geschreven. Echter, zonder de hulp, steun en adviezen die ik van velen heb gekregen, had dit proefschrift nooit tot stand kunnen komen.

Allereerst wil ik mijn promotor prof.dr. G.B. Snow graag bedanken voor de gelegenheid die ik heb gekregen om op de afdeling KNO mijn promotie-onderzoek te verrichten.

Veel heb ik geleerd van mijn co-promotoren, Guus van Dongen en Ruud Brakenhoff. Samen hebben we altijd naar een hoge mate van perfectie gestreefd, hetgeen ondermeer tot uiting komt in het aantal keren dat er een artikel werd omgegooid. Guus, mede door jouw optimisme heb ik de tegenslagen in mijn onderzoek goed weten te relativiseren. Aan de vanzelfsprekendheid waarmee je me altijd hielp, was niet te merken hoe druk je het eigenlijk hebt. Ruud, jouw goede ideeën en uitgebreide kennis van de moleculaire biologie zijn van grote waarde geweest voor de koers van mijn onderzoek. Het af en toe "even doordouwen" om resultaten te krijgen, is een belangrijke eigenschap van ons beiden. Ook zal ik het aantal decibel dat gepaard gaat met jouw aanwezigheid niet snel vergeten.

Prof.dr. S.T. Pals, prof.dr. R.J. Scheper, dr. K.-H. Heider, prof.dr. J.M.M Walboomers, prof.dr. S.O. Warnaar en prof.dr. P.C. Huijgens wil ik hartelijk danken voor de tijd die ze aan dit proefschrift hebben willen besteden en de bereidheid om zitting te nemen in de promotiecommissie.

Tal van resultaten zijn tot stand gekomen met de hulp van mensen buiten de vakgroep KNO. Van de afdeling Pathologie wil ik Paul van der Valk hartelijk danken voor het beoordelen van de immunohistochemieresultaten. Petra, alle immunohistochemische kleuringen die je voor me hebt gedaan, en Thea, de geduldig gesneden coupes voor mijn microdissectie-experimenten zijn niet voor niets geweest. Ze vormen een belangrijk onderdeel van mijn proefschrift. Jim Herron (University of Utah), we had a valuable e-mail correspondence. I'd like to thank you for spending your Christmas holiday to derive an equation, which barely fits to the page size of my thesis. Irene Rech-Weichselbraun and Karl-Heinz Heider (Bender Medsystems), unfortunately, in research you do not always get the data that you want.

Ook mijn studenten verdienen een speciaal plekje in dit dankwoord. Petra, hopelijk zijn je nachtmerries over de sequentieplaten inmiddels voorbij.

Davy, ik herinner me nog een gezellig middagje kolonie-prikken met de hele KNO-afdeling. Ioana, jouw werklust en doorzettingsvermogen zijn ongekend. Simone, al kunnen transformaties nog zo lastig gaan: de aanhouder wint!

En dan wil ik natuurlijk mijn collega's van KNO-tumorbiologie bedanken voor de gezellige tijd. Alle analisten waren bereid om mij zo nu en dan een handje helpen. Corlinda, jij hebt meer gedaan dan alleen een helpende hand toe te steken, daarom ben je straks mijn paranimf. Hopelijk hoeft je die search in Paradox niet nog een keer over te doen. Mirjam, het is moeilijk de orde te handhaven op een afdeling met zoveel gestresste AIO's. Kreeg je nou nog klonenformulieren van mij? Ellen, die screeningsmethode was toch wel erg effectief. En ook jouw hulp, Marijke, was bijna als vanzelfsprekend.

Bijna niemand kent het promotie-gevoel beter dan je mede-AIO's. Jacqueline, als ex-AIO wist jij je altijd precies in mijn situatie in te leven. Bij jou, Marij, kan ik alles voor de laatste keer afkijken. En Frank, wat zei je ook alweer? Is promoveren leuk? Dat proefschrift komt vanzelf wel af? Ingeborg, Maarten & Maarten, Viola, Iris en David, ik verzeker jullie: sommige gedeelten van promoveren zijn niet leuk, en dat proefschrift komt ook echt niet vanzelf af.

Boudewijn, San Diego was een leuke stad maar die bagels en dat Mexicaanse eten gingen op den duur toch wel wat vervelen. Voor alle technische en organisatorische ondersteuning wil ik Ton, Fred en het secretariaat KNO hartelijk danken. Pieter (Universiteit Utrecht), door jou was het toch nog mogelijk om mijn ontwerp op de voorkant van dit boekje te krijgen. Verder alle oud-studenten bedankt voor de gezelligheid op het lab en het halen van de koffie tijdens werkbesprekingen. Ook alle labgenoten van andere afdelingen, vroeger bij Moleculaire Pathologie op de brug en later op het IMBL, bedankt voor alle hulp en gezelligheid.

En dan tot slot natuurlijk mijn ouders, ik vind het knap dat jullie met zoveel begrip en interesse mijn promotie hebben gevolgd. Ik weet het, de laatste tijd kon ik over niets anders meer praten. Leonie, vroeger deden we al veel samen. Straks zullen we ook samen voor de commissie staan.

Okke, we hebben heel wat uurtjes met z'n tweeën op de studeerkamer doorgebracht. Het was een zware tijd, maar ik zal er straks met een goed gevoel aan terugdenken. Een periode waarin je toch altijd aandacht voor mij had. Kom, de proefschriften zijn af, zullen we samen de studeerkamer uit ons nieuwe leven instappen?

List of abbreviations

[Ag ^{tot}]	total concentration of surface antigen
[Ag ^{unb}]	concentration of unbound surface antigen
APAAP	alkaline-phosphatase anti-alkaline-phosphatase
b-FGF	basic-fibroblast growth factor
BSA	bovine serum albumine
CD	cluster of differentiation
cMAb	chimeric monoclonal antibody
DAB	3,3'-diaminobenzidine
DMEM	Dulbecco's modified Eagle's medium
EGFR	epidermal growth factor receptor
ELISA	enzyme-linked immunosorbent assay
[F _{ab} Ag]	concentration of the complex of antigen-combining sites with the surface antigen
[F _{ab} ^{tot}]	total concentration of antigen-combining sites
[F _{ab} Pep]	concentration of the complex of antigen-combining sites with the peptide
[F _{ab} ^{unb}]	concentration of unbound antigen-combining sites
FCS	fetal calf serum
HA	hyaluronic acid
HAMA	human anti-mouse antibody
HEPES	<i>N</i> -(2-hydroxyethyl)piperazine- <i>N'</i> -(2-ethanesulfonic acid)
HB-EGF	heparin binding-epidermal growth factor
HEV	high endothelial venule
HNSCC	head and neck squamous cell carcinoma
HPV	human papilloma virus
HS	heparan sulfate
K _d ^{Ag}	dissociation constant for the surface antigen/antigen-combining site complex
K _d ^{Pep}	dissociation constant for the peptide/antigen-combining site complex.
LOH	loss of heterozygosity
MAb	monoclonal antibody
MAd	mucosal vascular Addressin
NRS	normal rabbit serum

PBS	phosphate buffered saline
PCR	polymerase chain reaction
[Pep ^{unb}]	concentration of unbound peptide
PHA	phytohaemagglutinin
p.i.	post-injection
RAMPO	rabbit anti-mouse immunoglobulin peroxidase conjugate
RIS	radioimmunosciintigraphy
RIT	radioimmunotherapy
RT-PCR	reverse transcriptase-polymerase chain reaction
SCC	squamous cell carcinoma
SDS	sodium dodecyl sulfate
SDS-PAGE	sodium dodecyl sulfate polyacrylamide gel electrophoresis
SSC	saline sodium citrate buffer
TRIS	tris(hydroxymethyl)aminomethane
UICC	Union Internationale Contre le Cancer